A COMPUTER INTERFACED HIGH TEMPERATURE/KNUDSEN CELL QUADRUPOLE MASS SPECTROMETER DATA ACQUISITION SYSTEM: APPLICATION TO THE INVESTIGATION OF THE VOLATILE ABUNDANCE OF SUBMARINE BASALTS FROM THE MARINA ISLAND-ARC AND TROUGH

A THESIS SUBMITTED TO THE GRADUATE DIVISION OF THE UNIVERSITY OF HAWAII IN PARTIAL FULFILLMENT OF THE REQUIREMENTS FOR THE DEGREE OF

MASTER OF SCIENCE

IN CHEMISTRY

AUGUST 1978

By

Norman Wai Kwong Liu

Thesis Committee:

David W. Muenow, Chairman
John J. Naughton
Michael O. Garcia

We certify that we have read this thesis and that in our opinion it is satisfactory in scope and quality as a thesis for the degree of Master of Science in Chemistry.

THESIS COMMITTEE

David W. Muenow, Chairman

John J. Naughton

Michael O. Garcia

ACKNOWLEDGEMENT

I thank my research advisor, Dr. David W. Muenow, for his guidance and for granting me an enjoyable degree of freedom and supports in my research efforts.

I thank emeritius Professor John J. Naughton who served as a member of my thesis committee in his retiring years.

I thank Dr. Michael O. Garcia for providing me sample and helpful discussion in the geology aspect of my research.

I am grateful to Mr. Gerald Gulden who has given me technical assistance in the development of the instrumentation portion of my research.

My thanks to Mr. Bill Barnes for his assistance in the construction of the Knudsen cell heating control circuit, Ms. Diana G. Graham for providing helpful suggestions during the development of the QMS program, and Mrs. Wendy Harrison for her assistance in repairing the interface electronics in the time of trouble.

I am grateful to the University of Hawaii and the Hawaii Natural Energy Institute for financial support.

ABSTRACT

A method for the controlled heating of a high temperature Knudsen-cell effusion source and an automatic data acquisition system for an interfaced quadrupole mass spectrometer are described. The method of controlled heating (with variable heating rates, 1.25 to 20°C/min. from 25°-1300°C) has been shown to allow accurate and precise heating of the high temperature vaporization source required for quantitative extraction of volatiles from igneous rocks. The automatic data acquisition system provides the accurate measurement of signals from the mass spectrometer and allows one to collect large quantities of data (e.g. 150-250 mass scans per experiment) and make the data available quickly (15 to 20 minutes) for examination. The system eliminates the necessity of repeating the same experiment many times.

The utility of the heating control and automatic data acquisition system is demonstrated by providing quantitative mass pyrograms for the complete characterization of the vaporization and degassing of glass samples selected from the rims of pillow basalts dredged from the Mariana island-arc and interarc basin. The mass pyrograms allow clear distinction of samples from different geologic environments and show the effects of alteration of samples from seawater contamination. The abundance of the volatiles H_2O, CO_2, SO_2, F, and Cl in the matrix glasses and phenocrysts of plagio-

clase have been obtained. The results of this study demonstrate the power of the automated high temperature/Knudsen cell mass spectrometer system to provide important new data for the characterization of the volatiles in samples of geochemical interest.

TABLE OF CONTENTS

TABLE OF CONTENTS (Continued)

LIST OF TABLES

LIST OF FIGURES

LIST OF FIGURES (Continued)

LIST OF FIGURES (Continued)

LIST OF FIGURES (Continued)

LIST OF FIGURES (Continued)

I. INTRODUCTION

A. Background

Mass spectrometry coupled with vacuum heating and a computer-controlled data acquisition system can be a powerful analytical method for the extraction and determination of volatiles and volatile forming elements from a wide variety of materials (Wyatt et al., 1971; Gibson, 1973).

Systems have been developed and used in the study of lunar samples by the Burlingame group at Berkeley (Burlingame et al., 1971; Holland et al., 1972; Simoneit and Burlingame, 1972; Simoneit et al., 1973). Their analytical system consists of a magnetic instrument with high sensitivity, medium-resolution and fast scanning capability. Data are taken continuously by a LOGOS computer system. The computer-generated mass pyrograms were used to determine the total carbon and nitrogen contents of Luna 16 and Luna 20 samples (Simoneit, 1973) and to illustrate the mode of release of inorganic and organic volatiles on heating. A second research group led by Gibson (NASA Manned Spacecraft Center, Houston) has also recently developed a TA-MS computer system. In this system, a Finnigan 1015 S/L quadrupole mass spectrometer coupled with a Mettler vacuum-recording thermoanalyzer and interfaced to a PDP-8/L computer, was used for the analysis of meteoritic and lunar samples (Gibson, 1973; Gibson and Moore, 1973; Gibson et al., 1974).

A particularly important technique, originally developed for the characterization of high temperature vapors and their thermodynamics (Grimley, 1967), involves the use of a Knudsen cell which serves both as the sample holder and effusion source for volatiles admitted into the mass spectrometer. Interfaced with a low-cost quadrupole mass spectrometer Killingley and Muenow (1975) have constructed a versatile Knudsen cell assembly and developed a method to obtain temperature and time-dependent gas-release profiles (mass pyrograms). Mass pyrograms and the weight loss of the sample may be used to quantitatively characterize the vaporization or degassing behavior of the sample. The system takes advantage of the quantitative nature of Knudsen cell mass spectrometry and the versatility, low cost and small size of a quadrupole mass filter. Recent investigations in this laboratory have used this system to obtain the abundance and distribution of volatiles (and their heats of vaporization and partial pressures) from materials of geochemical interest. Among these are milligram-size samples of submarine basalts and their separated mantle-derived phenocrysts of olivine and plagioclase, meteorites, synthetic and natural glasses, calcareous and siliceous material from the marine environment and ore-forming fluids in inclusions (Delaney, Muenow and Graham, 1978; Gooding and Muenow, 1977).

B. Proposed Research

The system developed by Killingley and Muenow (1975) is capable of providing important information about the composition, abundance, and mode of release of volatiles in igneous materials. In order to utilize this system to the fullest advantage, it is the purpose of this research to:

(a) Develop methods for the accurate vacuum-heating-control required for quantitative extraction of volatiles from igneous rocks.

(b) Implement an efficient data acquisition system by interfacing the high temperature quadrupole mass spectrometer to an on-line real-time minicomputer (PDP-11/45).

(c) Demonstrate the utility of the data acquisition system by performing measurements for the volatiles released from selected samples of glassy rims of submarine basalts and their associated plagioclase and/or olivine phenocrysts.

The basic requirement of a high temperature mass spectrometric facility is the production of a beam of molecules representative of the volatiles released or vaporizing from a heated sample and their mass analysis as a function of temperature. To obtain mass pyrograms which allow quantitative characterization of the total volatilization process the most important criteria for the temperature control and data acquisition system are: (1) a variable and precise control of sample heating rate (e.g., from 1 to 20 °C/min.

over the range 25°-1500°C); (2) rapid and variable sampling rate of signals which accurately represent cell temperature, molecular mass and ion-intensity; (3) storage of data on a disk for later processing, analysis and graphical display; (4) elimination of operator intervention after the sample has been placed in vacuum; and (5) eliminate the necessity of repeating the same experiment many times so that all important data are collected.

In the first part of this thesis I describe a method for the controlled heating of a Knudsen cell vaporization source and a data acquisition system for an interfaced quadrupole mass spectrometer. The data acquisition system consists of computer-terminal interactive programs giving flexibility in selection of instrumental settings (e.g., data sampling and heating rates) thus permitting a wide variety of high temperature studies. The remaining portion of this thesis demonstrates the utility of the automated system by describing high temperature volatilization studies of submarine basalts from the Marianas Trough and Arc regions. The geochemical importance of these results are also discussed.

II. HIGH TEMPERATURE MASS SPECTROMETRY

A. Instrumentation

1. The High Temperature Mass Spectrometer System:

The high temperature quadrupole mass spectrometer facility consists of a specially designed high temperature Knudsen effusion cell assembly interfaced with a quadrupole mass filter which are both housed inside a Varian (model 934-1110A) vacuum system. The apparatus was largely assembled by Killingly (1975). A schematic diagram of the high temperature mass spectrometer facility is shown in Figure 1.

The mass filter is an Electronic Associates Incorporated (EAI) Quad 1110 residual gas analyzer". The Quad 1110 consists of three units. (1) Control unit; (2) Head electronics; (3) Analyzer assembly. Since the rf/dc generator needs to be located in close proximity to the filter the head electronics and the analyzer are fastened together. The control unit (positioned in an instrument rack with the Vacuum system controls) established and maintains operating conditions for the ionizer, rf/dc generator, and the detector. In addition, the control unit provides the amu correlation signal (horizontal sweep) to the recording instrumentation. The rf/dc generator drives the quadrupole filter which selectively passes properly accelerated ions from the ionizer to the detector. The analyzer assembly was flanged into the bell jar by means of a 4-inch Conflat flange. The Quad 1110 has a mass range of 1 to 300 amu, a sensitivity

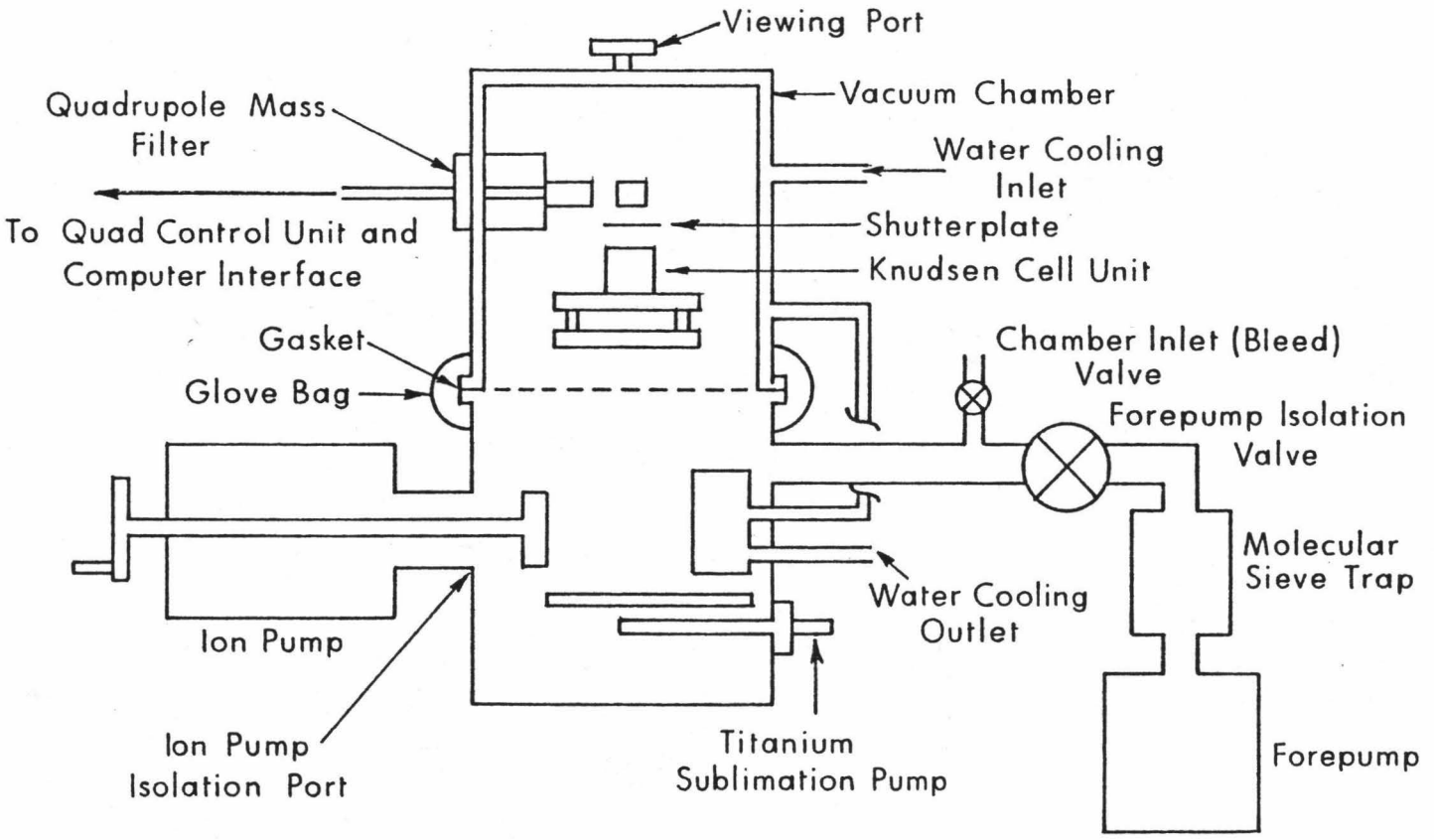

Figure 1. Schematic of the High Temperature Quadrupole Mass Spectrometer Facility.

(at electron multiplier output) of 100A/torr for N_2 with unit resolution, a resolution of $\frac{M}{\Delta M} > 2M$, where ΔM is peak width at half height, and a vacuum range of 10^{-4} torr or lower. Scan rates on the Quad 1110 can be changed in discrete steps from 0.1 to 900 sec/scan. The instrument has dual emission filaments, premounted and prealigned, which are switchable on the control panel. The analyzer system will withstand bake-out temperatures of 250°C (and 400°C with the rf/dc unit removed). The analyzer materials are stainless-steel, tungsten, and alumina.

The analyzer-detector system consists of a secondary emission multiplier-- a 14-stage beryllium-copper discrete dynode type. Output from the electron multiplier was fed to an EAI (ESA Model 75A) electrometer which is mounted next to the Quad rf/dc unit (not shown in the figure) on the bell jar. The ESA 75A electrometer is a single-ended current-in/voltage-out amplifier of the non-inverting type. The four linear ranges of the electrometer will produce an output of 10 volts dc, full-scale, for any input currents of 10^{-5} to 10^{-8} amps. A fifth range provides a logarithmic scale.

The dc voltage output of the electrometer is carried by coaxial cable from the bell jar unit to the control console where it is split to simultaneously drive an oscilloscope (integrated into the Quad control unit) and the computer interface electronics for online data acquisition, or alternatively drives a fast response Texas Instrument recorder (Model FS01W6D).

The high vacuum pumping system consists of a mechanical roughing pump (Welch Model 1402) incorporated with a molecular-sieve trap with a bake-out heater which can achieve a vacuum of $5x10^{-5}$ torr, a titanium sublimiation pump (TSP) Varian Model 916-0017, for high speed pumping for all active gases and to increase system pumping speed at pressure below 10^{-6} torr, and a 140 L/min. VacIon pump (Varian Model 916-7001) which operates in vacuum ranges from 10^{-5} to 10^{-12} torr.

The vacuum housing consists of a double-wall, water cooled, stainless steel bell jar with numerous viewing ports and feed-thrus which facilitate the attachment of various components-- the cell temperature-sensing thermocouple, the mass filter, the shutter plate and the high current feed-thrus. The bell jar is seated on a fixed base with a Viton gasket for high vacuum sealing which permits convenient access to the bell jar interior for sample introduction and maintenance work. The exterior of the bell jar around the perimeter of the Viton seal is enclosed in a plastic glove bag which is inflated with high-purity nitrogen during the sample introduction and retrieval operation to prevent the vacuum system from being excessively "contaminated" by atmospheric gases.

The computer is a PDP-11/45 minicomputer (a disk-operated system) emphasizing time share/real time operation. A CAMAC interfacing module is used for on-line data acquisition from instruments. The computer facility also contains

a magnetic tape unit for off-line data storage, a high capacity disk unit for on-line data storage, and a VERSITAC electrostatic printer/plotter.

2. The Knudsen Cell Assembly:

The high temperature Knudsen cell assembly is illustrated in Figure 2. Details of the high temperature Knudsen cell have been previously described (Muenow, 1973). The Knudsen cell is supported by tungsten rods and heated by radiation (to 1500°C) from a coiled tantalum resistant element (6.5 in. length, 0.05 in. diameter). A set of four concentric molybdenum cylinders surrounds the cell and serves as a radiation shield. At high temperature a molecular beam of released volatiles from the sample emerges through the orifice in the cell lid and is directed through a movable shutter-plate (bolted to the vacuum end of a linear feed-through) and into the ionizer of the quadrupole mass spectrometer. An important feature of this arrangement is the short and direct line-of-sight placement of the ion source with respect to the 0.040-in. diameter cell orifice. This permits essentially 100% transmission of volatiles (including condensable species) from the sample to the ionizer. Use of the shutterplate allows distinction between molecular species emitted directly from the Knudsen cell and those reemitted and scattered from other surfaces of the system.

The cell temperature is measured by a Pt/Pt-10% Rh thermocouple secured into the base of the cell and is fed to

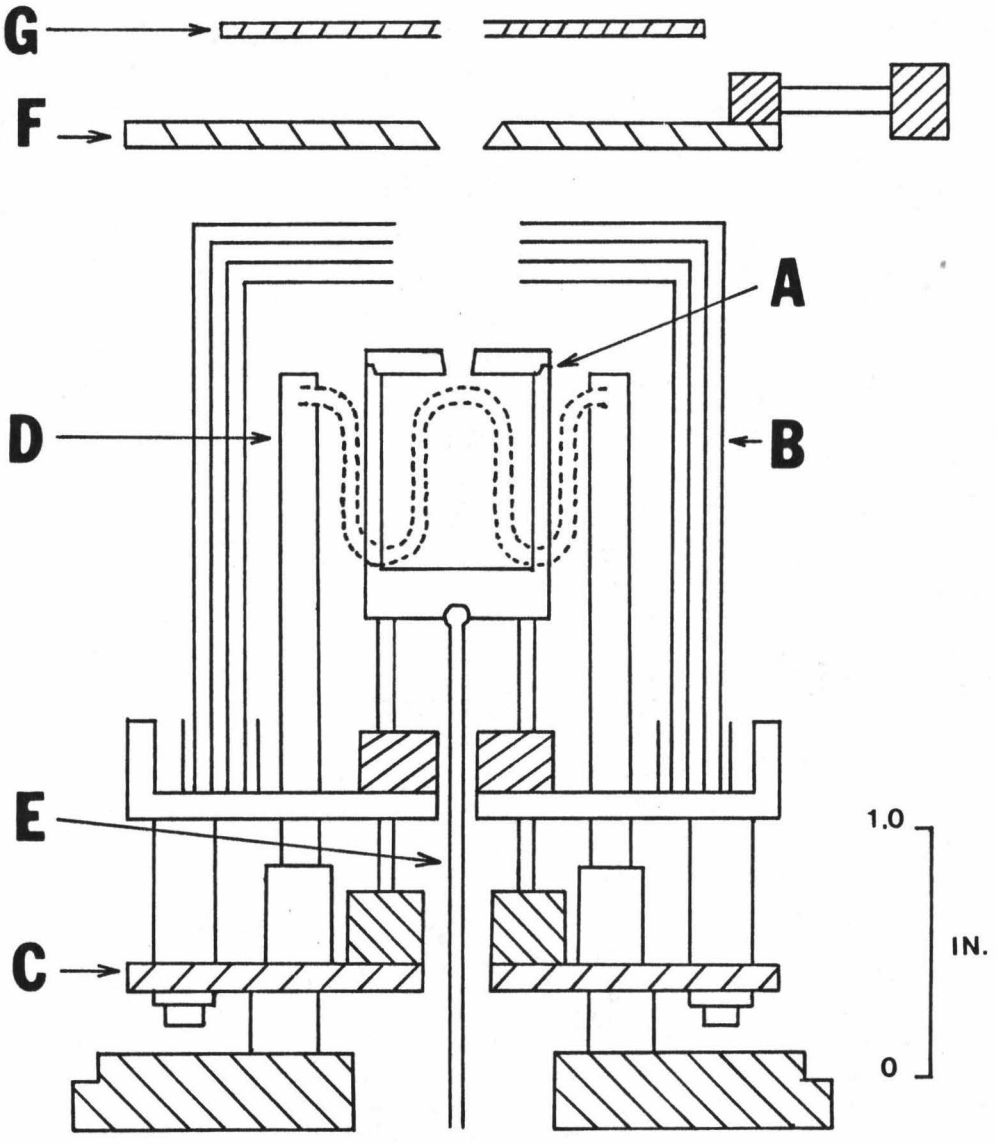

Figure 2. Schematic of the High Temperature Assembly (adapted from Muenow, 1973). The components are the Knudsen Cell (A), heat shields (B), positioning plate (C), resistance heating element (D), thermocouple (E), shutter-plate (F), and the ionizer (G).

an external digital temperature indicator (Newport Laboratories Inc., model 2600SC).

To eliminate (or minimize in some cases) reaction between the sample and the cell material at high temperature, samples are contained within a high purity Lucalox (99.99% Al_2O_3) cell liner. Each liner (shown in Figure 3) is fabricated to slip-fit into the Knudsen cell. The liners are reusable with proper cleaning procedures.

3. The Operation of and Theory of the Quadrupole Mass Filter:

The quadrupole mass analyzer, first developed by Paul and co-workers (1958), eliminated magnetic requirements and achieved mass separation solely with electric fields. The analyzer transmits only those ions whose mass to charge ratio lines within a band of easily variable width. The sensitivity increases, and the resolution decreases, as the width of the passband is increased. The fact that these parameters can be readily controlled is a distinct advantage of this instrument.

The theoretical design of the quadrupole mass filter describes an ideal quadrupole array consisting of four hyperbolic cylinders in a square configuration with the inside radius of the array equal to the smallest radius of curvature of the hyperbola. In practice this is approximated by four cylindrical rods mounted precisely at the corners of a square, at a distance 2r from each other, with opposite

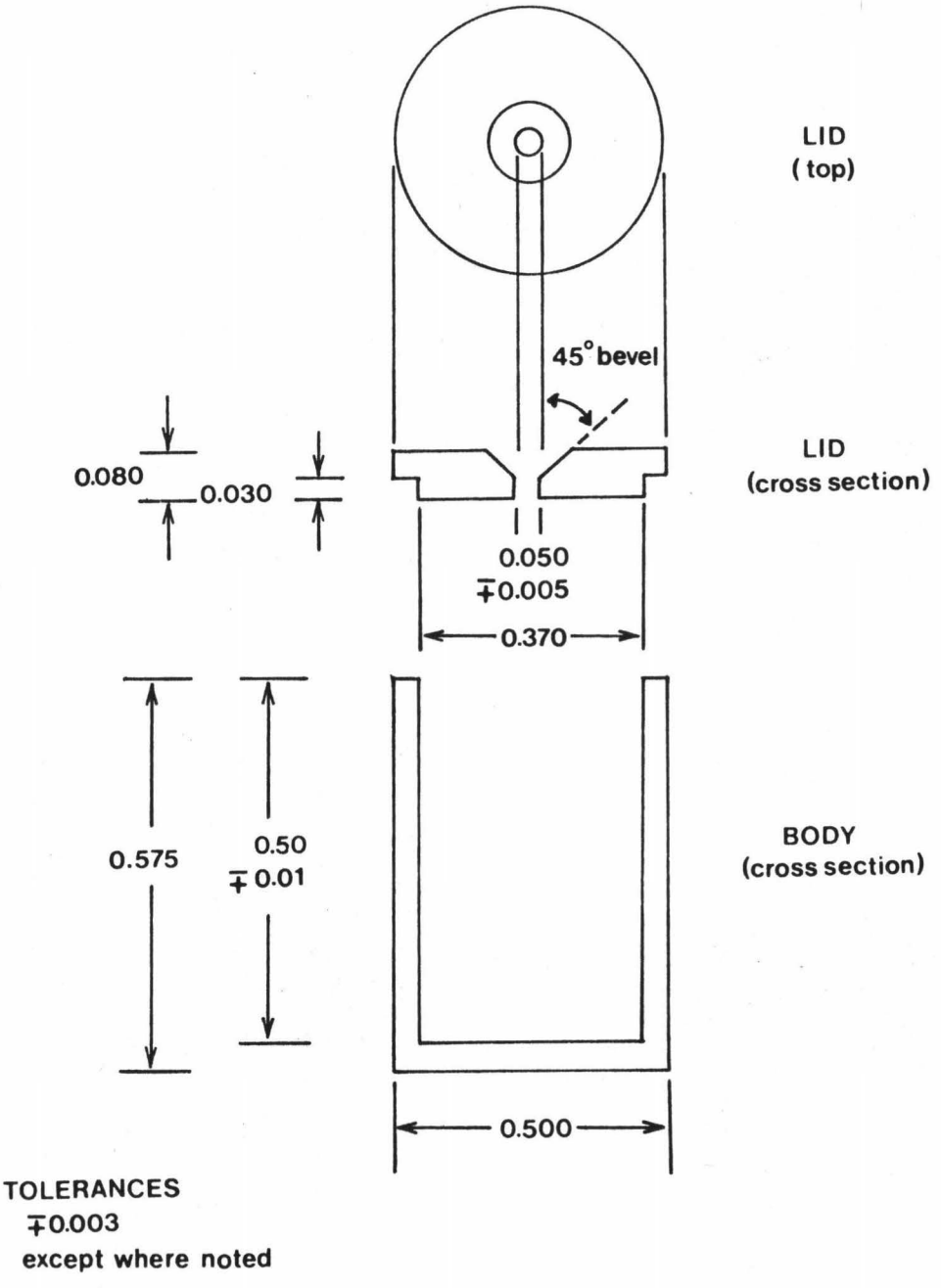

Figure 3. Schematic of Knudsen Cell Lucalox[R] Liner Cup. (Dimensions are in inches.) (after Gooding, 1975).

rods having common electrical inputs. An rf potential, V cos ωt, and a dc potential, U, are applied to the rods and a two-dimensional quadrupole field is produced with a potential at any point in the field:

$$\Phi\ (x,y,z,t) = (U + V \cos \omega t)\ (x^2 - y^2)/r^2 \qquad (1)$$

The two pairs of rods receive potentials of equal magnitude with the dc component of one pair being of opposite sign to that on the other pair and the ac component having a 180° phase difference between the two sets of rods. Ions produced in the ion source of a quadrupole mass filter are accelerated into one end of the quadrupole array and encounter the potential existing between the rods.

The distribution of the electric field in the region is given by the first differential of Φ:

$$E_x = -\frac{d\Phi}{dx} = -2\ (U + V \cos \omega t)\ \frac{x}{r^2} \qquad (2)$$

$$E_y = -\frac{d\Phi}{dy} = 2\ (U + V \cos \omega t)\ \frac{y}{r^2} \qquad (3)$$

$$E_z = 0 \qquad (4)$$

The force on a singly charged ion is eE in a field of strength E. Therefore, equations of motion of such an ion injected in the z (axial) direction of this field are given by:

$$m\ddot{x} = eE_x = -2e(U + V \cos \omega t)\ \frac{x}{r^2} \qquad (5)$$

$$\text{or, } m\ddot{x} + (2e/r^2)(U + V\cos\omega t)x = 0 \qquad (6)$$

$$\text{and similarly, } m\ddot{y} - (2e/r^2)(U + V\cos\omega t)y = 0 \qquad (7)$$

$$m\ddot{z} = 0 \qquad (8)$$

It follows that $m\dot{z}$ = constant which means that the axial velocity component of the ion in the quadrupole field is constant. Factors which govern the stability of the ion in the quadruple field are therefore determined by solutions of equations (6) and (7).

The equations may be rewritten in the normal forms of the Mathieu equation by substituting the following non-dimensional coefficients (Brubaker, 1960).

$$\theta = \omega t \qquad (9)$$

$$\alpha = \frac{e}{m} \cdot \frac{2V}{r^2\omega^2} \qquad (10)$$

$$\beta = \frac{U}{V} \qquad (11)$$

The differential equations then become:

$$\ddot{x} + \alpha(\beta + \text{Cos}\ \theta)x = 0 \qquad (12)$$

$$\ddot{y} - \alpha(\beta + \text{Cos}\ \theta)y = 0 \qquad (13)$$

The regions of interest are those where both x and y solutions to these equations are stable simultaneously so that the resultant trajectory of the ion is stable and the ion is unperturbed in its transit of the region between the

four poles. The boundaries of the region of interest are shown in Figure 4.

For ions of specific $^{m}/e$ values the quadruple is traversed without incident while lighter, or heavier, ions increase in oscillations and collide with the analyzer rods.

For a given rf field frequency ($f = \omega/2\pi$), the mass to frequency relationship is given by:

$$M = \frac{0.136V}{r^2 f^2} \tag{14}$$

where V is in volts, r in cm, f in megacycles, and M in amu (Roboz, 1968).

Mass scanning is achieved either by varying U or V while keeping the U/V ratio constant and f constant or by varying f at fixed voltages. The former procedure is the more common.

A suitable ratio of the peak ac to dc voltage (U/V) is selected to provide the appropriate operating line. The value of r is fixed and ω is held at a fixed value. Selectivity of the filter is controlled by use of the rf voltage (V).

The range of masses which traverse the quadrupole unimpeded may be determined from the two points where the operating line intersects the stable region boundaries.

B. Analytical Techniques:

Using a Knudsen cell arrangement of the type described, permits one to use techniques originally developed for

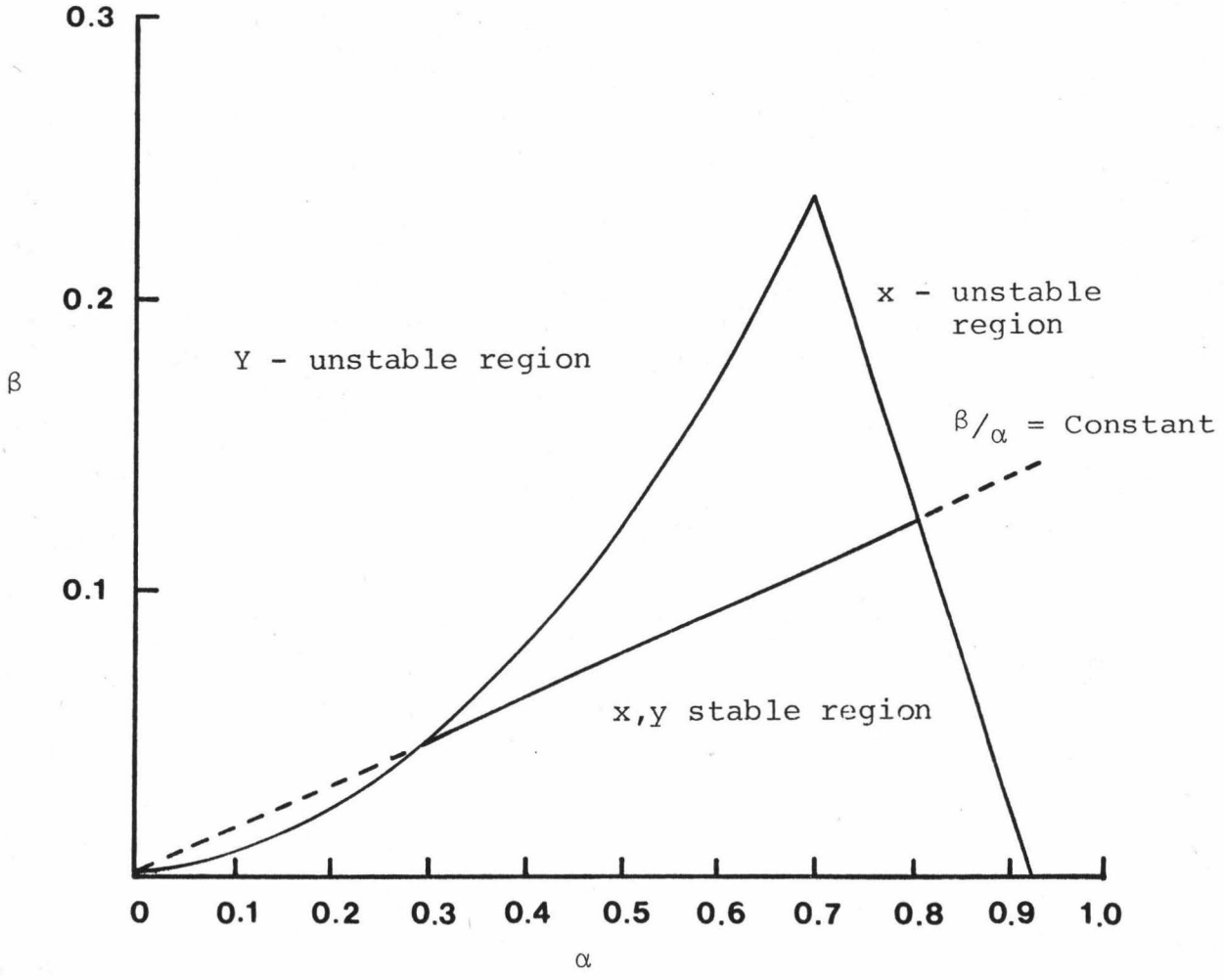

Figure 4. The Stability Domain for the Operation of a Quadrupole Mass Filter (after Dawson and Whetten, 1969).

thermodynamic measurements in high temperature inorganic mass spectrometry. A fundamental relationship (Grimley, 1967) is the one expressing the number of molecules (N_i) of species (i) released from a heated sample as a function of their measured isotope-corrected ion intensities (I_i^+), the mean thermal velocity ($\bar{c}_i$) of molecular species within the effusion cell, and the time interval (t_2-t_1) the sample is maintained at high temperature. It is given by the equation:

$$N_i = K_i \int_{t_1}^{t_2} I_i^+ \bar{c}_i dt \qquad (15)$$

The constant (K_i) is the instrumental sensitivity constant and is obtained by vaporizing a standard whose vapor pressure is well established over a large temperature range. Its value is computed from the relation:

$$K_i = \frac{P_s}{I_s^+ T_s} \cdot \frac{\delta_s}{\delta_i} \cdot \frac{\gamma_s}{\gamma_i} \cdot \frac{(E_s - AP_s)}{(E_i - AP_i)} \cdot \frac{\tau_s}{\tau_i} \qquad (16)$$

where P_s is the vapor pressure of the calibration standard; I_s^+, its measured ion-current intensity; T_s, the absolute temperature of the Knudsen cell; (δ), the ionization cross section; (γ), the electron multiplier efficiency; (E), the energy of ionizing electrons; (AP), the appearance potential; and τ, the quadrupole efficiency.

These two expressions allow one to compute the weight (or number of moles) of each volatile released from a sample

subject to controlled vaporization. The calculation is made in the following way: A mass pyrogram is obtained at a controlled heating rate (r) so that r = dT(°K)/dt(sec). Since $\bar{c}_i$ may be expressed as $(8RT/\pi M_i)^{1/2}$, where M_i is the molecular weight of the ith species, it follows from integration of equation (15) over the time of heat treatment that

$$N_i = \frac{8R}{\pi}^{1/2} \cdot \frac{M_i}{r}^{-1/2} \cdot (K_i) \cdot (A_i) , \quad (17)$$

where A_i is the value for the integrated area under the $(I^+_i T^{1/2})$ vs. T curve obtained from the output signals recorded on magnetic tape. Letting W_i and W_s be the respective amounts of the ith and calibration-standard species vaporized (where W (grams) = $\frac{NM}{\text{Avogadro's No.}}$), the combined equations (16) and (17) one finally obtains for the weight in grams of the ith species released,

$$W_i = W_s \cdot \frac{M_i^{1/2}}{M_s^{1/2}} \cdot \frac{A_i}{A_s} \cdot \frac{\delta_s}{\delta_i} \cdot \frac{\gamma_s}{\gamma_i} \cdot \frac{(E_s - AP_s)}{(E_i - A_i)} \cdot \frac{\tau_s}{\tau_i} \cdot \quad (18)$$

For each species a correction is made to (A_i) to take into account fragmentation patterns and isotopic abundances.

III. IMPLEMENTATION OF THE TEMPERATURE CONTROL AND AUTOMATIC DATA ACQUISITION SYSTEM

A. Heating and Temperature Control

Heating of the Knudsen cell is achieved by passing an A.C. current through the resistance element. In order to obtain a variable and precise heating rate of the Knudsen cell, a heating voltage control unit with a cell temperature feed-back loop was designed and constructed.

A block diagram of the heating control of the Knudsen cell is shown in Figure 5. The temperature of the Knudsen cell is sensed by the thermocouple and the voltage signal is fed into a digital thermometer by which a four digit Binary-Coded-Decimal (BCD) signal is produced. The BCD signal is converted to an analog signal by a 4-digit BCD digital-to-analog converter (DAC) and is calibrated at 1 millivolt per degree C.

A temperature ramp control voltage of opposite sign is generated by an electronic circuit. A crystal oscillator (a frequency generator) serves as a clock. Its output is split into different frequencies using a binary counter (the frequency divisor). Each of these frequencies (the outputs of the binary counter) corresponds to a quotient of the oscillator frequency divided by a power of 2. One of the binary counter outputs is selected to serve as heating rate control signal. A 12-bit binary up-down counter samples and stores the control signal. A 12-bit binary DAC converts the con-

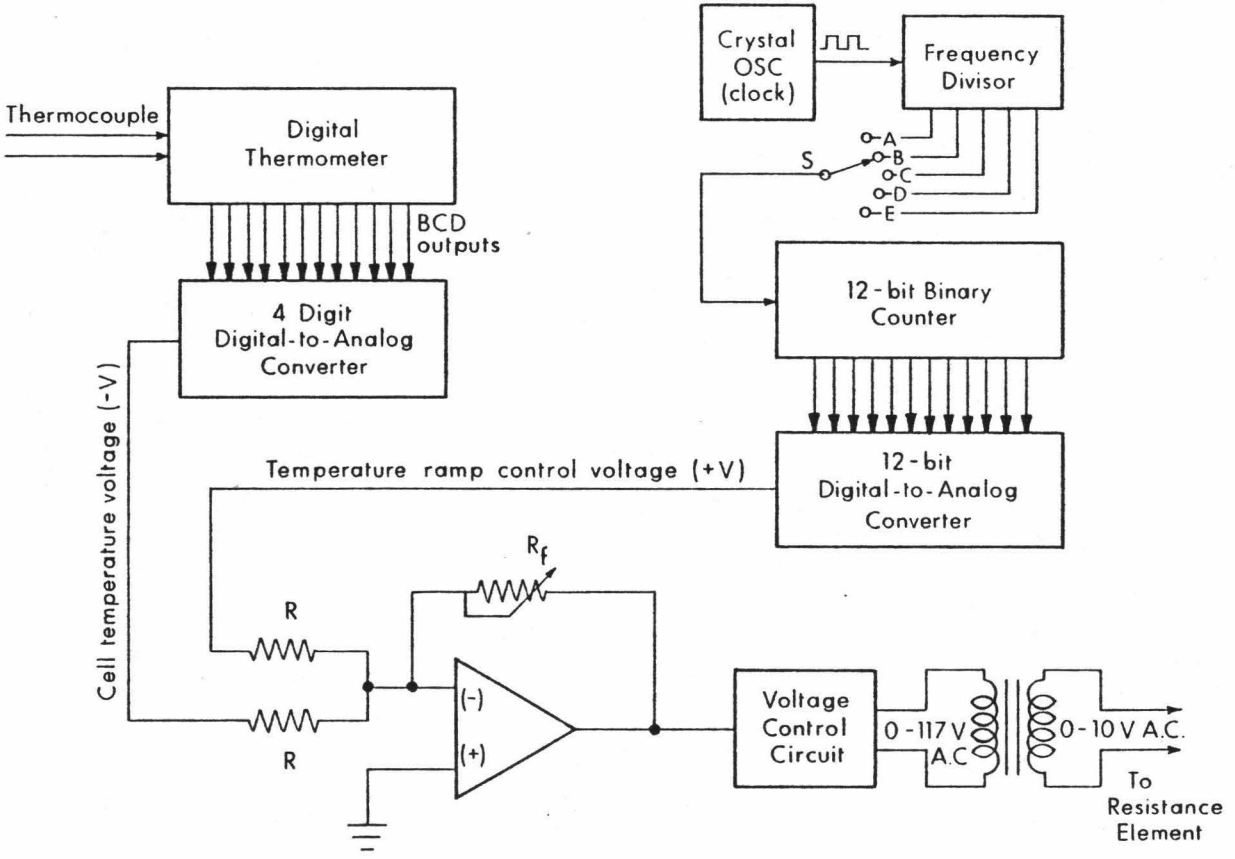

Figure 5. Block Diagram of the Heating Control Circuit for the Knudsen Cell.

tent of the counter to an analog voltage, also calibrated at 1 millivolt per degree C. The voltages from both DACs are compared at the summing point to an operational amplifier. The difference of the two voltages is amplified to control the voltage regulating circuit which then supplies 0 to 117V a.c. (stepped down by a high current transformer) required by the heating element.

B. Method of Automatic Data Acquisition

The implementation of the automatic on-line computer data acquisition system for the mass spectrometer involves the conversion of analog outputs of the mass spectrometer to digital signals suitable for sampling and processing by the computer. A block diagram outlining the method of signal digitization, data collection and data reduction is shown in Figure 5. The signals from the mass spectrometer are the ion intensity (0 to -10 v), mass ramp (0 to +10 v), temperature (0 to +2.0 v), and heating voltage (0 to +10v, not shown in Figure 6). Each of these signals is converted to a frequency via an INTECH A-8000 monolithic voltage-to-frequency converter, "V/F", which converts an input voltage of 0 to 10V to a frequency of 0 to 100 kHz of 5-volt pulses. The pulse signals are received by the computer via an optical coupler (HP4350-443) to avoid potential problems with ground loops between the mass spectrometer and the computer. These are then counted by a 15-bit counter for a short sampling period (e.g. 0.03 sec.). This data sampling rate

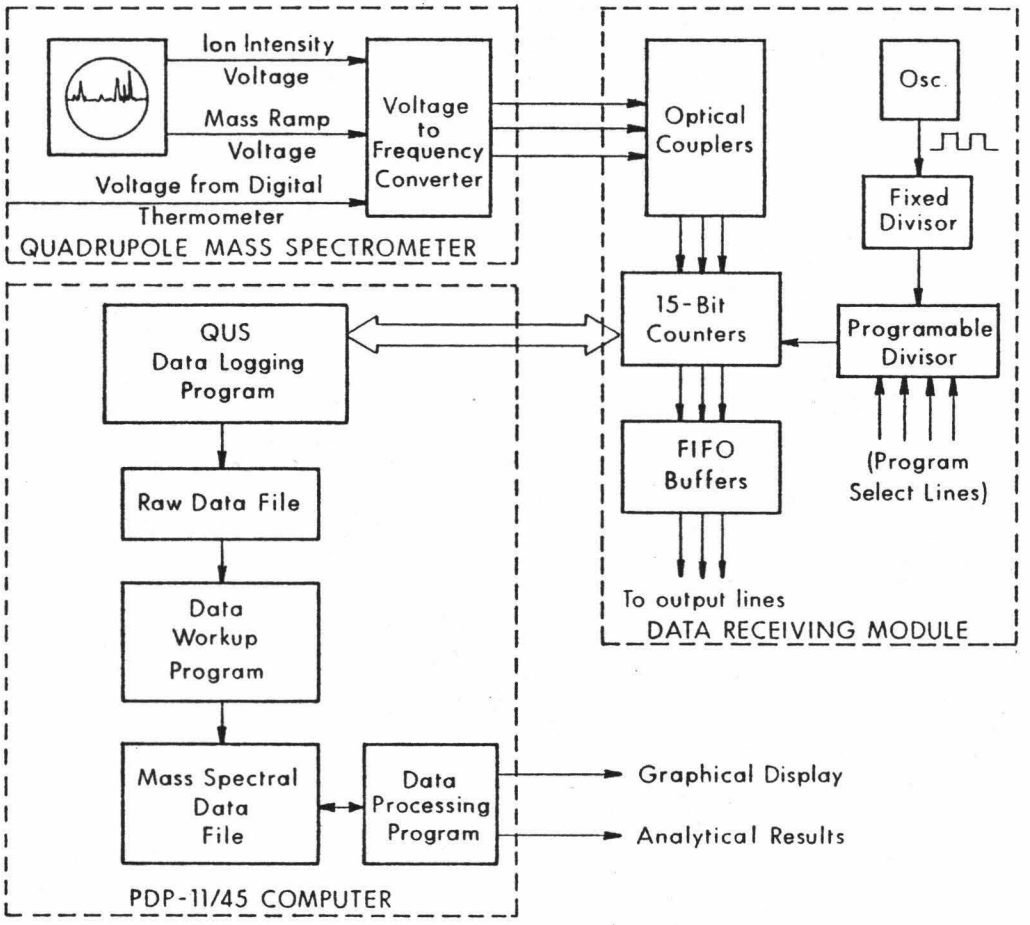

Figure 6. Block Diagram Outlining Method of Signal Digitization, Data Collection and Reduction.

is dictated by a crystal oscillator whose frequency is divided by a fixed divisor and a programmable divisor to allow flexible selection of data sampling rate. At the end of the period all the counter outputs are clocked into a FIFO buffer, to avoid possible data back logging problems before output onto a disk file. The data logging operation is controlled by a computer program (QUS, written in assembly language) to allow flexibility in the selection of data sampling rate and sampling period of a mass spectrum. The data logging program is able to restart itself at a constant time interval while the mass spectrometer is scanning continuously and without operator intervention. Detailed operation instructions of the data acquisition system is given in Appendix C.

C. Data Reduction and Analysis

1. QRDMAS -- Data Work Program:

The transformation of the collected raw data into useful spectral information involves the determination of the occurrence of mass peaks, peak positions and their intensities, cell temperatures, and heating voltage. The results are stored onto a permanent mass spectral data file for later analysis. A computer plot of a typical mass scan is shown in Figure 7.

The data transformation operation is done by a FORTRAN data work-up program (called QRDMAS) which can be run uninterrupted or in an interactive mode to allow handling of

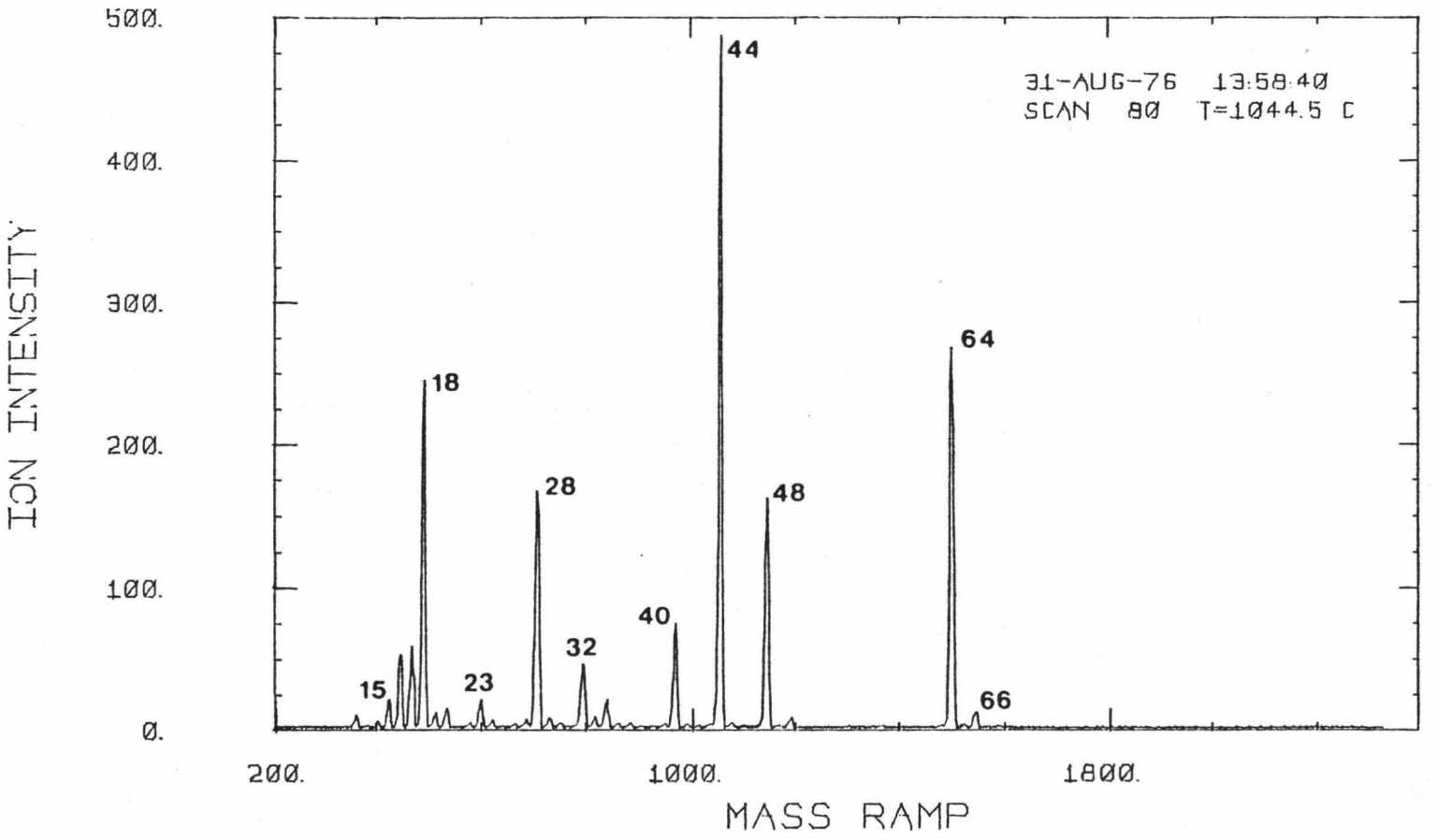

Figure 7. A Computer Plot of a Typical Mass Scan.

error in the data. QRDMAS searches the data for the occurrence of mass peaks. The intensity of each peak is given by the sum of sample points V_i to V_n from X_i to X_n, the positions at which a peak begins and ends. (The voltages are subtracted for baseline signal which is calculated in the program since no threshold rejection of the baseline signal is done during signal digitization.) Ion intensity data are converted back to its corresponding input voltage signals according to a simple relationship governed by the characteristics of interface electronics, V = N/ft, where V is the input voltage of the "V/F" in volts, N is the number of pulses counted by the binary counter, f is the conversion factor of the "V/F" (10^4 Hz/V) and t is the sampling time per data point. The center of the peak is calculated using the centroid method, $\Sigma V_n X_n / \Sigma V_n$. The centroid method was shown to be fundamentally correct in peak center calculations (Klimowski, et al., 1970).

After all mass peaks are found and their intensities calculated the proper m/e-value is assigned to each peak. Since m/e is linear with respect to the mass ramp sweeping voltage, the mass assignment of peaks found is reduced to a simple calculation using a linear equation which is characteristic of the mass spectrometer. In order to obtain this characteristic equation, the positions of at least two reference peaks must be known. Water, nitrogen and carbon dioxide are common background gases and provide convenient reference peaks at m/e = 18, 28 and 44, respectively. The m/e = 18

position is first identified by using the fragmentation pattern of H_2O (m/e = 18, 17 and 16) and the intensity-ratio of m/e = 17 to 18. A first order approximation of the characteristic function is then found by performing a linear-least squares calculation using these three consecutive peaks. Using this equation, peaks for m/e = 28 and 44 are identified, and against a least squares calculation is performed with the addition of these two peaks and their known positions. This gives the characteristic equation, M = AX + B, where M is the m/e-value for the peak found, X its position and A and B are the slope and offset, respectively.

The resulting spectral information (the mass peaks, ion intensities, temperature and heating voltage) of each scan is output to a data file. This data file is kept for subsequent analysis. The raw data file can then be discarded.

2. QMS -- Data Analysis Program:

The determination of analytical information from the spectral data is done by an independent FORTRAN program, QMS, which is a fully terminal-interactive program and allows the operator to select the types of analyses to be performed on a data file. The important functions of this program are: 1) to provide a qualitative "picture" of the system being studied; 2) to provide quantitative information about the system being studied; and 3) to provide flexibility in data analysis and facilitate the search for new and and important information.

QMS is structured in modular form and each of the different functions it performs is implemented by a subroutine function. The main program acts as a monitor which interacts with the operator via a computer terminal. The monitor asks the operator the functions (each is encoded in a four-character code) to be performed. The monitor then transfers control to the selected subroutine. After the subroutine is completed its task control is returned to the monitor. This process is repeated until the analysis is completed.

This arrangement of the program has several advantages: 1) it provides maximum flexibility in data analysis; 2) it minimizes the modification of the existing program when future expansion is necessary; and 3) subroutines can be overlaid to reduce memory requirement (memory is a limiting resource in any mini-computer system).

The QMS program is documented in detail in the FORTRAN source code. A brief outline of QMS in the form of flow diagrams is given in Appendix D. The QMS's subroutine names and their functions are listed in Table 1.

D. System Performance

1. The High Temperature Vaporization Unit:

The performance of the high temperature vaporization source (consisting of the specially designed Knudsen cell interfaced with the quadrupole mass spectrometer) has been thoroughly evaluated and has proved to be sensitive, versatile and reliable (Killingley, 1975).

Table 1. QMS Subroutine Code Names and Functions.

Name	Function
AREA	For each of the masses being processed, calculate the temperature-dependent area (A_1 in equation 17) under the mass pyrogram using a background file for background correction.
BACK	Read in the background data file.
CORR	Subtract background intensities from sample intensities.
DATA	Read in the sample data file.
ERRO	Inspect the input data from terminal.
EXIT	Ending the QMS main program.
HELP	Print a summary of the QMS subroutines and their functions to the user terminal for a quick reference.
PEAK	Calculate the temperature dependent area, A_i, of a mass peak envelope under the mass-pyrogram by drawing a straight line at the base of the mass envelope for background correction.
PLTS	Plot temperature or heating voltage vs. time.
PYRO	Plot the mass pyrogram for the masses selected.
RATI	Calculate the temperature dependent area ratio of two masses.
STAR	Select masses to be processed by the above subroutines.

The heating control circuit described in Section III-A allows precise controlled heating of the high temperature vaporization unit. The outputs of the frequency divisor labeled A, B, C, D and E are selectable via the switch S and allow for a variable heating rate. The 12-bit binary up-down counter also permits the controlled cooling of the Knudsen cell from high temperature. At position A the heating rate is calibrated at approximately 1.25°/min., and at positions B, C, D, and E the heating rates are increased sequentially by a factor of 2 to provide a maximum rate of 20°/min. The performance of the heating control circuit is evaluated by heating the Knudsen-cell at each rate setting and measuring the cell temperature at fixed time intervals. Figure 8 shows a computer plot of cell temperature vs. time at three different heating rates. The number of data points on lines C, D and E are approximately 250, 110, and 60, respectively. The measured heating rates and standard deviations are calculated by a linear least-square program, and are also shown in Figure 8.

2. The Automatic Data Acquisition System:

The data resulting from digitization of the signals from the mass spectrometer must, after proper conversion, represent as precisely and accurately as possible the original mass spectrometer signals so that one obtains the desired quantitative information about the system being studied. To determine the precision and accuracy of the data

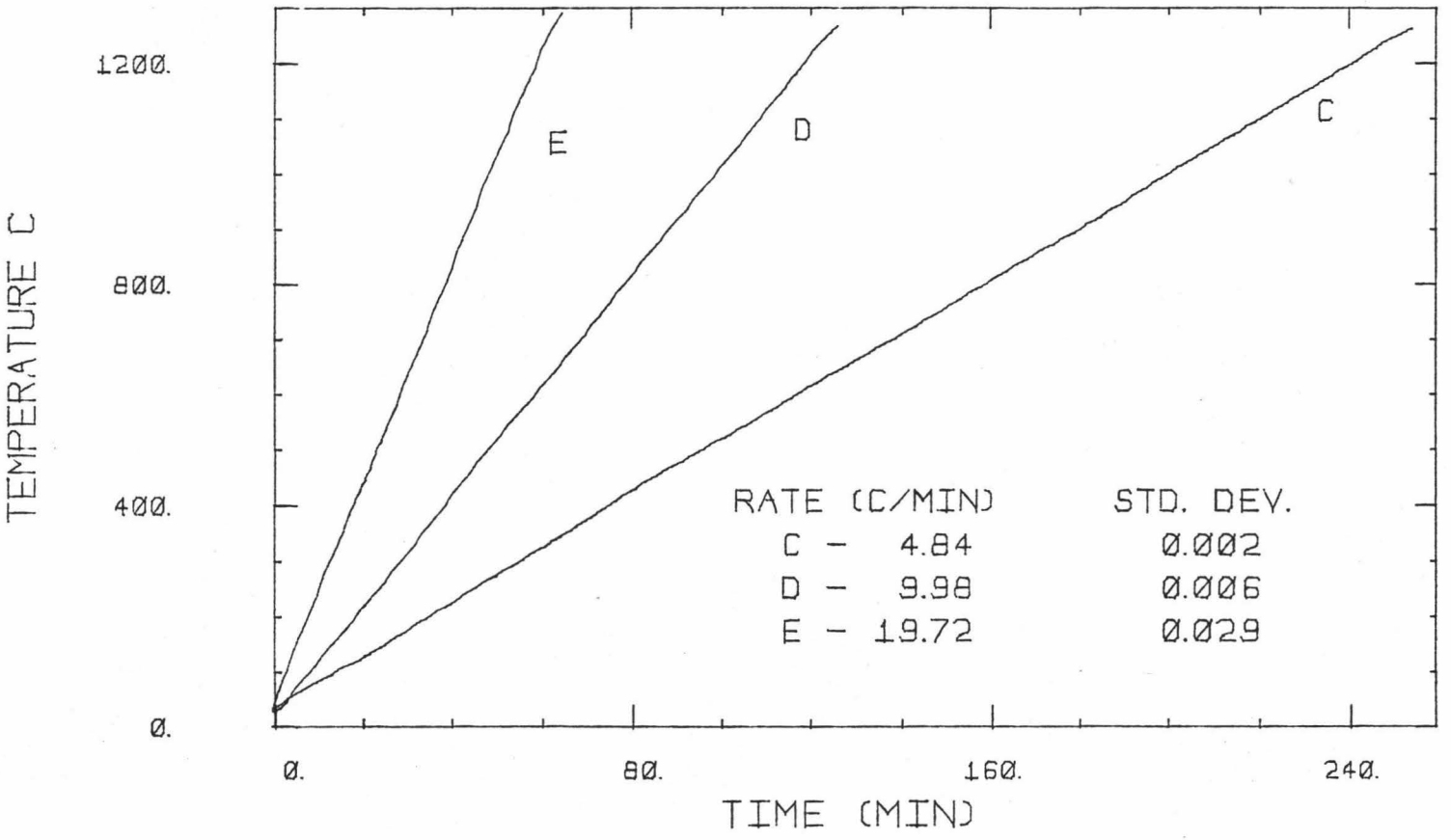

Figure 8. Computer Plot of Cell Temperature vs. Time for Three Heating Rates.

acquisition system, a range of voltages from a precision DC power supply was used to simulate input signals to the interface electronics. The measured signals (after digitization and proper conversion) were compared with the corresponding inputs. The results are summarized in Table 2.

The accuracy and precision of the data acquisition system range from ±8.5% to 10.00% and 1.68% to 5.39% respectively, for input voltages at or below 10 millivolts. The mass spectrometer noise level is approximately 10 millivolts, but normally the mass peak signals are much greater than this voltage (>1.0 volt for H_2O, >0.2 volt for CO_2, and 0.02 to 1.0 volt for SO_2). For the mass spectrometer signals above 10 millivolts, the accuracies are very good as shown in Table 2b. For example, even for weak ion intensities of 0.1191 volt (for M/C = 29) and 0.0782 volt (for m/e = 40) the standard deviations are 0.31% and 4.80%, respectively. The deviation of the measured voltage of the precision power supply inputs compared to those of the mass spectrometer (for similar voltages) are much less. This indicates that the data acquisition system is capable of sampling accurately and precisely the mass spectrometer signals.

3. Limitation of the System:

The high temperature vaporization assembly has been used to achieve cell temperatures as high as 1620°C (Killingley). However, for the protection of the mass

Table 2a. Precision and Accuracy of the Interface Electronics.

Input Voltage (volts)	Measured Voltage (volts)	Standard Deviation (%)
0.001	0.00090 ±10.00%	5.39
0.005	0.00542 ± 8.40%	3.10
0.010	0.01085 ± 8.50%	1.68
0.050	0.05106 ± 2.12%	0.53
0.100	0.10095 ± 0.95%	0.15
0.500	0.50129 ± 0.38%	0.06
1.000	1.00375 ± 0.37%	0.018
5.000	5.01543 ± 0.31%	0.006
10.000	10.03161 ± 0.31%	0.003

Table 2b. Accuracy of Ion Intensity Measurement.

Ions	m/e Ratio	Ion-intensity (volts)*	Standard Deviation (%)
H_2O+	18	5.9780	0.98
$(^{15}N^{14}N)+$	29	0.1191	0.31
Ar+	40	0.0782	4.80

*Measured mass peak intensity using constant background signals.

filter and detector units from excessive heat caused by radiation, most experiments are normally confined to cell temperatures <1300°C. For cell temperatures higher than 1300°C, extreme care and close monitoring of the system by the operator are required.

For any computer system, memory is one of the major limitations to the size of the program which can be run. The PDP-11/45 is no exception. For this reason certain requirements have been imposed upon the input data of the QRDMAS and QMS programs. QRDMAS limits the number of data points in a mass scan to a maximum of 2000. Data points in excess of 2000 will be discarded. The total number of scans which can be processed is limited by the capacity of the on-line storage medium (the system disk) of the computing facility and by the QMS program. QMS limits the number of masses which can be processed at a given time (a maximum of 5), and the total number of scans (a maximum of 250) of any QMS input data file.

Currently, the system disk has approximately 6000 blocks of available space for on-line storage. The number of blocks of disk space needed per mass scan by QMS is 24, with a sampling speed of 9 and a sampling (scan) time of 30 seconds.

The total number of blocks, B_t, of disk space required for a vaporization experiment can be computed by

$$B_t = B_s \quad \frac{T_r}{H} \quad \frac{1}{t_R} \tag{19}$$

where B_s is the number of blocks per mass scan, T_r is the temperature range (°C) during which data is acquired, H is the heating rate (°C/sec), and t_R is the rescheduling time (seconds) of the data logging program, QUS. During the vaporization experiment (which requires QUS to log data), the number of blocks of disk space used by QUS plus the available space must be greater than or at least equal to B_t. If no disk space is available for QUS to output data, the data will be lost.

The above limitations must be observed when planning an experiment. Of course, the above requirements may be changed by modifying the existing programs if future expansion is necessary.

IV. APPLICATION: INVESTIGATION OF THE VOLATILE ABUNDANCE OF SUBMARINE BASALTS FROM THE MARIANA ISLAND-ARC AND TROUGH

A. Importance of the Volatile Content in Submarine Basalts

Volatiles from igneous rocks provide important information about chemical and physical properties associated with volcanism at divergent plate margins. Petrogenetic models for the origin and evolution of magma depend critically upon the abundance and character of volatiles in the system (Holloway and Burnham, 1972; Kushiro, 1972; Eggler, 1976). Therefore, knowledge of the absolute and relative abundances of volatiles in different magma types is essential to the understanding of their origin and evolution.

Numerous studies on the volatiles in basalts have been made in an attempt to explain volcanic eruptive behavior (e.g., Anderson, 1975; Naughton et al., 1969; Killingley and Murrow, 1975a,b; Watson, 1976). Attention has been focused upon magmatic source conditions and evolution from studies of readily available products, such as sub-alkalic basalt dredged from the ocean floor. Of particular geochemical and petrologic interest are volatile abundances within Mid-Ocean Ridge Basalts, MORB (Delaney et al., 1978; Muenow et al., 1978).

In contrast to basalts from mid-ocean spreading centers those from island-arc systems represent materials of an entirely different geologic environment where subduction of a lithospheric plate has taken place. It has been proposed

from recent petrologic studies that materials from volcanic arc systems have been contaminated by material from remelting of the subducting crustal plate (Armstrong, 1968, 1971; Ringwood, 1974). Figure 9 shows a schematic diagram of the principal geologic features of a mid-ocean spreading center, a subducting ocean lithosphere (under an island arc), and a spreading center within a marginal basin. Approximate depths and pressures are indicated on the vertical scales. The pressure below sealevel is estimated to be 30 kilobar per 100 kilometer of depth (Ringwood, 1975).

The primary source of magmas in island arcs is believed to contain either slices of a subducted lithosphere and/or the overlying wedge of perididite (Boettler, 1977; Wyllie, 1973; Ringwood, 1974; Garcia, 1978a). The abundance of CO_2 and H_2O in the source during partial remelting of lithosphere material greatly influences the character of the resulting magma (Holloway and Burnham, 1972; Eggler and Rosenbauer, 1978).

Recent studies have also indicated great interest in the origin and evolution of marginal basins (e.g. Dietrich, et al., 1978, Hawkins, 1976, 1977; Meijer, 1976). Attention has been focused on comparing marginal basin lavas with lavas from mid-ocean ridges and island arcs (e.g. Hawkins, 1977; Hart et al., 1972; Gill, 1976; Hawkesworth et al., 1977). In general, marginal basin basalts have a broad composition overlapping with MORB and it does not seem possible at this point to distinguish geochemically between the mar-

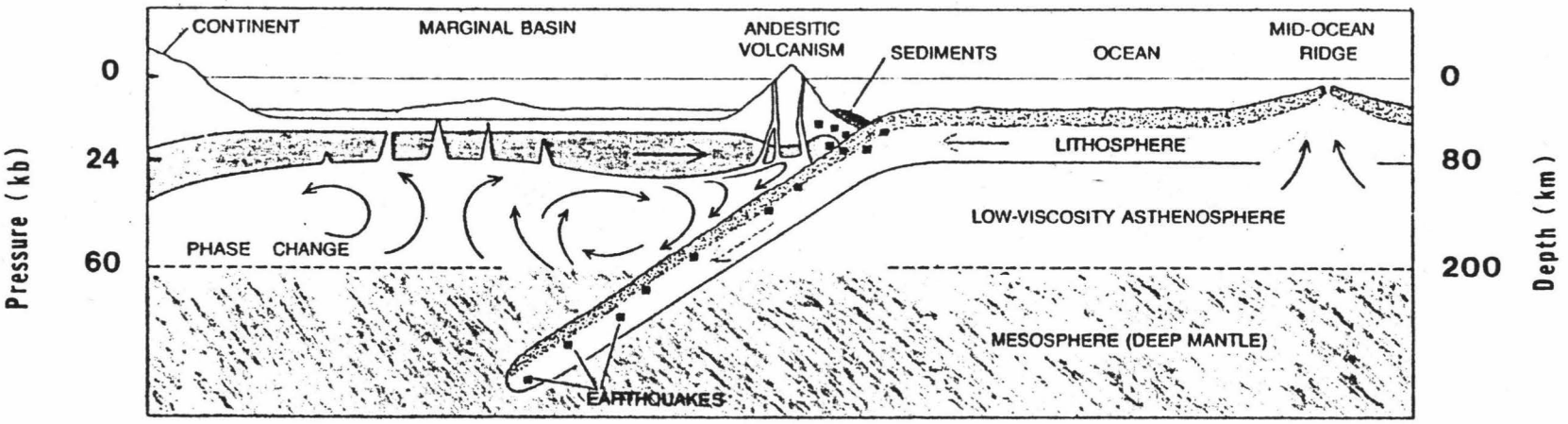

Figure 9. A cross sectional diagram showing the formation and subduction of lithosphere. New lithosphere is created at a mid-ocean ridge. A trench forms where the lithosphere slab descends into the mantle. Secondary convection currents in asthenosphere may form small spreading centers under marginal basins. Arrows in asthenosphere indicate direction of possible convective motion (after Toksoz, 1975).

ginal basins and mid-ocean ridge spreading environments (Hawkins, 1977; Hawkesworth et al., 1977).

B. Sample Description:

The samples studied in this investigation were selected from unaltered submarine pillow basalts and are principally from the Mariana island-arc and interarc basin (Mariana trough). A generalized bathymetric map of the Mariana island-arc and trough is shown in Figure 10. The regions on the map labelled A and T indicate the approximate locations of the arc and trough samples, respectively. The exact locations and descriptions of the samples are given in Table 3a; their depth and chemical compositions (major elements) are given in Table 3b. Basalts from the trough typically contain 40% phenocrysts, 10% vesicle and 50% fine grained ground mass (Meijer, 1976). Samples from the arc contain 15% to 30% phenocrysts, 10% to 30% vesicles and 40 to 70% fine grained ground mass (Garcia, 1978). All the samples studied have spherical vesicles quenched in the glassy portions of the pillow basalt rims and contain phenocrysts of plagioclase.

Unaltered glassy rims of pillow basalts were selected since they are the quench products of volatile rich lavas erupted on the ocean floor (Moore and Fabbi, 1971) and may be expected to contain volatile abundance patterns close to that of their magmatic source (Delaney et al., 1978). That these types of samples contain primordial gases from the

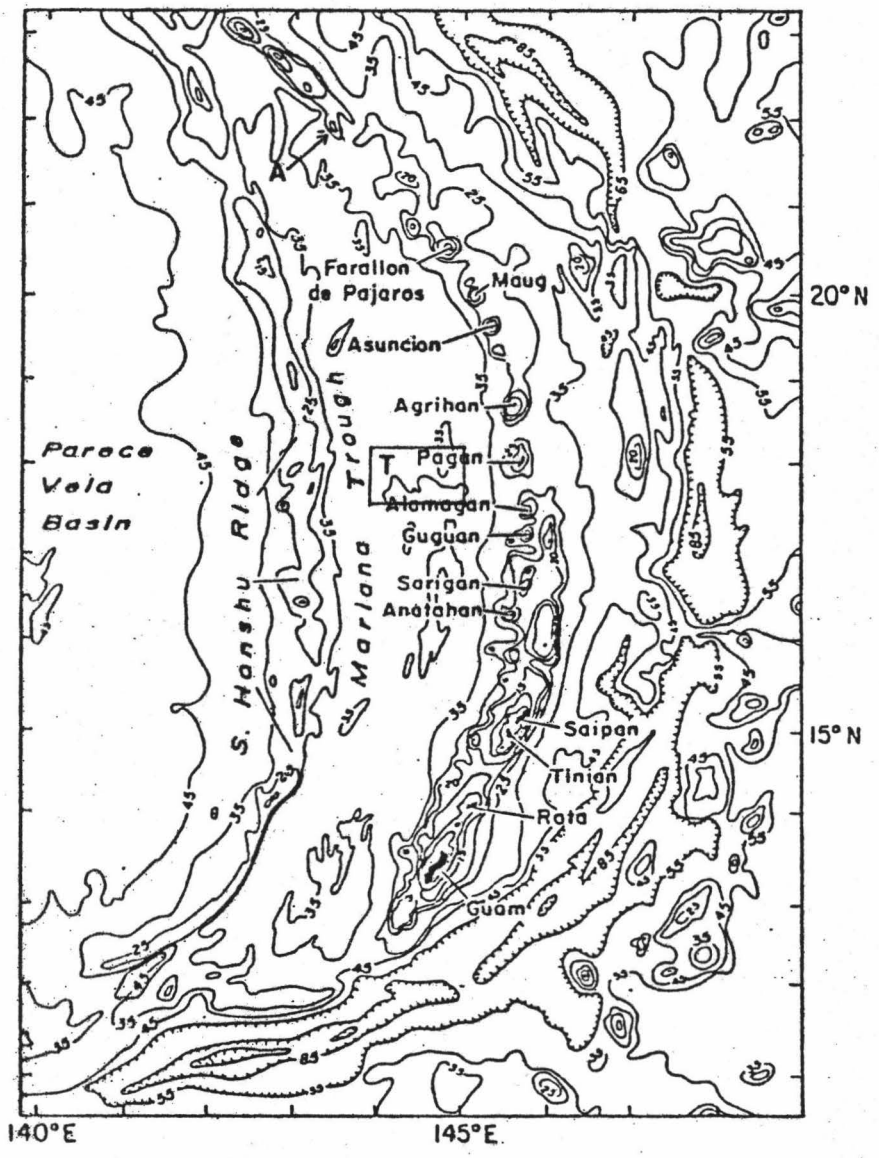

Figure 10. Generalized Bathymatric Map of Marian Island Arc System, and the Mariana Interarc Basin (the Mariana Trough) (after Meijer, 1976).

Table 3a. Sample Localities and Description

Sample No.	Location (lat.)	(long.)	Description
MV1506*	21°55.5'N	143°25.1'E	Andesite, hyalopolitic texture, phenocrysts 30%, ground mass 40%, vesicles 30%; Plagioclase 40%, augite 5%, opaques 1%, remainder is very fine grained ground mass. Not altered.
MV1514*	Same as MV1506		Andesite, hyalopolitic texture, phenocrysts 25%, ground mass 65%, vesicles 10%; Plagioclase 30%, augite 10%, opaques 1%, remainder is very fine grained ground mass. Not altered.
MV15220*	Same as MV1506		Andesite, hyalopolitic texture, phenocrysts 20%, ground mass 55%, vesicles 25%; Plagioclase 30%, augite 10%, opaques 1%, remainder is very fine grained ground mass. Not altered.
MV15227*	Same as MV1506		Basaltic andesite, hyalopolitic texture, phenocrysts 15%, ground mass 70%, vesicles 25%; Plagioclase 10%, olivine 2%, augite 2%, opaques 1%, remainder is very fine grained ground mass. Not altered.

Table 3a. (Continued) Sample Localities and Description

Sample No.	Location (lat.)	(long.)	Description
MV1349*	18°00.1'N	144°43.1'E	Basalt, hyalopolitic texture, phenocrysts 20%, ground mass 80%; Plagioclase 14%, olivine 6%, opaques 5%, remainder is very fine grained ground mass. Not altered.
46D** Series	17°10.1'N	144°50.5'E	Basalt, hyalopolitic texture, phenocrysts 40%, ground mass 50%, vesicles 10%; phenocrysts: plagioclase 20%, augite 5%, olivine 15%, remainder is very fine grained ground mass. Not altered.

* The sample descriptions are hand specimen descriptions made by Garcia (1978); sample locations were provided by Patricia Fryer (Dept. of Geology, Univ. of Hawaii).

** The sample locations and descriptions are taken from Meijer (1976).

Table 3b. Major Elemental Analysis of Selected Arc and Trough Basalts

Sample Depth Type*	MV1506 1170M Arc	MV1514 1170M Arc	MV15220 1170M Arc	46 D1 (3465 to Trough	46 G1 4415M) Trough
S_i0_2	61.05	55.40	56.50	51.25	51.23
T_i0_2	0.91	0.96	1.01	1.60	1.40
$A/_20_3$	15.12	15.94	15.52	16.76	17.80
Fe_20_3	1.99	1.99	1.39	8.63	7.70
Fe 0	6.54	7.58	7.86		
Mg 0	2.09	3.57	2.98	5.95	4.86
Mn 0	0.17	0.17	0.17	0.17	0.15
Ca 0	6.24	9.16	8.12	11.22	11.22
Na_20	3.41	2.67	2.83	3.04	2.86
K_20	1.38	1.06	1.07	0.44	0.56
H_20**	0.85	1.03	2.12	--	--
P_20_5	0.27	0.18	0.22	0.13	0.18

* Analysis of arc samples were done by K. Ramlal, Department of Earth Sciences, University of Manitoba. Data of the trough samples were taken from Meijer (1974).

** Determined by heating sample in a stream of dry oxygen in an induction furnace (temp. 1100°C). H_20 collected on Anhydrone and weighed.

mantle is supported by rare gas isotope studies (Craig and Lupton, 1976).

Plagioclase crystals separated from the glassy rinds of the arc and trough basalts were also studied. The separated plagioclase range from 0.1-1.0 mm in diameter and contain variable amounts of glass-vapor inclusions which can be seen under a binocular microscope. It has been the conclusion of most studies of volatile phase glass-bearing inclusions (contained within phenocrysts of plagioclase and divine) that they have sampled magma at a depth greater than that of eruption onto the sea floor (c.f. Anderson, 1974; Delaney et al., 1978; Roedder, 1965; Watson, 1976; Roedder and Weiblen, 1972, 1973a, 1973b). Textural evidence of these phenocrysts also favor post-entrapment vapor phase development. That is, the inclusions did not trap vapor plus magma. The volatile content of the inclusions can therefore be directly related to the mass of glass in the inclusion (Delaney, 1977).

The 46D-series of samples were provided to this laboratory by J. R. Delaney (Dept. of Oceanography, Univ. of Washington) and are described by Meijer (1974, 1976). The MV-series of samples were obtained from M. O. Garcia (Geology Dept., Univ. of Hawaii) and were dredged by the R/V KANA KEOKI during an IPOD site-survey cruise during 1977. These are described by Garcia et al. (1978).

C. Method of Analysis

1. Sample Preparation:

Samples were prepared according to procedures previously described (Delaney et al., 1978).

Glassy portions of the basalt rims were chipped away from the rock sample and crushed with an agate mortar and pestle. A size fraction of the sample of 0.5 to 1.0 mm diameter was separated and ultrasonically cleaned with distilled water and 0.2N HCl solution (to remove any carbonate which might have formed on fracture surfaces), rewashed with distilled water and dried at approximately 200°C for 1/2 hour with a laboratory heat gun. Glass and phenocrysts were handpicked under a binocular microscope. Glass fragments with alteration of any type were rejected. Considerable care was taken to exclude phenocryst fragments with glass adhering to outer surfaces. Only those free of clinging matrix glass were used for analysis.

2. High Temperature Vaporization of Matrix Glass:

The volatile content and degassing behavior of all the samples were studied with the computer interfaced high temperature/Knudsen cell quadrupole mass spectrometer system described in a previous section of this thesis (Section II).

Glass samples (40-60 mg) were weighed and placed into a prebaked high purity alumina cell liner and heated under a vacuum of ~ 2×10^{-8} torr at a rate of approximately 5°C/min. to 1250°C. Cell liners were prebaked to temperatures ex-

ceeding those of sample-degassing temperatures. During the entire degassing period, the mass spectrometer was operated in a rapid-scan mode with a scan rate of 30 sec/scan from approximately 1 to 100 amu. Mass spectra and cell temperatures were sampled by QUS at a time interval of approximately 2 minutes. The mass spectral data were subsequently processed and analyzed by QRDMAS and QMS, respectively (see Section III of this thesis).

3. High Temperature Vaporization of Phenocrysts:

For degassing plagioclase phenocrysts, the mass spectrometer was operated in a switchable fixed-mass mode. By continuously monitoring a major ion-mass characteristic to any volatile of interest (or several, by periodically switching from mass to mass), it is possible to observe rapid changes in the ion intensity as sharp spikes on a fast-response, strip-chart pen recorder and oscilloscope. For minerals containing volatile-bearing inclusions, the ion-current signal spikes appear at high temperature and correspond to vapor release from one or a number of ruptured inclusions. This phenomenon has previously been observed (Killingley and Muenow, 1974) and is believed to be the result of cracking caused by stresses due to temperature gradients within the plagioclase grains (Killingley and Muenow, 1975b). The detection limit of the instrument for spike release of the volatiles CO_2, H_2O, and SO_2 is 5×10^{-13} mole per spike. Each sample was heated at 10°C/min.

to 1300°C and monitored for its vapor burst-release behavior.

D. Results and Discussion

The mass pyrograms of the volatiles released from matrix glass samples were plotted by the computer. A typical mass pyrogram showing the release behavior of the three principle volatiles H_2O, CO_2 and SO_2 is shown in Figure 11. The mass pyrogram provides a "picture" of sample volatility up to 1250°C. Ion-intensities, plotted along the verticle axis, are proportional to the partial pressures of each of the volatiles and the area under each curve is proportional to the total amount of each volatile released over the temperature (or time) interval. Each curve contains approximately 200 data points representing a vaporization period of approximately 4 hours. Ion-intensities for all mass peaks below temperatures of approximately 500°C are at background levels. A mass pyrogram for a background ("blank") run is shown in Figure 12.

Most of the glass samples studied were taken from the glassy rims of pillow basalts. Typical weight losses range from 1.24 to 2.54 wt-% with an exception of 4.44 wt-% for the pillow interior glass sample (46D I1). Interior glass of the pillows are sometimes partly crystalline and are subject to alteration through seawater contamination. A mass pyrogram of 46D I1 interior glass (Figure 13) shows a broad water release between 200°C and 500°C which is indicative of

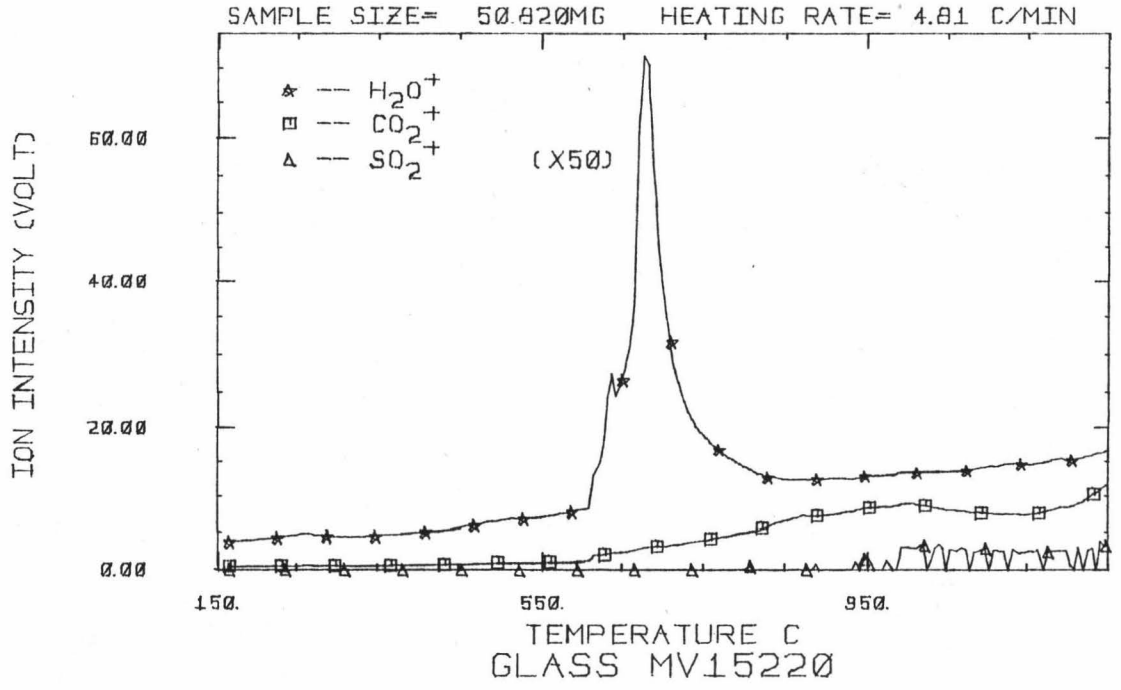

Figure 11. Mass Pyrogram Showing the Release of H_2O, CO_2 and SO_2 from MV15220 Glass.

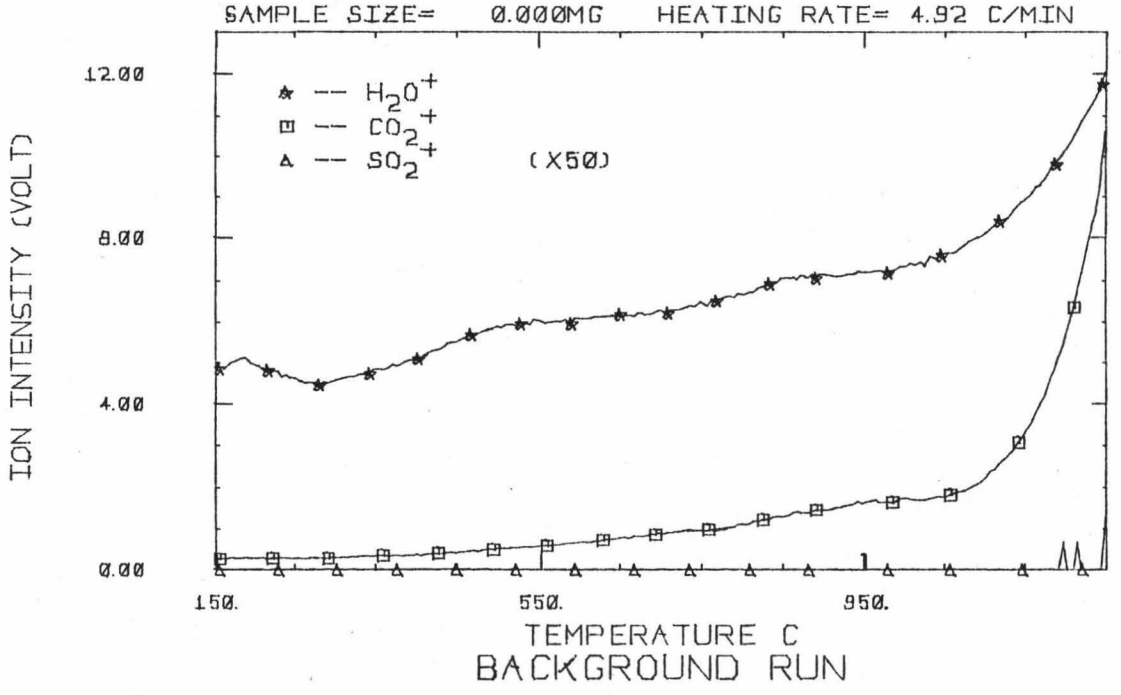

Figure 12. Mass Pyrogram Showing the "Release" of H_2O, CO_2 and SO_2 During a "Blank" Run.

nearly all basalt samples altered by reaction with seawater during slow cooling of the pillow interior. For comparison, Figure 14 shows the mass pyrogram for an unaltered glass rim of 46D I1.

For the quantitative determination of volatiles released, the areas under each curve are used. Here, the ion-intensities of all mass peaks must also be corrected for background and other (instrumental sensitivity, isotopic abundance and fragmentations) effects. From the areas under the pyrogram curves, the heating rate, the instrumental sensitivity and calibration constants, and the total sample weight loss the volatile content of any sample can be determined. This is accomplished by use of the equation,

$$\text{Wt. \% } X_i = \frac{K_i A_i}{\sum_{i=1}^{n} K_i A_i} \cdot \text{\% wt. lost} \qquad (20)$$

where X_i is the volatile in question, K is the instrumental sensitivity constant of species i, A_i is the temperature-dependent area of species i (given in Section II-B), and the summation index n is the total number of different volatiles released from the sample.

Mass pyrograms showing release of volatiles (H_2O, CO_2, SO_2, F and Cl) typical to matrix glasses of arc (MV15220) and trough (46D A1) environments are shown in Figures 15 to 18 (mass pyrograms of all the samples studied are presented in Appendix E). Only data above 500°C are shown

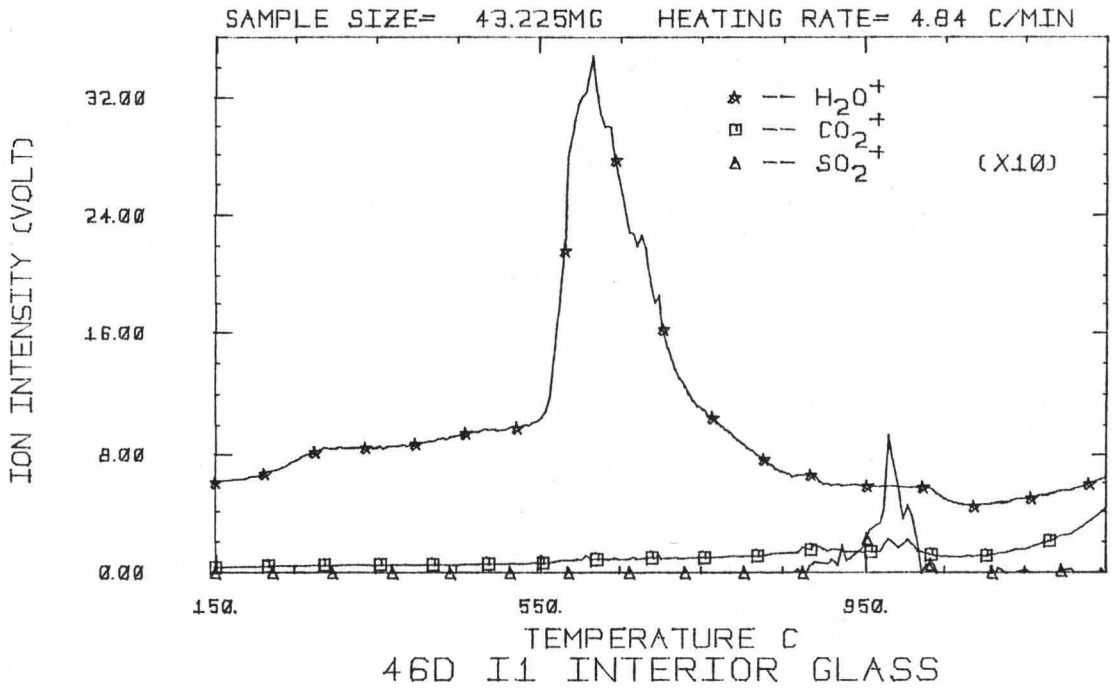

Figure 13. Mass Pyrogram Showing the Release of H_2O, CO_2 and SO_2 from 46D I1 Interior (Altered) Glass.

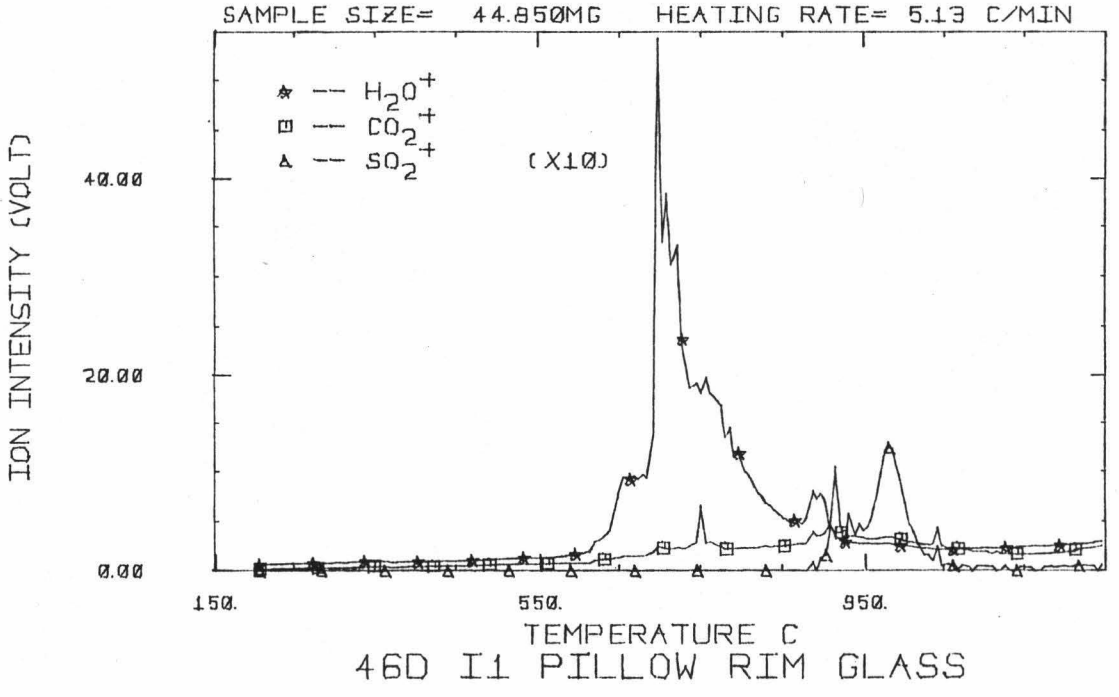

Figure 14. Mass Pyrogram Showing the Release of H_2O, CO_2 and SO_2 from 46D I1 Unaltered Glassy Rim

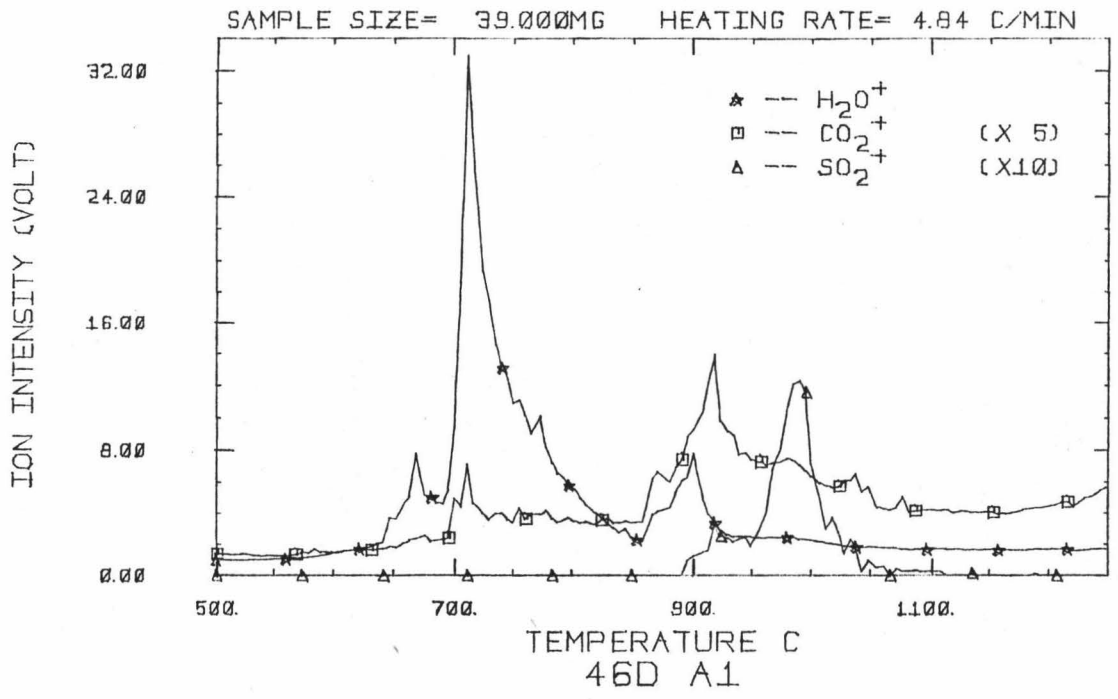

Figure 15. Mass Pyrogram Showing the Release of H_2O, CO_2 and SO_2 from 46D Al Glass.

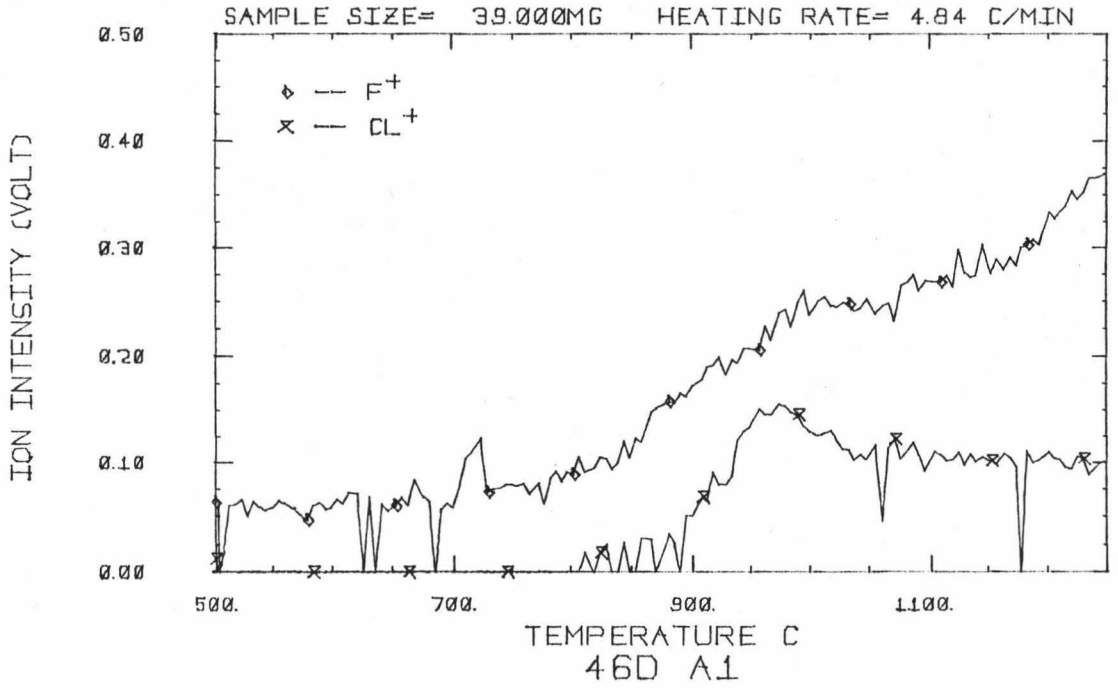

Figure 16. Mass Pyrogram Showing the Release of F and Cl from 46D Al Glass.

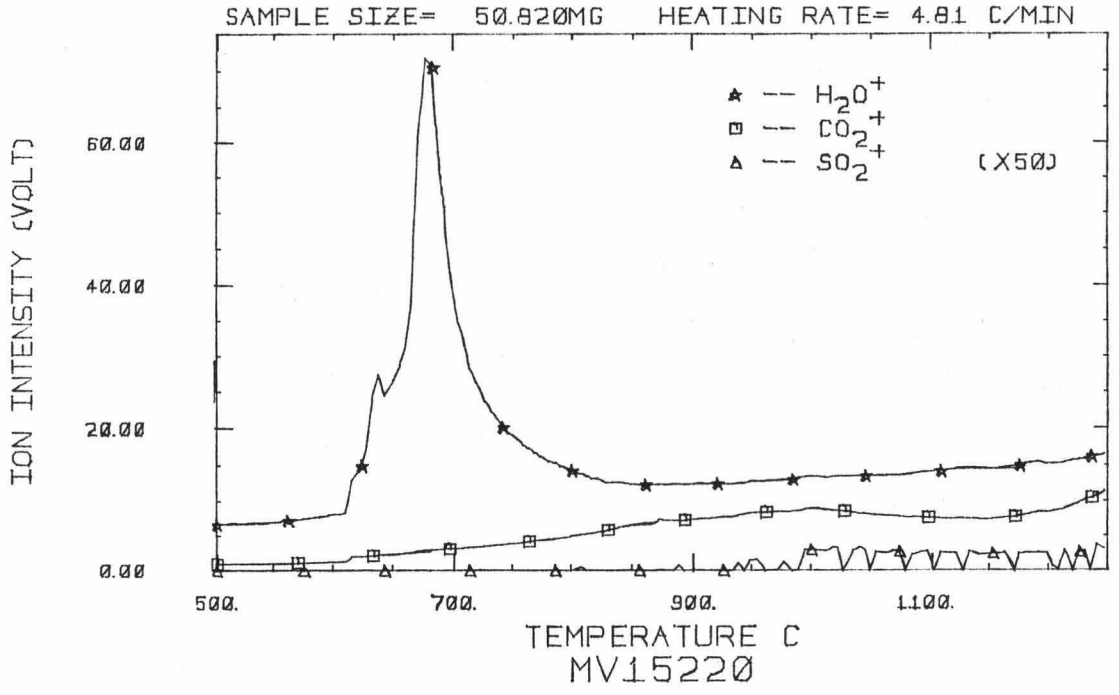

Figure 17. Mass Pyrogram Showing the Release of H_2O, CO_2 and SO_2 from MV15220 Glass.

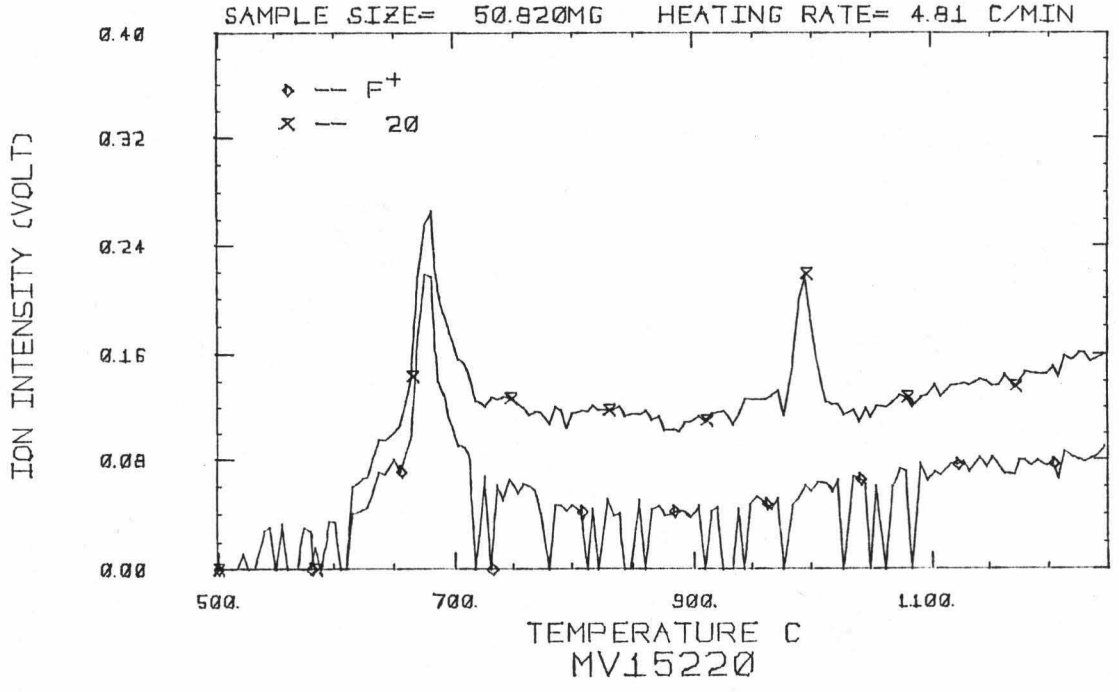

Figure 18. Mass Pyrogram Showing the Release of F and Cl from MV15220 Glass.

since below this temperature there was no degassing activity from the samples. The major water release occurs between 600°C to 925°C and 600°C-800°C for trough and arc samples, respectively. For both types of samples all detectable water is removed by 970°C. The CO_2 release patterns for both types of samples show large differences but are remarkably consistent among samples of the two groups. Most of the CO_2 is released between 700°C to 1050°C. The release of SO_2 corresponds to melting of the samples and only minor amounts are seen to be released from the arc samples. Release patterns of fluorine and chlorine are similar for both the arc and trough samples. The release of F seems to be closely related to the release of H_2O. In some cases this is less obvious. The release of Cl seems to be associated with the initial release of Na and K and corresponds to glass decomposition temperatures beginning at approximately 950°C (for both the arc and trough samples). After the initial release of Na and K at 950°C, their corresponding intensities continue to increase rapidly with temperature until cell temperatures of about 1200°C are reached. From 1000° to 1050°C alkali release decreases, then remains fairly constant to 1150°C, and finally rapidly increases again with increasing temperature and silicate decomposition (no quantitative data for Na and K are given since decomposition at maximum cell temperatures of 1300°C is not complete). Alkali release is shown in Figure 19.

The apparent concurrent release of F with H_2O may be

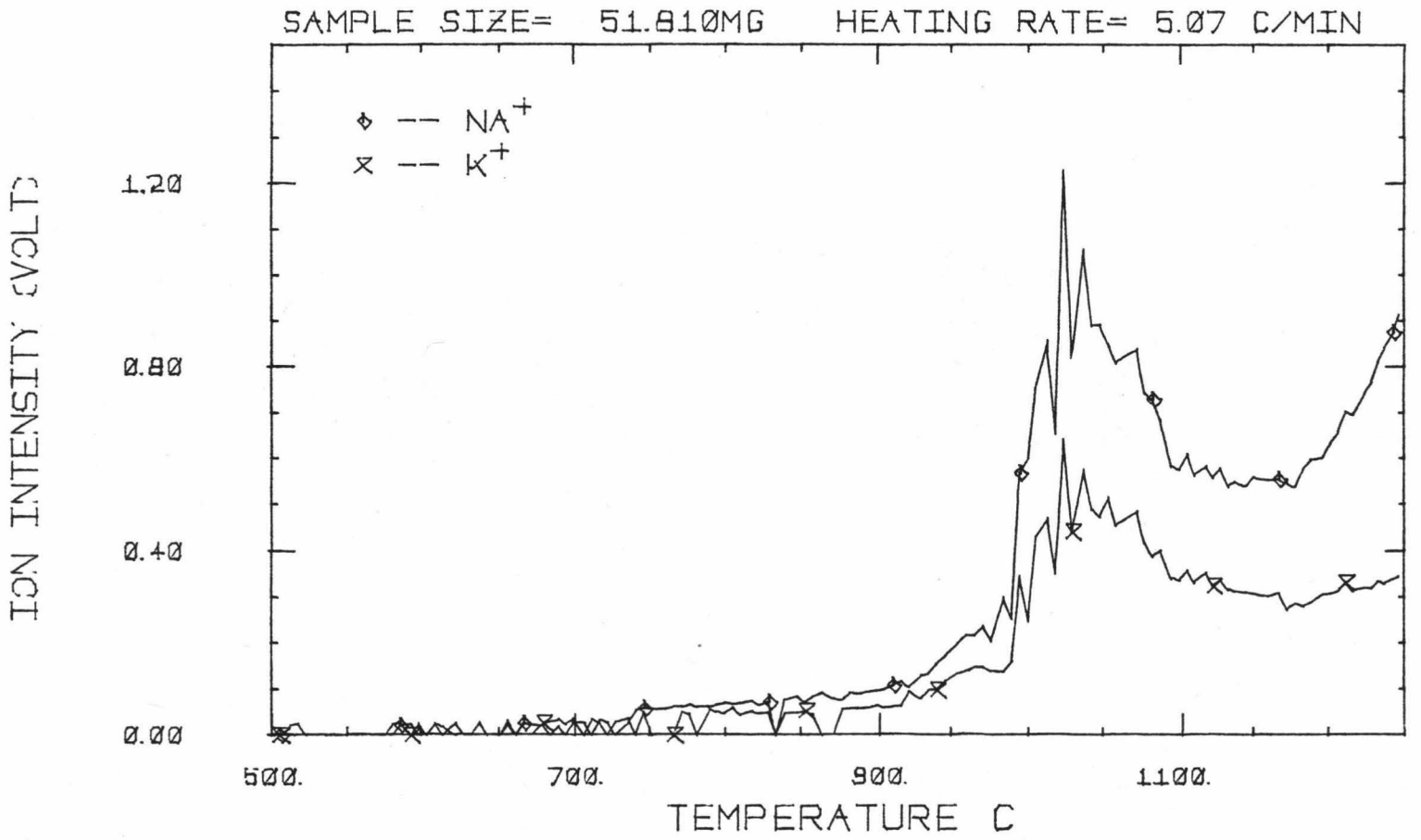

Figure 19. A Typical Mass Pyrogram Showing the Release of Na and K from Pillow Rim Glass.

due to the partial replacement of OH^- ions with F^- ions within the silicate. The similarity in their sizes (1.40Å for OH^- and 1.36Å for F^-) (Huheey, 1972) and charge densities support this view. This close association with water-release, however, is not observed for chlorine, even though the chemistry Cl^- and F^- are quite similar.

Release of Cl with Na and K between 950° to 1150°C may suggest that these three elements exist in some common compound (e.g. KCl and NaCl) which dissociates into its atomic components during melting of the glasses. This phenomena is also observed for F, but to a smaller extent.

The release patterns of H_2O, CO_2 and SO_2 distinctly distinguish samples from the trough (Figure 15) and arc (Figure 17) environments. The water release envelope is confined to a narrow temperature range for the arc samples but for the trough samples it extends over a wider temperature range with more than one water release peak. Mass pyrograms showing release of volatiles H_2O, CO_2 and SO_2 from samples typical to mid-ocean ridge spreading centers (MORB) and Hawaii (plume oceanic island, referred to as POI, an intraplate mantle-plume derived oceanic island) are shown in Figures 20 and 21. The mass pyrograms of Hawaii basalts (Figure 21) and the Mariana arc (Figure 17) both show a single H_2O-release envelope, however, the Hawaii mass pyrograms show a shoulder on the low temperature end of the H_2O-release envelope. The corresponding CO_2-release show rather poorly defined release envelopes (broad and low density). In contrast, mass pyro-

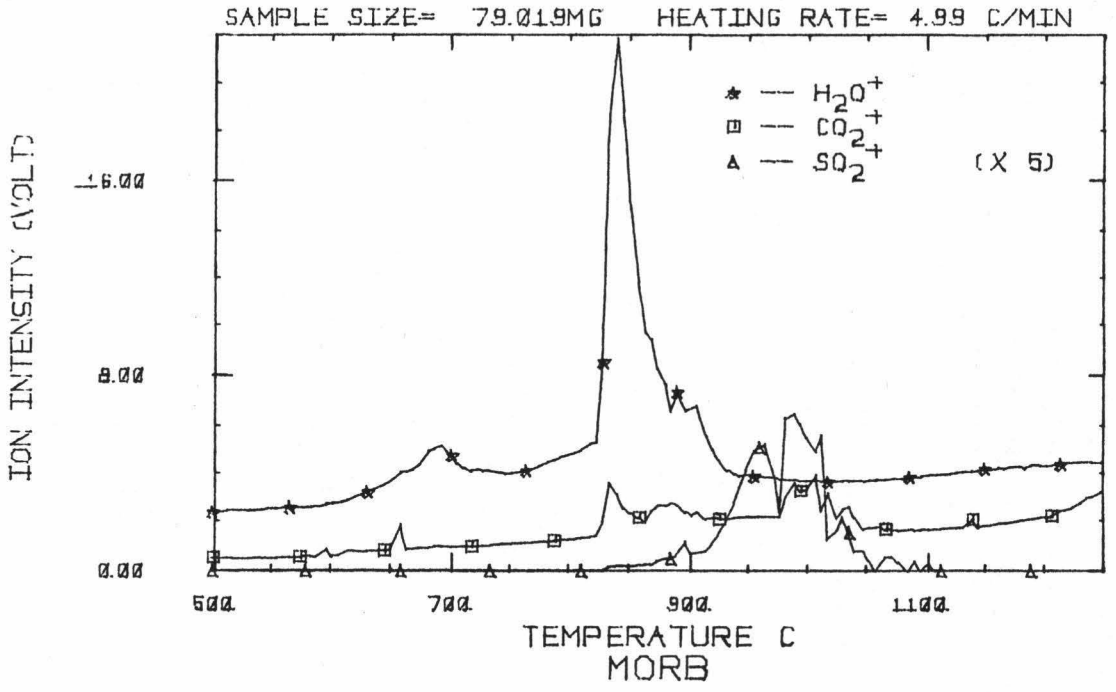

Figure 20. Typical Mass Pyrogram Showing the Release of H_2O, CO_2 and SO_2 from Mid-Ocean Ridge Glass.

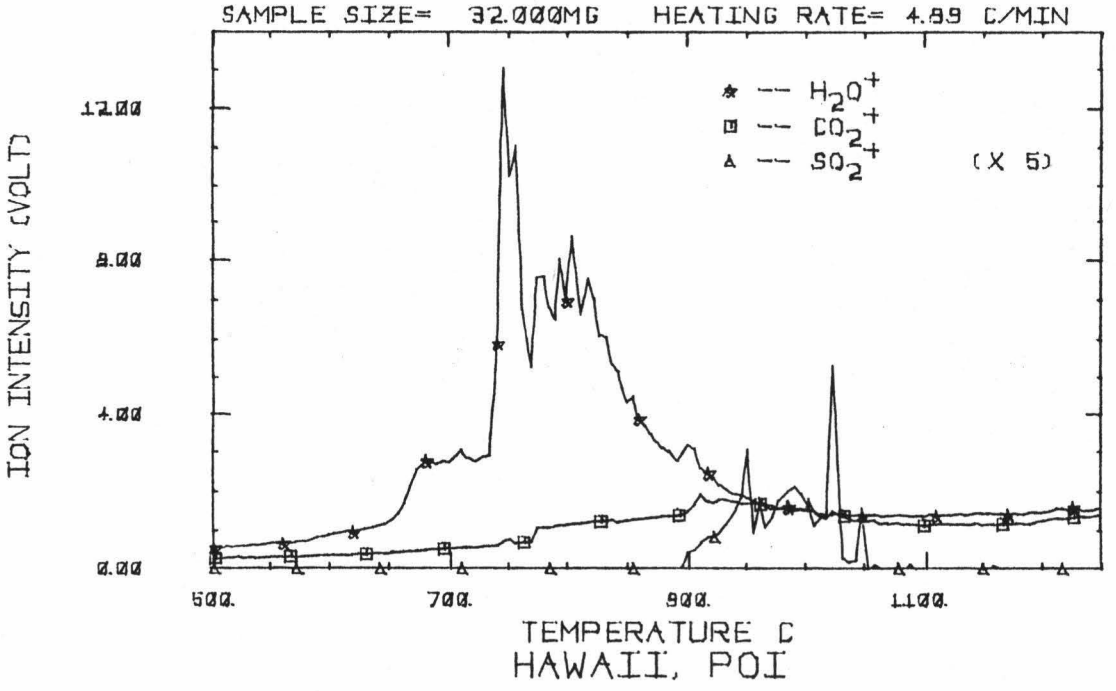

Figure 21. Typical Mass Pyrogram Showing the Release of H_2O, CO_2 and SO_2 from Hawaii Submarine Basalt Glass.

grams for samples from MORB (Figure 20) and the Mariana trough (Figure 15) show bimodal releases of H_2O and CO_2 and this may indicate that H_2O and CO_2 exist in two different types of molecular "environments" within the silicate. Primary investigations along this direction has been done by Graham (1978).

The release behavior of SO_2 (900°-1100°C) is similar for all sample types except those for the Mariana arc which show only extremely small amounts released.

Release patterns for the other volatiles F, Cl, Na and K from the MAR, Hawaii, Mariana arc and Mariana trough samples are all quite similar with only minor differences.

The number of analyses made for each of the glasses ranges from 2 to 4 depending on sample availability. Differences in mass pyrograms for replicate samples were minor. Weight losses are essentially due to release of the volatile H_2O, CO_2, SO_2, Cl, F, Na, and K. The volatile data (excluding Na and K) are summarized in Table 4. Average values obtained for basalts from the Mid-Atlantic Ridge (MAR) and Hawaii (Delaney et al., 1978; Graham, 1978) are included for comparison. Glass rims of both arc and trough samples contain approximately 1.0 wt-% H_2O and 0.25 to 0.26 wt-% CO_2. Sulfur content in the arc samples average 0.006 wt-% and is considerably higher in the trough samples at 0.082 wt-%. Generally, F and Cl contents are higher in the arc samples compared to those in the trough.

Table 4. Volatile Abundance in Glassy Rims of Marianas Arc and Trough Pillow Basalts

Sample	H_2O (wt %)	CO_2 (wt %)	S (wt %)	F (wt %)	Cl (wt %)	CO_2/H_2O (mole ratio)	Location
MV15247	1.034	0.253	0.003	0.024	0.046	0.094	Arc
MV15220	0.898	0.433	0.010	0.029	0.049	0.197	Arc
MV1514	0.837	0.128	0.008	0.025	0.101	0.042	Arc
MV1506	1.494	0.165	0.003	0.332	0.232	0.045	Arc
Ave.	1.066	0.245	0.006	0.103	0.107	0.095	
46DI1	1.000	0.410	0.083	0.028	0.017	0.168	Trough
46DG1	1.220	0.224	0.058	0.068	0.084	0.047	Trough
46DC1	1.263	0.202	0.075	0.021	0.024	0.065	Trough
46DA1	0.711	0.224	0.086	0.019	0.030	0.129	Trough
MV1349	0.898	0.268	0.108	0.015	0.012	0.122	Trough
46DI1-I[a]	3.280	0.126	0.112	0.041	0.010	0.058	Trough
Ave.	1.018	0.249	0.082	0.032	0.033	0.106	
MAR (Ave.)*	0.210	0.132	0.117	0.023	0.006	0.27	
Hawaii (Ave.)**	0.621	0.095	0.099	0.045	0.019	0.06	

Precision: ±10%

a Interior glass of 46DI1 not used in average calculation.

* Average values of 28 mass spectrometric analyses on 9 unaltered pillow basalt samples dredged from the interior rim valley of the Mid-Atlantic Ridge between 25-30°N latitude, including the FAMOUS area and Kolbiensey Ridge (Delaney et al., 1978).

** Average values of 18 mass spectrometric analyses of 5 fresh tholeiitic basalts dredged (2960-5000 m) from east rift, Kilauea Volcano, Hawaii (Graham, 1978).

Plagioclase samples show no significant degassing behavior below 1000°C. At approximately 1020°C, the mass peaks corresponding to H_2O, CO_2 and SO_2 begin to spike, indicating burst-release of these volatiles. Spiking is most vigorous in the temperature range 1030°-1120°C. No SO_2 spikes were observed from the arc plagioclase. Figure 22 shows "simplified" mass pyrograms showing the release behavior of H_2O, CO_2 and SO_2 constructed from ion-intensities obtained by continuously monitoring either one mass per degassing experiment or several by periodically switching from mass to mass on a fast-response strip-chart recorder. The two methods of recording volatile spikes yield similar results on identical samples.

The concentrations of the volatiles H_2O, CO_2 and SO_2 within the inclusions are difficult to establish because it is presently not possible to identify the number and size of inclusions per spike or to accurately determine the mass of glass inclusions being analyzed in the mass spectrometer. However, an estimate can be made from the measured size distributions of H_2O, CO_2 and SO_2 spikes. By switching between masses 18(H_2O^+), 44(CO_2^+) and 64(SO_2^+) and measuring the corresponding spike intensities it is possible to establish a size distribution of spikes for these volatiles. Since spike intensities are proportional to the total amounts of the corresponding gases released their ratio will approximate the average molar ratio of the volatiles. The CO_2/H_2O mole ratio is calculated from the ratio of the sum of the

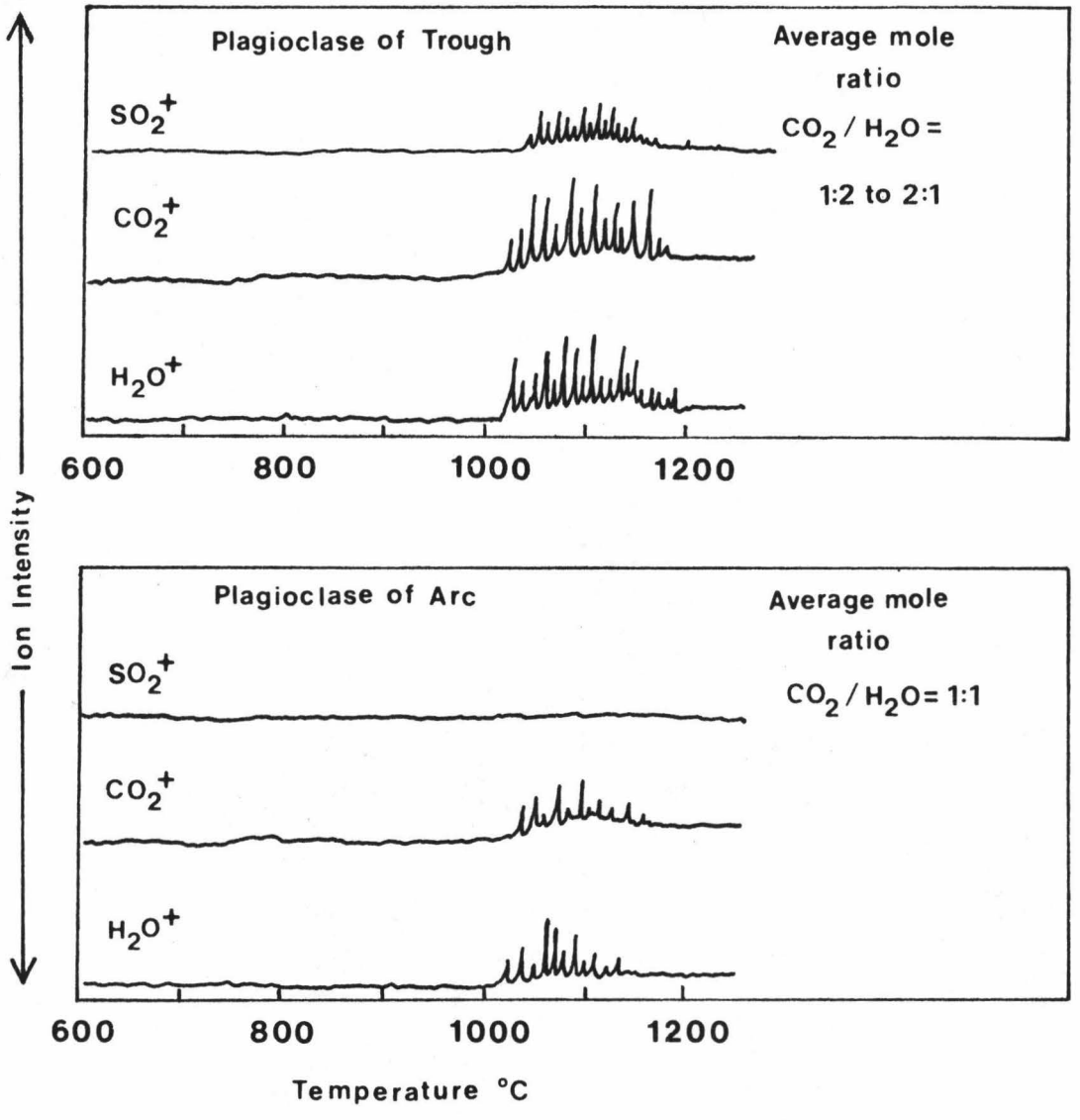

Figure 22. Schematic Diagram of H_20, $C0_2$ and $S0_2$ Burst-Release from Glass-Vapor Inclusions in the Plagioclase Phenocrysts from the Trough (top) and Arc (bottom) Samples.

CO_2 spikes and H_2O spikes and corrected for the instrumental sensitivity constants and fragmentation effects. The average CO_2/H_2O mole ratio obtained ranges from 1/2 to 2/1 for the trough plagioclase and to be approximately 1/1 for the arc plagioclase. For the trough samples the molar amount of SO_2 is comparable to the amounts of CO_2 and H_2O. However, virtually no SO_2 is released from the arc plagioclases; this compares with only minor amounts of SO_2 observed in the corresponding matrix glasses.

There were two and six degassing experiments done with plagioclase separated from the arc and trough samples, respectively. Sample size ranged from 37 mg to 90 mg. One degassing experiment was done with plagioclase separated from the interior portion of a pillow basalt from the trough (46DI1). The H_2O, CO_2 and SO_2 spike distribution patterns recorded from this sample showed no significant difference from those of plagioclase taken from the pillow rim.

Results obtained from this study indicate that samples from the Mariana arc and trough contain substantially more H_2O and CO_2 than samples from MAR and Hawaii. Glass-vapor inclusions within plagioclase phenocrysts also indicate the presence of water. This is in marked contrast to results of similar studies made on plagioclase and olivine phenocrysts from Hawaii and MAR which show no release of water. These results support models for the production of island arc magmas from a subducted slab of oceanic lithosphere, rather than from the overlaying mantle wedge which require high

volatile content (5-15 wt-%) to produce island arc magma (Garcia et al., 1978). The trough samples, although nearly identical in non-volatile composition to mid-ocean ridge rocks, have much higher H_2O, CO_2 and lower S content. Either near surface addition of volatile has enriched the magmas or H_2O must be an important component in the generation and evolution of bac-arc basin lavas (Garcia, 1978b).

The data from these studies also point out the potentially important correlation among the chlorine and water concentrations for any given sample. Sigvaldason et al. (1976) have pointed out that, "arguments involving the origin of excess volatiles lead to the assumption that the H_2O/Cl-ratio in the magmatic gas phase may be the same as that of ocean water and sediments". On this basis, measured Cl values have been used to assign H_2O contents of basaltic magma in Iceland and these are in agreement with values assumed by other independent methods. Using the H_2O/Cl-ratio in seawater plus sediments (H_2O = 35 Cl, wt-%) and measured chlorine contents from subaerial and submarine basalts Sigvaldason et al. (1976) obtain the values of 0.3 - 0.6 wt-% H_2O for low-K tholeiites and 0.9 - 1.2% H_2O for high-K tholeiites. The H_2O and Cl data from the present studies (and others made in this laboratory) are summarized in Table 5 and show a similar striking correlation of H_2O/Cl-values among the seawater plus sediment value and those for glasses from spreading centers, the Mariana Trough (a back-arc spreading center) and Hawaii (a mantle-plume-

Table 5. Variation Among Water and Chlorine Contents for Pillow Basalt Glasses.

Geologic Environment	Wt-% H_2O	Wt-% Cl	Wt-% H_2O/Cl
Mariana Arc	1.006	0.107	9.4
Mariana Trough	1.020	0.033	31.0
MORB[a]	0.180	0.006	30.1
Hawaii	0.621	0.019	32.7

[a] Average value of MAR, Juan DeFuca Ridge, Paul Revere Ridge, Gulf of California, and FAMOUS Samples.

derived ocean island). The notable exception is the value (H_2O/Cl = 9.4) for the Mariana Arc (derived in part from subducted ocean lithosphere?). A similarly low value has been reported by Anderson (1974) for Mt. Shasta andesites. These data demonstrate that while chlorine is both very soluble in magma and is perhaps easily fluxed out of magma by water during effervesence (Unni and Schilling, 1978), it is not necessarily a key indicator of total volatile content (Anderson, 1974), particularly for water. Correlation among water and chlorine in magma might be expected to be clarified by future studies on the Cl-content of glass inclusions within plagioclase and olivine phenocrysts from glassy basalts.

V. SUMMARY

A. The Automatic Data Acquisition System

An automatic data acquisition system for a high temperature quadrupole mass spectrometer has been designed and implemented as stated in the objectives of this research. A heating control circuit was developed which allows the accurate and precise heating of the high temperature vaporization unit required for quantitative extraction of volatiles from igneous rocks. The data acquisition system has been shown to accurately and precisely sample all the mass spectrometer output signals. The data acquisition system is used routinely for the acquisition and reduction of large quantities of data (150 to 250 mass scans per experiment). The system makes the data available quickly (15 to 20 minutes after each experiment) for examination and releases the operator from 4 to 5 hours of painstaking effort. In contrast, the manual mode of operation typically allows the operator to collect only 10 to 20 mass spectra per experiment, requires several hours for data reduction, and usually several identical experiments are required to obtain all important data.

B. Application

Glasses selected from the rims of pillow basalts dredged from the Mariana island-arc and interarc basin were studied using the automated data acquisition system. Mass

pyrograms showing the release of volatiles from these samples were obtained and compared with those from samples from other geologic environments. The mass pyrograms provide a quantitative "picture" of sample volatility and also provide important information on the relationships between the various volatiles within each sample. The mass pyrograms allow one to clearly distinguish among samples from different geologic environments and show the effects of alteration of samples through seawater contamination. The abundance of the volatiles H_2O, CO_2, SO_2, F and Cl in matrix glasses and phenocrysts have been obtained. The results of this study demonstrate the power of the automated high temperature mass spectrometer system to provide important data for the characterization of the volatiles in samples of geochemical interest and ultimately to provide clues to the origin of volatiles and their evolution from within the earth.

APPENDIX A

Mass Pyrograms

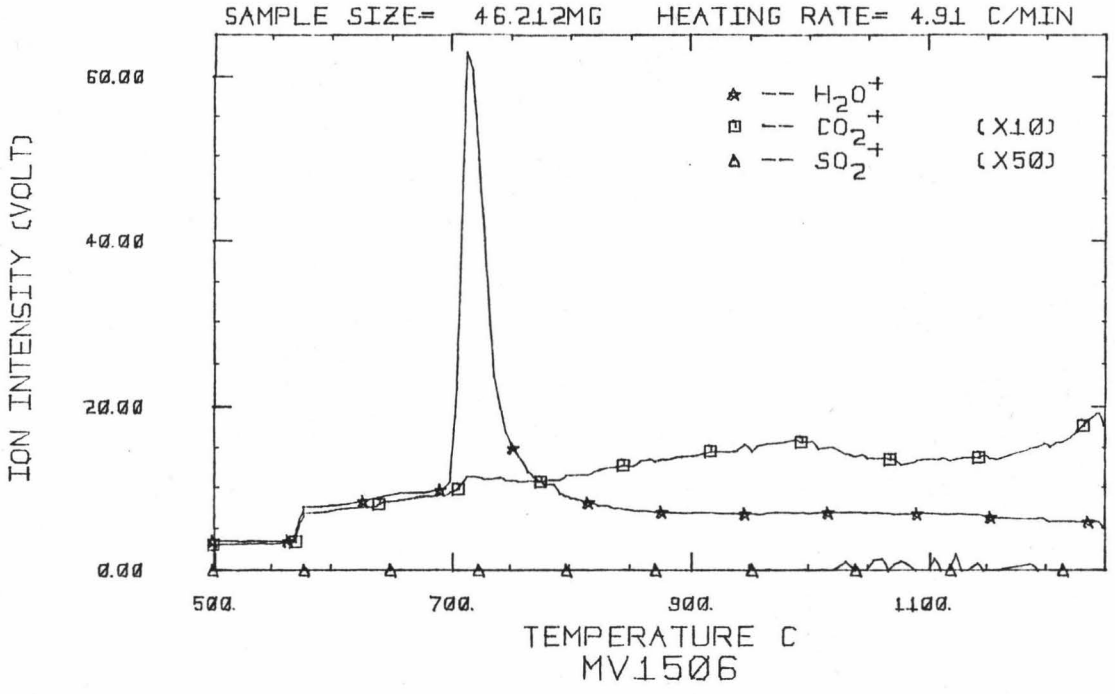

Figure 23. Mass Pyrogram Showing the Release of H_2O, CO_2 and SO_2 from MV1506 Glass.

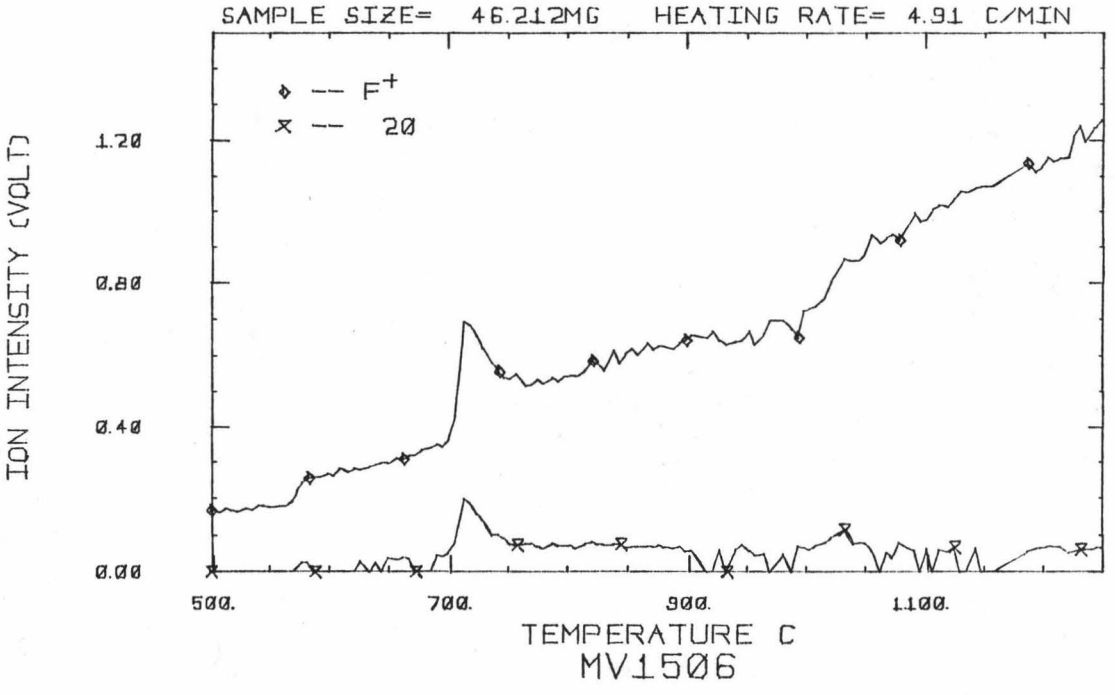

Figure 24. Mass Pyrogram Showing the Release of F and Cl from MV1506 Glass.

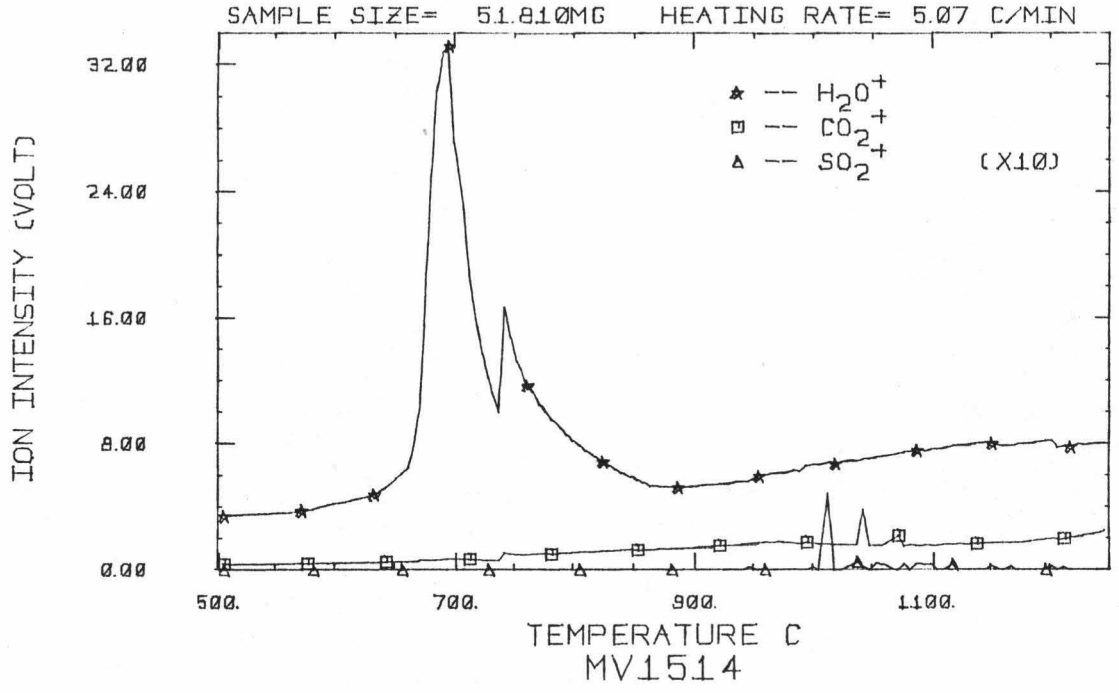

Figure 25. Mass Pyrogram Showing the Release of H_2O, CO_2 and SO_2 from MV1514 Glass.

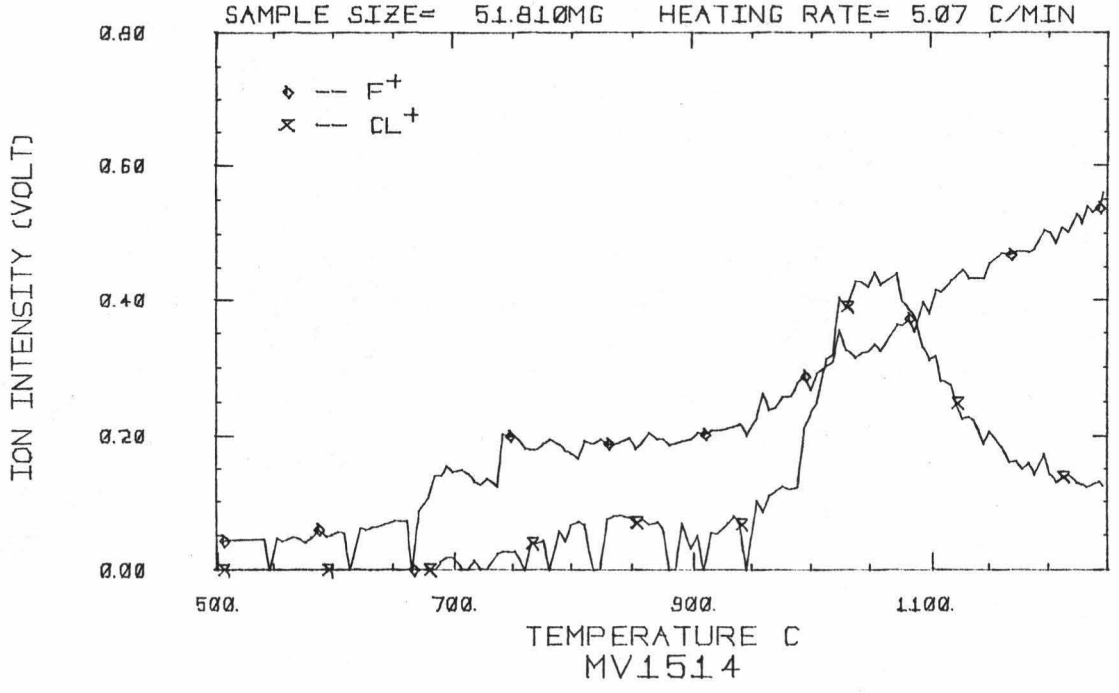

Figure 26. Mass Pyrogram Showing the Release of F and Cl from MV1514 Glass.

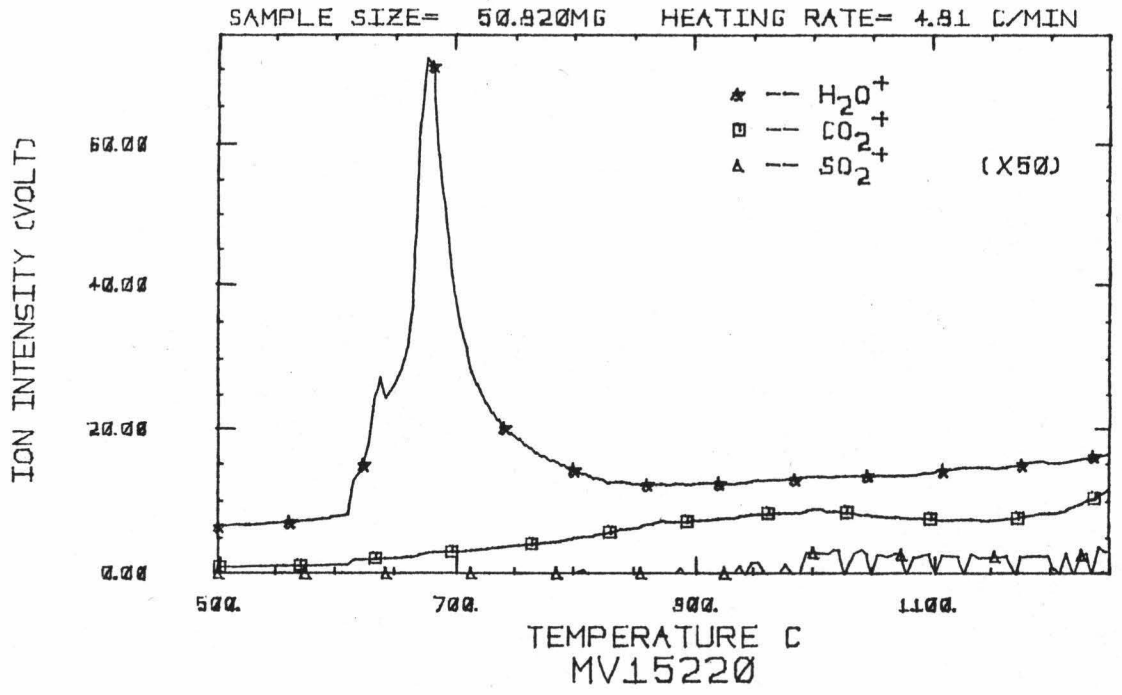

Figure 27. Mass Pyrogram Showing the Release of H_2O, CO_2 and SO_2 from MV15220 Glass.

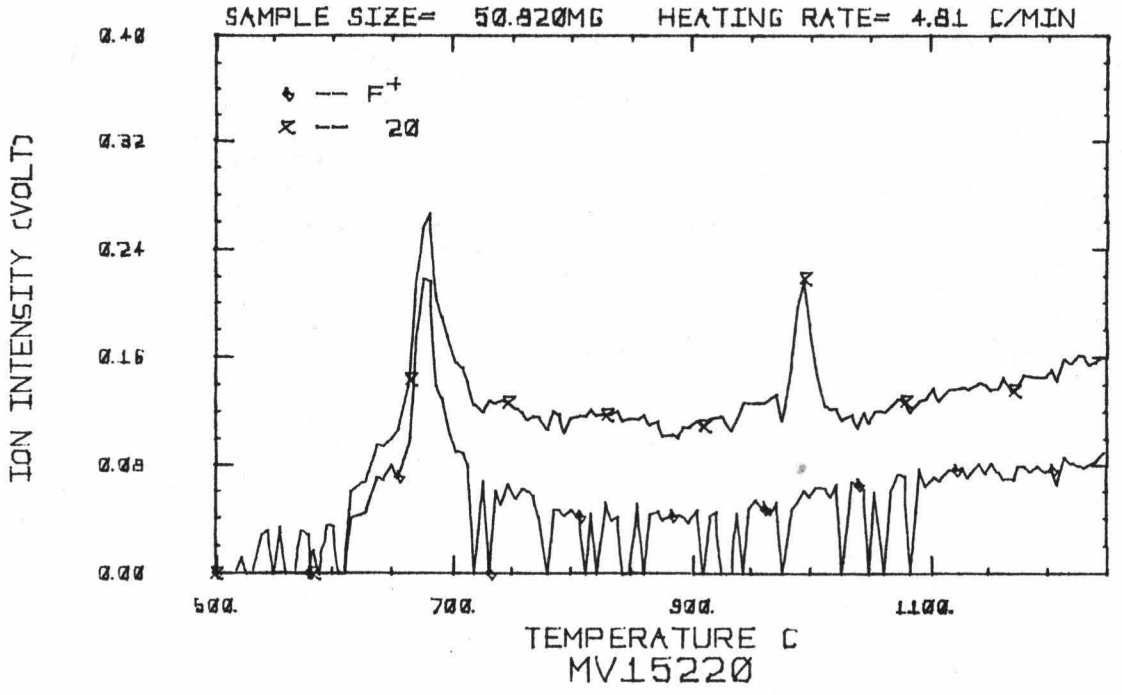

Figure 28. Mass Pyrogram Showing the Release of F and Cl from MV15220 Glass.

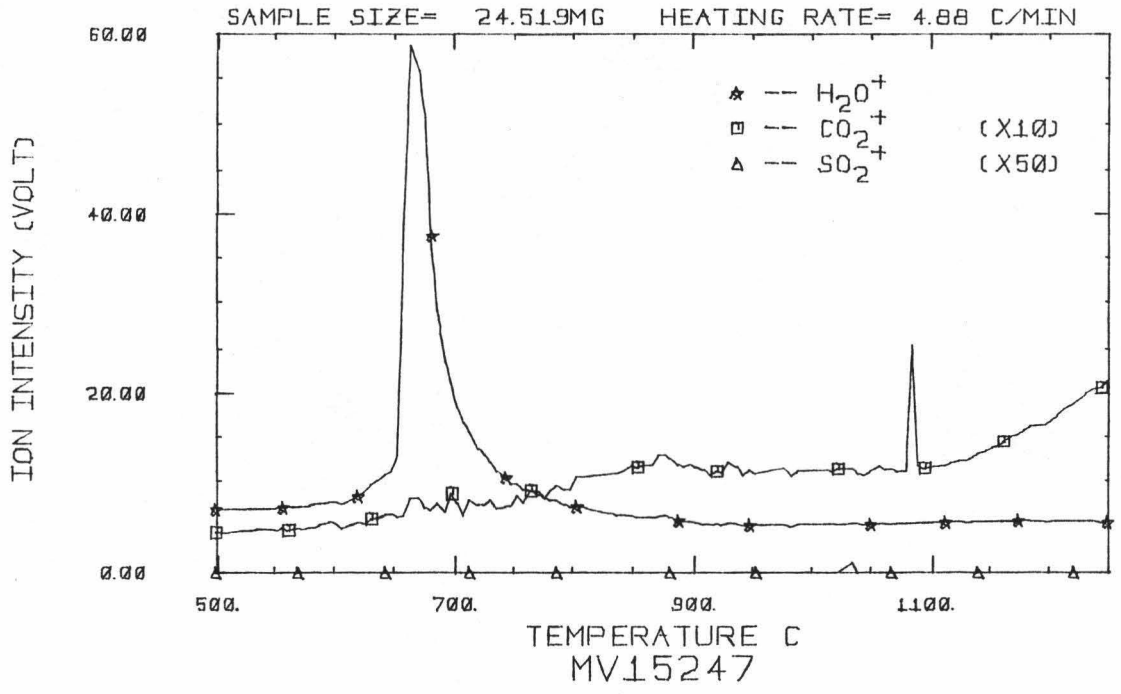

Figure 29. Mass Pyrogram Showing the Release of H_2O, CO_2 and SO_2 from MV15247 Glass.

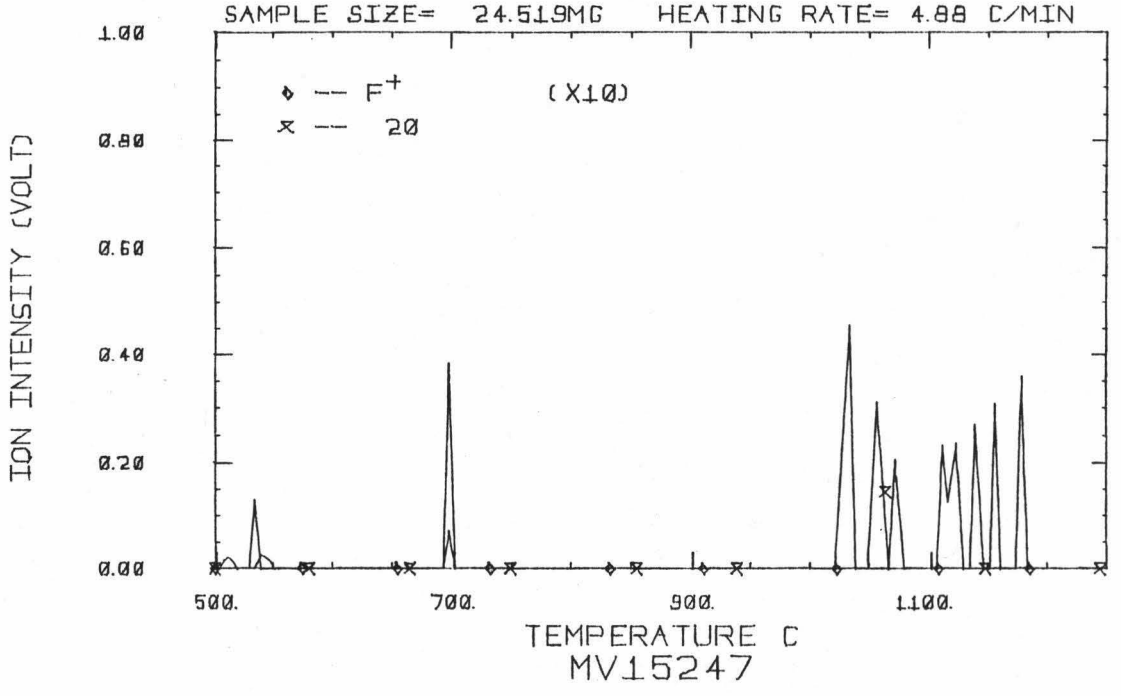

Figure 30. Mass Pyrogram Showing the Release of F and Cl from MV15247 Glass.

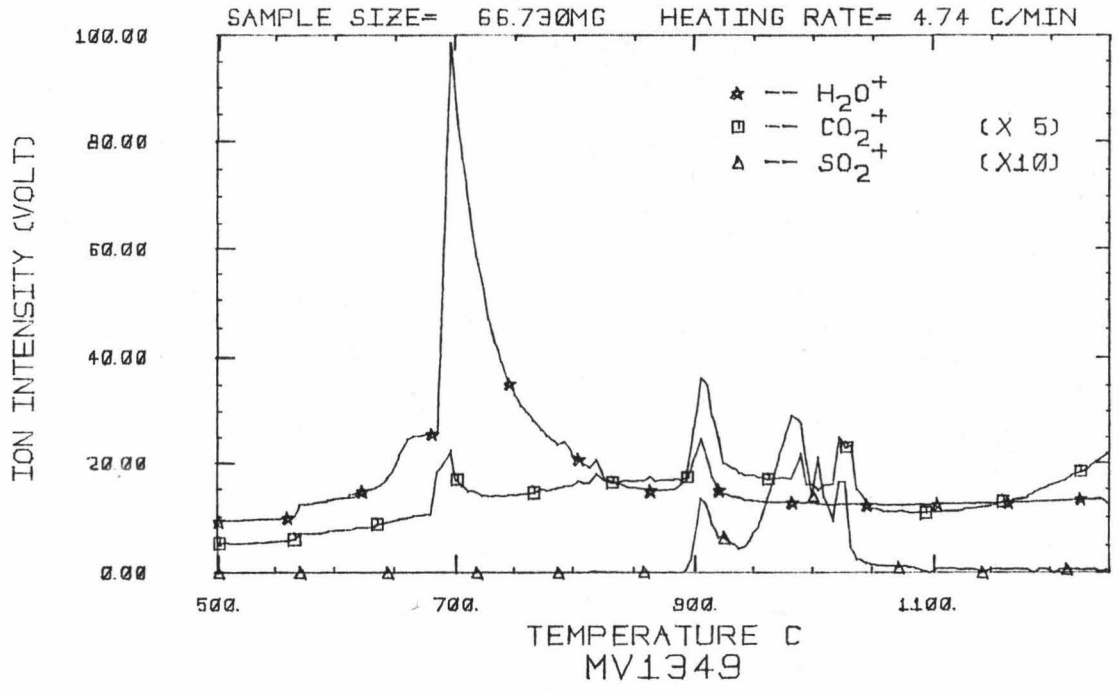

Figure 31. Mass Pyrogram Showing the Release of H_2O, CO_2 and SO_2 from MV1349 Glass.

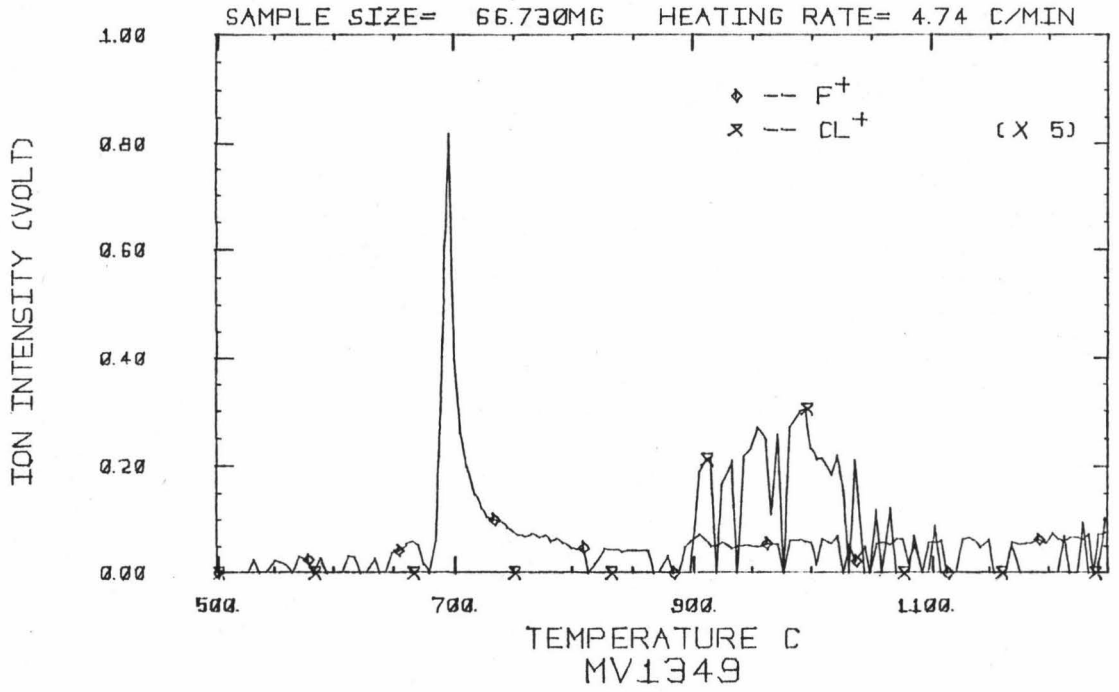

Figure 32. Mass Pyrogram Showing the Release of F and Cl from MV1349 Glass.

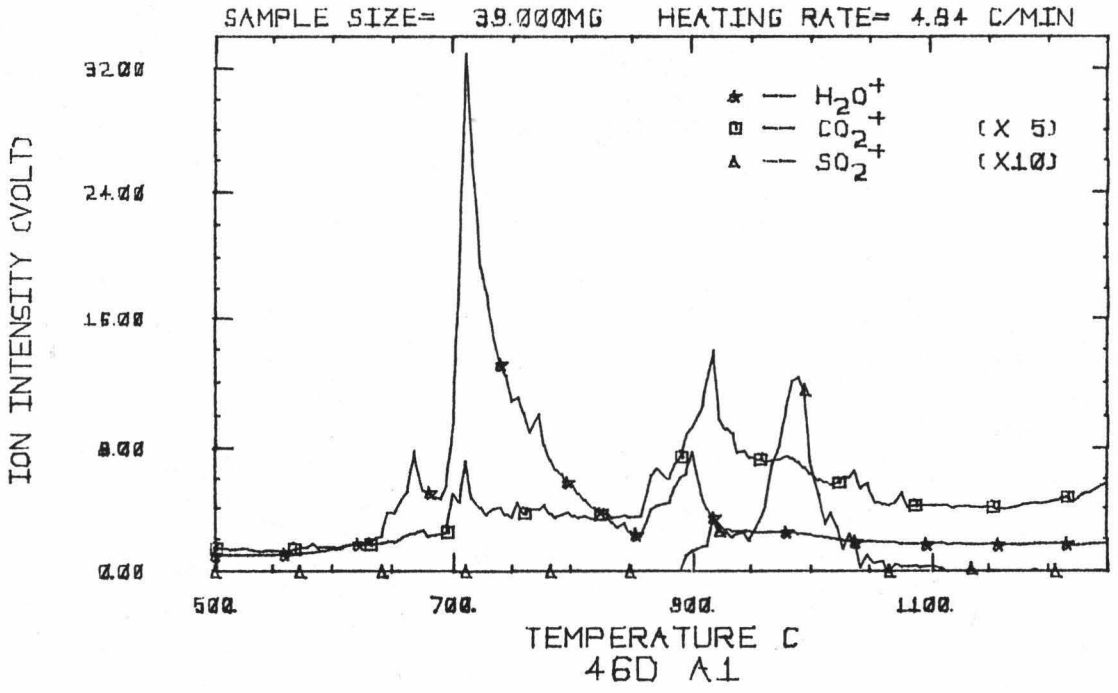

Figure 33. Mass Pyrogram Showing the Release of H_2O, CO_2 and SO_2 from 46D Al Glass.

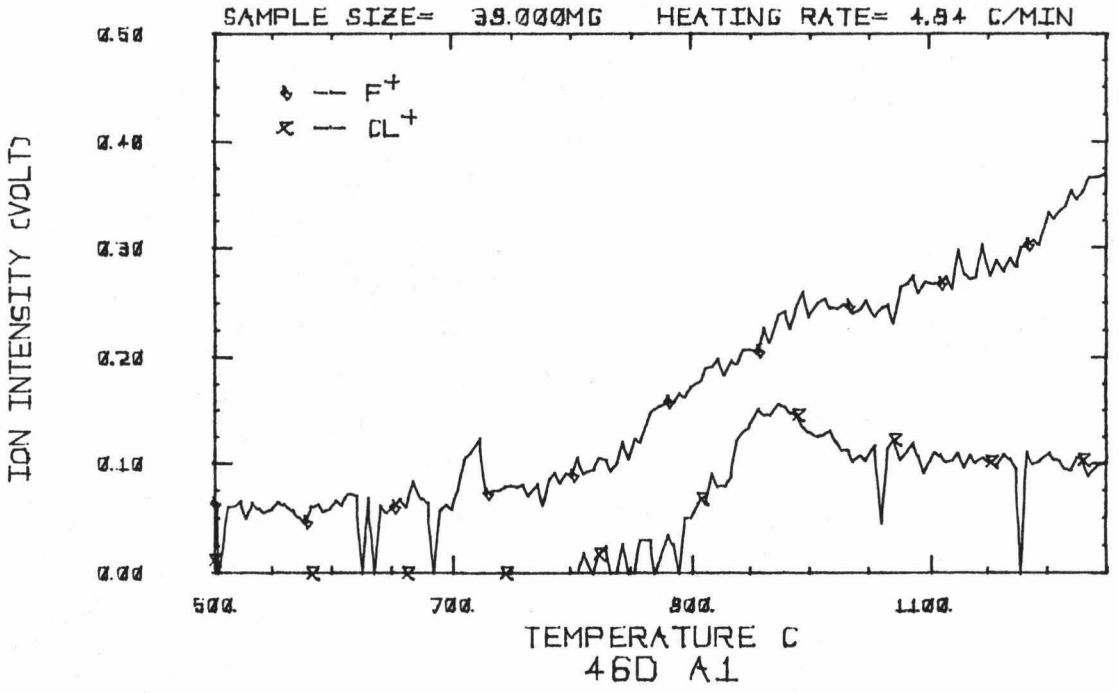

Figure 34. Mass Pyrogram Showing the Release of F and Cl from 46D Al Glass.

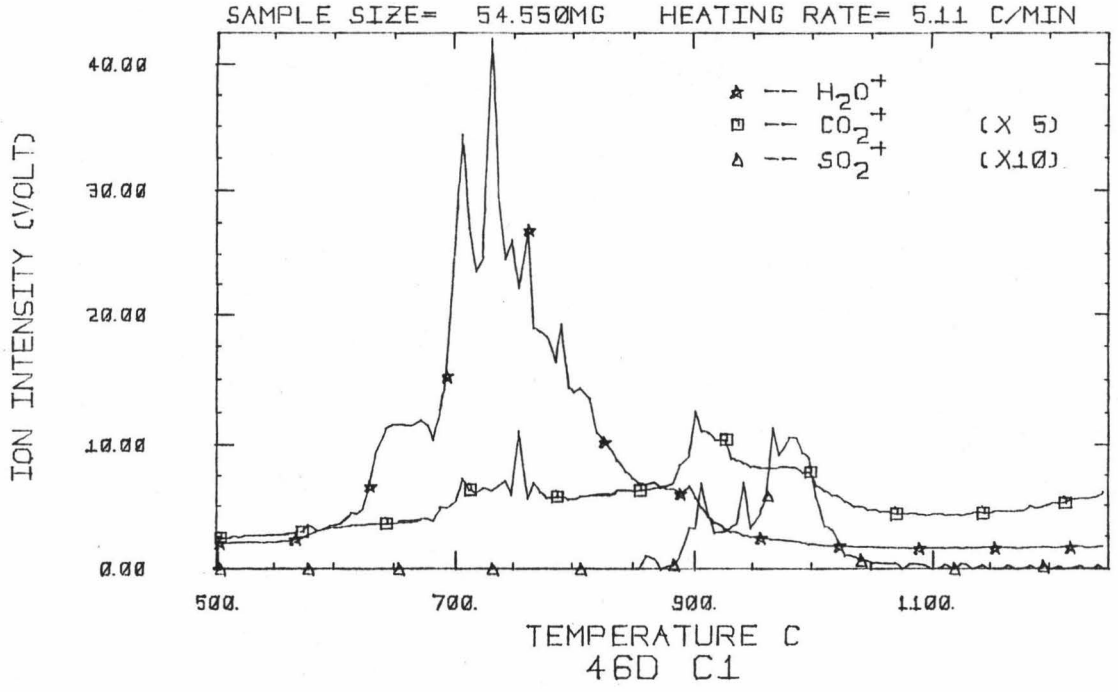

Figure 35. Mass Pyrogram Showing the Release of H_2O, CO_2 and SO_2 from 46D Cl Glass.

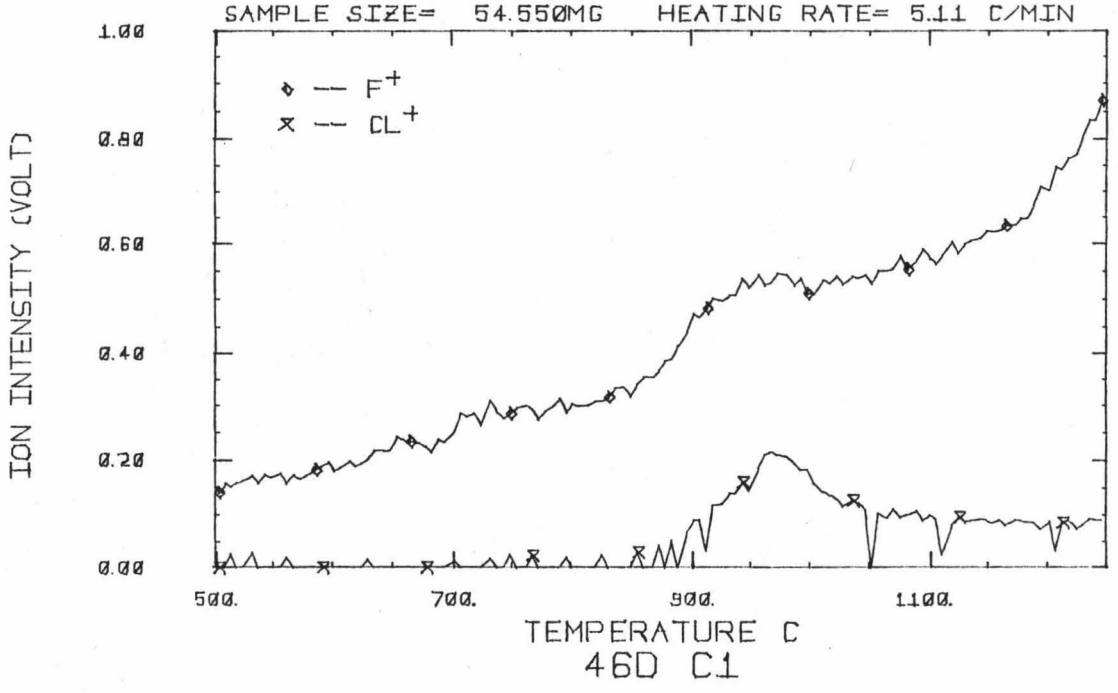

Figure 36. Mass Pyrogram Showing the Release of F and Cl from 46D Cl Glass.

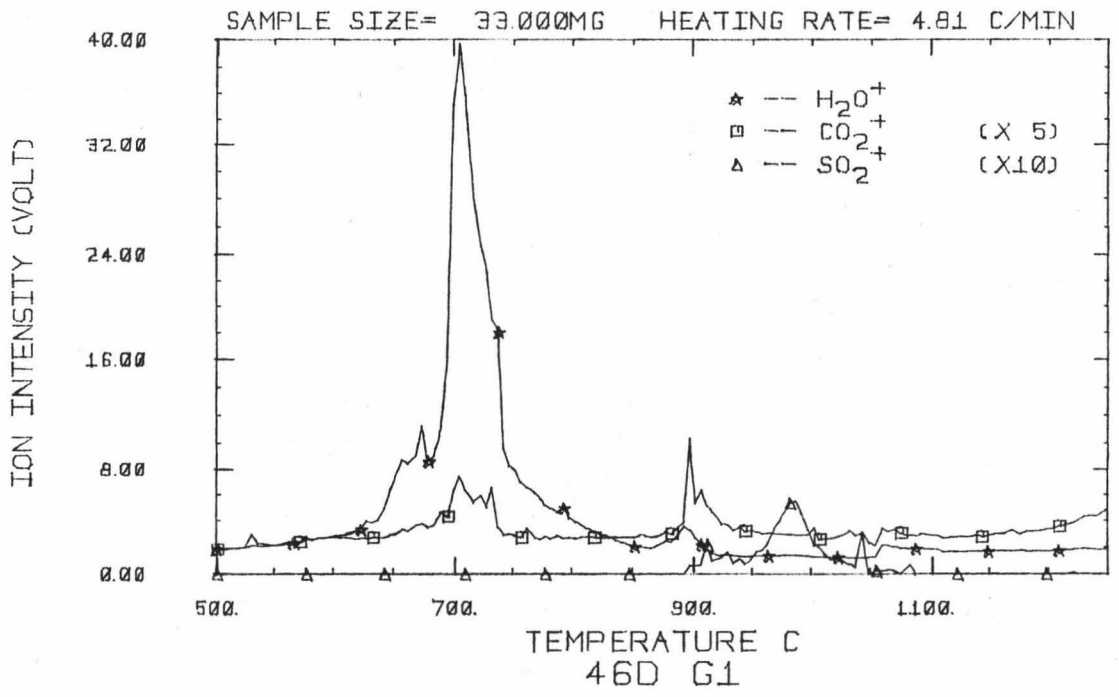

Figure 37. Mass Pyrogram Showing the Release of H_2O, CO_2 and SO_2 from 46D G1 Glass.

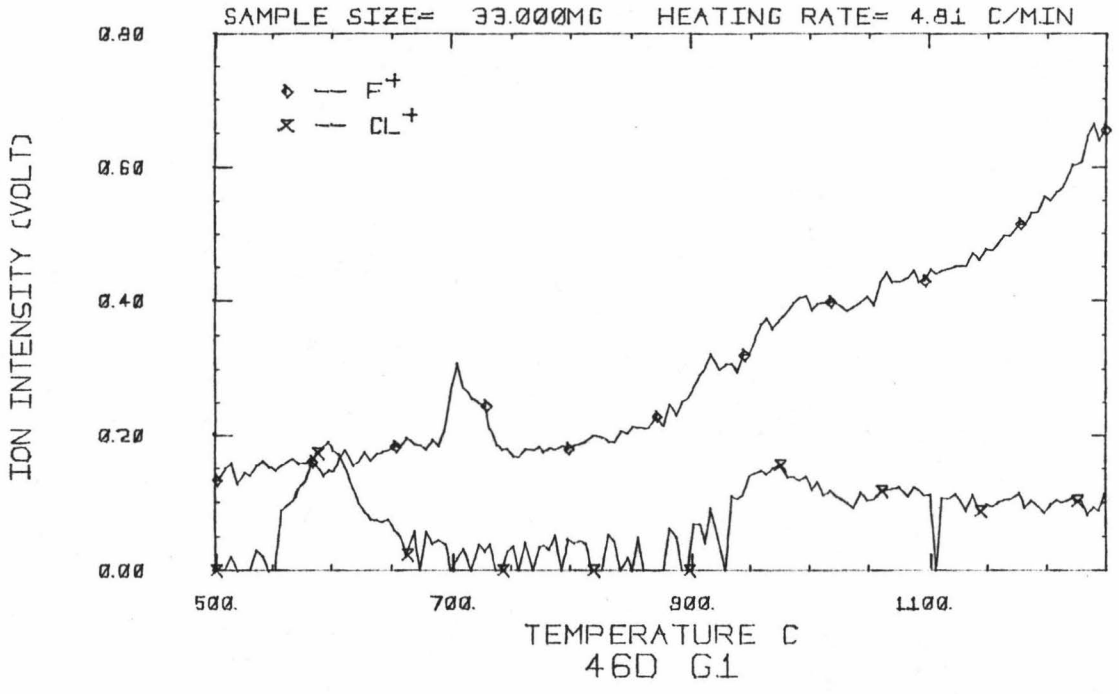

Figure 38. Mass Pyrogram Showing the Release of F and Cl from 46D G1 Glass.

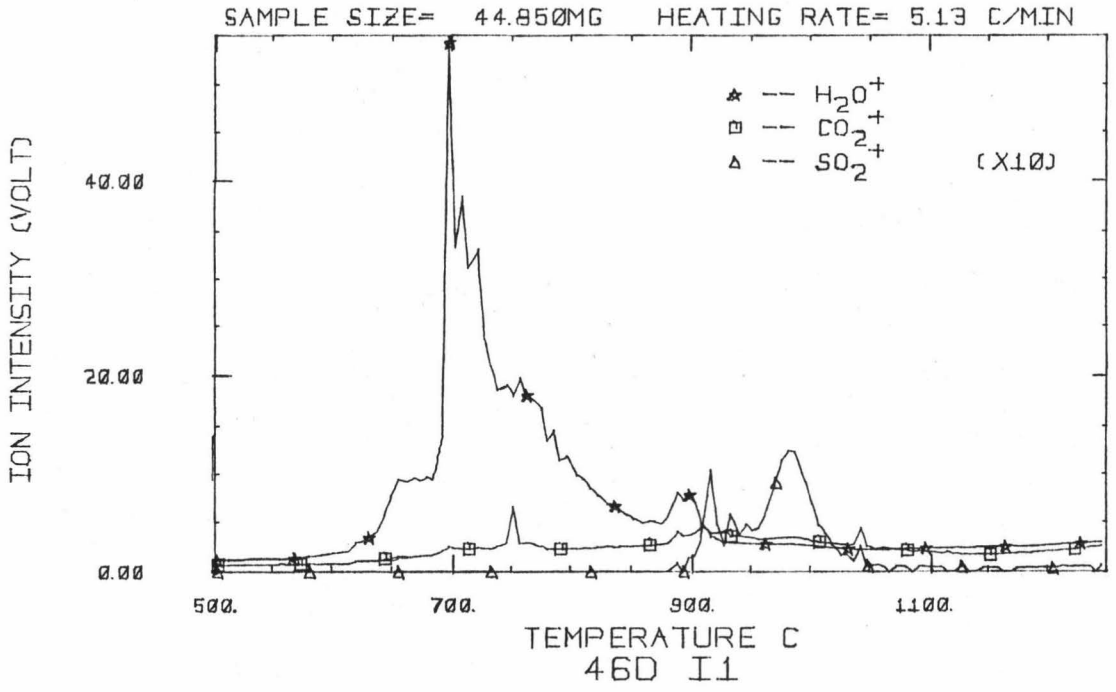

Figure 39. Mass Pyrogram Showing the Release of H_20, $C0_2$ and $S0_2$ from 46D I1 Glass.

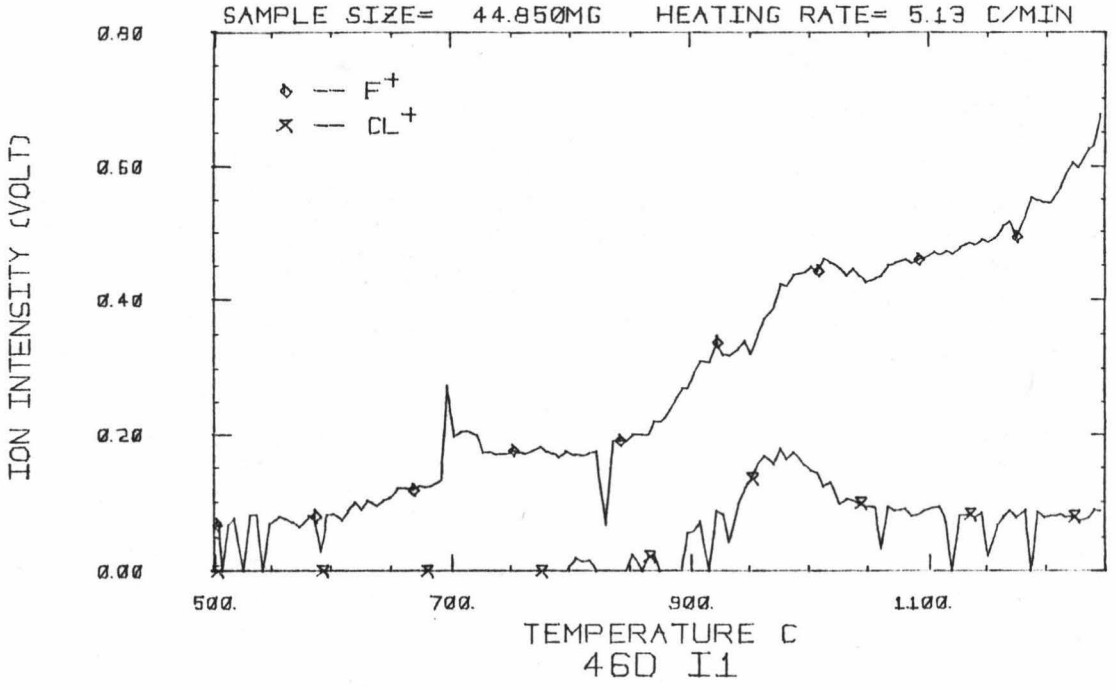

Figure 40. Mass Pyrogram Showing the Release of F and Cl from 46D I1 Glass.

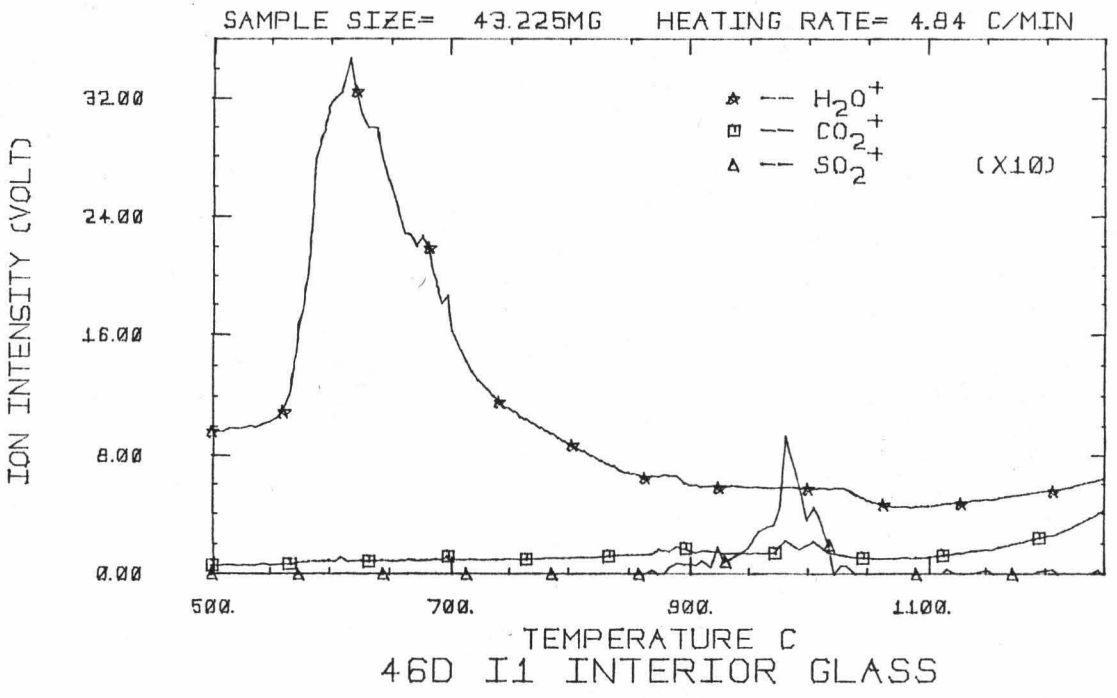

Figure 41. Mass Pyrogram Showing the Release of H_20, $C0_2$ and $S0_1$ from 46D I1 Interior Glass.

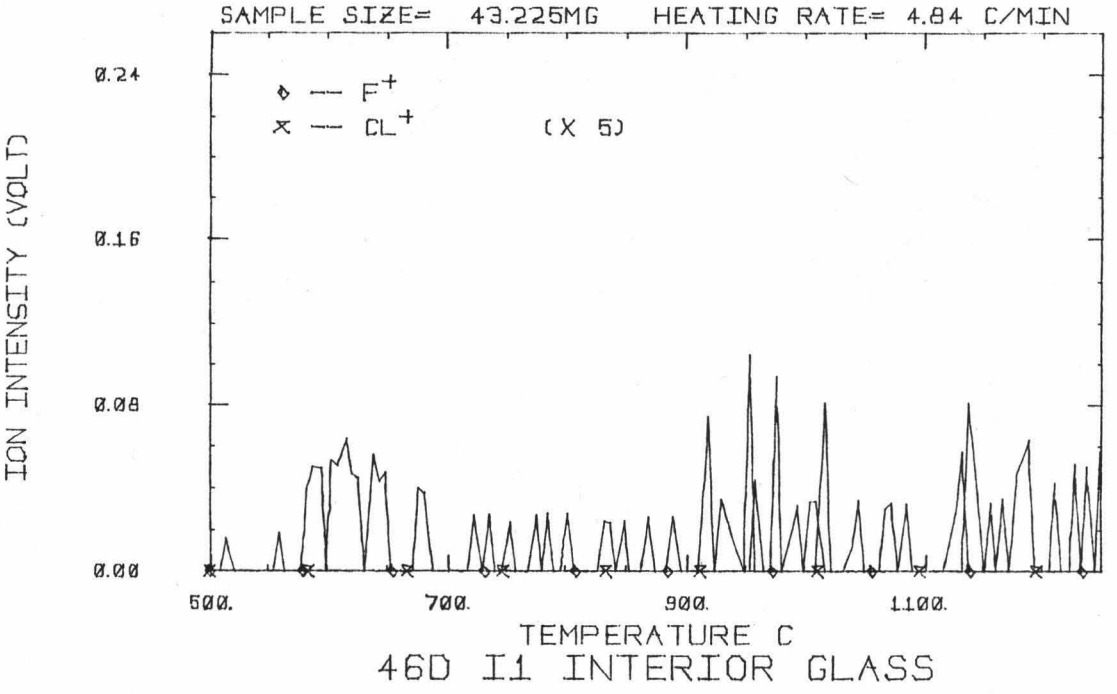

Figure 42. Mass Pyrogram Showing the Release of F and Cl from 46D I1 Interior Glass.

APPENDIX B

Sample Calculations of Volatile Abundance from Matrix Glass

Two methods for calculating the volatile abundance from matrix glass summarized by Graham (Ph.D. Thesis, 1978, Appendix B) are given here for convenience reference. Calculation of the amount of any volatile (i) present in the glass sample can be made using the following formulas:

Method I.

$$\text{Wt-\% of Species i} = \frac{Wt_{Mg}}{Wt_{sample}} \cdot \frac{K_i}{K_{Mg}} \cdot \frac{r_{Mg}}{r_i} \cdot \frac{A_i}{A_{Mg}} \cdot 100 \qquad (21)$$

Method II.

$$\text{Wt-\% of Species (i)} = \frac{K_i A_i}{\sum_{\text{all i}} K_i A_i} \cdot \frac{\text{Wt. of Volatiles}}{\text{Wt. of Sample}} \cdot 100 \qquad (22)$$

Where

Wt_{Mg} = Weight of magnesium standard vaporized

Wt of Volatiles = total weight of all volatiles released from the sample - the sample weight loss.

$K_i = M^{1/2} Fi \left[\delta_i \gamma_i (E-AP_i) \cdot \tau_i\right]^{-1}$

M = Molecular weight of species i

F = Correction factor of fragmentation pattern and isotopic abundances

δ = ionization cross section

γ = election multiplier efficiency

E = Energy of ionizing electrons (e.g. 50 eV)

AP_i = appearance potential of species i

τ = quadrupole efficiency

r = heating rate (°C/min)

A = area under the $IT^{1/2}$ vs. T curve

Values of the parameters used to determine K_i are shown in Table 6. The fragmentation patterns were determined experimentally by Killingley (1975). Ionization cross sections (δ) were evaluated by reference to a curve of ionization vs. atomic number (Figure 43-a; Flaim and Ownby, 1971). The electron multiplier efficiency (γ) is given by a $M^{1/2}$ vs. amu curve (Figure 43-b; Bunyard, 1972). The quadrupole transmission efficiency (τ) for an ion is dependent on its mass (Figure 43-c; Bunyard, 1972). Appearance potentials and isotopic abundance were obtained from Roboz (1968). Areas are calculated by the QMS program.

Table 6. Values of Parameters Used in Volatile Abundance Calibrations

Specie	M/e	F	δ	γ	AP	τ	K
H_2O	18	1.22	0.82	1.25	12.8	1.00	0.136
F	19	1.00	0.82	1.21	17.4	1.00	0.135
Na	23	1.00	0.87	1.10	5.1	0.90	0.126
Mg	24	1.27	0.91	1.08	7.6	0.90	0.126
N_2	28	1.07	1.00	1.00	15.6	0.80	0.206
CO	28	1.11	1.00	1.00	14.0	0.80	0.204
H_2S	34	1.94	1.17	0.91	10.4	0.75	0.358
Cl	35	1.33	1.13	0.80	13.0	0.75	0.314
HCl	36	1.62	1.17	0.88	12.8	0.75	0.338
K	39	1.07	1.22	0.85	4.40	0.70	0.201
CO_2	44	1.21	1.35	0.80	13.8	0.65	0.317
Fe	56	1.09	1.61	0.70	7.9	0.55	0.327
N_i	59	1.47	1.70	0.68	7.6	0.55	0.430
SO_2	64	2.19	1.78	0.66	12.4	0.55	0.72

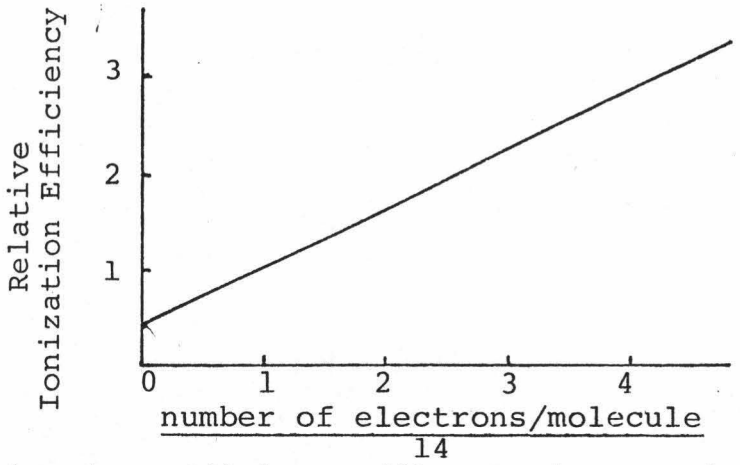

a. Ionization Efficiency (δ) Relative to Nitrogen (After Flaim and Ownby, 1971)

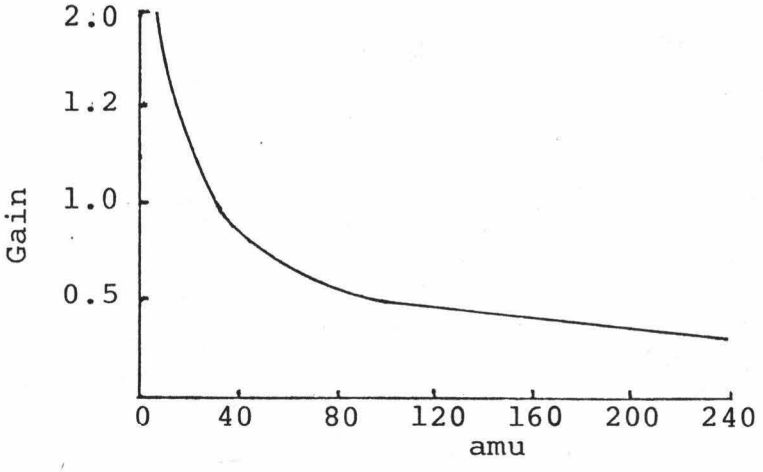

b. Electron Multiplier Efficiency (γ) Versus amu (After Bunyard, 1972)

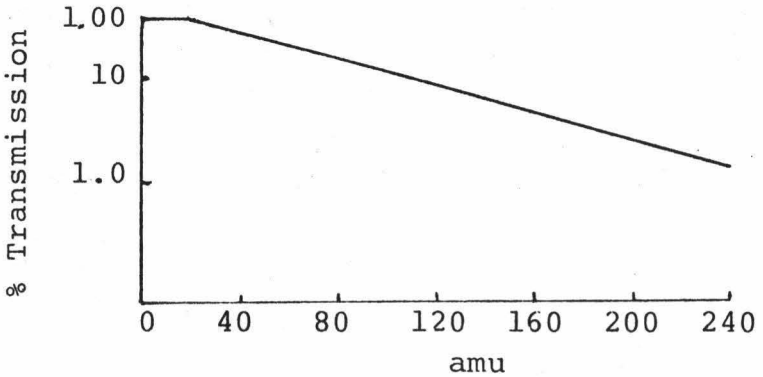

c. Quadrupole Relative Transmission (τ) Versus amu

Figure 43. Quadrupole Correction Factors

Example: Hawaii Basalt, 5000 M.

Sample size - 37.933 mg, wt. loss = 0.434 mg, r - 4.95°C/mtn.

Magnesium standard: wt = 0.642 mg; A_{Mg} = 8426, r_{Mg} = 2.5°C/min

Table 7. Sample Calculation Data

Species m/e	H_2O 18	F 18	Na 23	Cl 35	K 39	CO_2 44	SO_2 64
A_i	8660	670	1062	96	276	351	304
K_iA_i	1178	90	134	30	55	111	219
Wt-%*	0.736	0.056	—	0.019	—	0.0694	0.137
Wt-%**	0.740	0.057	—	0.019	—	0.0698	0.138

* Value obtained using Method I, equation 21.

** Value obtained using Method II, equation 22.

APPENDIX C

Instructions for the Operation of the Data Acquisition System (DAS)

a. Introduction

b. Heating Control of the Knudsen Cell

c. Quadrupole Mass Spectrometer Setting

d. QUS command file (CMI·CMD)

e. Running the QUS Program

f. Running the QRDMAS Program

g. Running the QMS Program

h. Planning for Future Experiments

a. Introduction

In this appendix, instructions for operating the automatic data acquisition system (DAS) are given. Instructions for the operation of the quadrupole mass spectrometer and vacuum system, and techniques for sample introduction and retrieval are found in various manuals collected in the laboratory. A summary of the "Operation Instructions for the Quadrupole Mass Spectrometer System" has been written by J. Gooding (M.S. thesis, 1975, Appendix A).

The operation of DAS commences after the sample has been introduced into the quadrupole mass spectrometer system, a vacuum of below 10^{-7} torr achieved, and the Knudsen cell heated to the desired starting temperature. DAS consists of three programs: 1) QUS, the on-line real time data logging program, which controls the data acquisition electronics; 2) QRDMAS, the data reduction program, which reduces the data acquired by QUS to a condensed mass spectral data file consisting of the mass peaks and their intensities, the cell temperature, and the heating voltage used during each mass scan sampled; and 3) QMS which performs the quantitative computation on the mass spectral data.

To operate DAS, one must first familiarize himself with the current PDP-11/45 operating-system commands. The communication between the computer and the user is established by a Monitor Control Routine (MCR) which can be invoked by typing "^C" (holding the control-key and typing the character "C" at the same time) on a computer terminal. The monitor

control routine will respond by printing on the computer terminal a "MCR>" and will wait for the user to type in further instructions (MCR> will "go away" after approximately one minute but can be invoked again by typing a "^c"). To communicate with the computer the user must log-on an existing work area designated by a "User Identification Code" (UIC). The UIC is designated by "[group number, project number]" (e.g. [201,1]). When logged on to a UIC, the user is allowed to execute any programs existing within the computer system providing certain system conventions and restrictions are obeyed. Detailed information can be found in the current PDP-11/45 operating system references (RSX-11D V6·2).

b. Heating Control of the Knudsen Cell

There are two temperature ramp signals which are used to control the heating rate of the Knudsen cell. One is supplied by QMS04 circuit. The other is supplied by the computer's digital-to-analog converter (DA1:). The voltage resolution of DA1: (10 bits) is inconsistent with the cell temperature digital-to-analog converter (12 bits) and for this reason signals from DA1: are not used. A switch S5 (in QMS05) is used for the selection of control signals from QMS04 or DA1:. It must be switched to position 1 (counter clockwise) to select the QMS04 control signal before starting the heating process.

To start heating:

1. Turn on the QMS interface electronics and the Newport-2600SC digital thermometer.
2. Turn the heating rate select switch S1 (see Fig. 44) to the desired heating rate setting (e.g. 5°C/min at C).
3. Switch S3 to count position.
4. Switch S4 to count-up position.
5. Push the reset switch S2.

   Note: The output of QMS04 (pin Z), connected to a volt meter, should read no more than 5 mV, otherwise problems have developed in the QMS04 circuit.
6. Turn the heater power on (see Fig. 45).
7. Watch the VOM (connected to the output of T1) to register at no more than 2V A.C. If it registers more than 2V A.C. and increases to a higher voltage rapidly, turn the heater power off immediately. This indicates problems have developed in the heating control circuit.

C. Quadrupole Mass Spectrometer Setting

1. Set Mode switch to SCAN.
2. Set SCAN SPEED to 900.
3. Turn S.E.M. voltage to maximum.
4. Set CENTER MASS to 0.90.
5. Turn the MASS RANGE knob until the H_2^+ peak is centered in the lower left 'centimeter box' on the

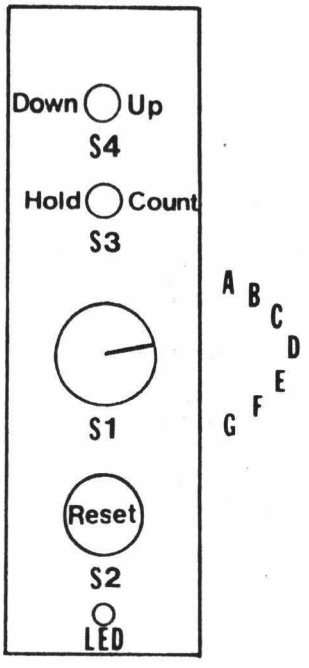

S1	Rate °C/min
A	1.25
B	2.50
C	5.00
D	10.0
E	20.0
F	40.0
G	40.0

Figure 44. Diagram of Heating Rate Control Switches. (Located in Front of QMS04 Circuit Card)

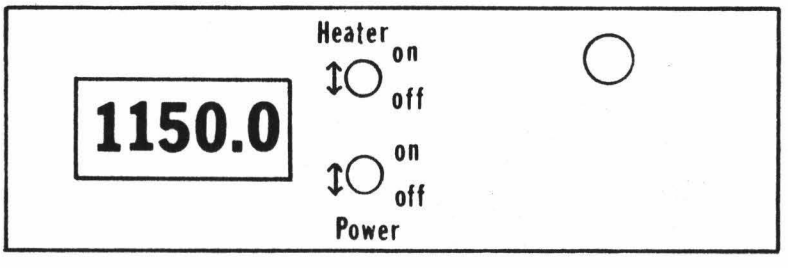

Figure 45. Diagram of Front Panel of Digital Thermometer.

oscilloscope.

6. Set SCAN SPEED to 30.

The above setting will give a mass range of -2 to 100 amu and a scan rate of 30 sec/scan.

d. QUS command file (CMI·CMD)

A command file named CMI·CMD file must be created in UIC=[201,7]. The CMI·CMD file must contain three (3) records of informations: Record 1 contains all the program control parameters (see Table 8). Record 2 contains the title of the experiment. Record 3 contains additional comments about the experiment.

Example of CMI·CMD:

```
FILENAME/TM:30/SP:9/RS:70/SZ:54·321/EC:M/RA:B/FI:4
THIS IS THE TITLE
THIS IS A COMMENT
```

To create CMI·CMD:

```
MCR>HEL [201,7]cr          (cr = carriage return)
MCR>RUN QUSCMD$            ($ = ALTMODE or ESC Key)
```

and answer all the questions asked by QUSCMD.

e. Running the QUS program

1. Install QUS program:

```
MCR>HEL [1,1]cr            (cr = carriage return)
MCR>INS [201,100]cr
```

(This will put QUS in the active task list in the system. At this time the CMI·CMD file must be created in UIC=[201,7].)

2. Run QUS:

```
MCR>HEL [201,7]cr
MCR>QUScr
```

Table 8. QUS Program Control Parameters

Parameter	Function	Value
FILENAME	The name under which QUS will output data	Maximum of 9 characters. The first character must be a letter of the alphabet.
/TM:	The scan time (sec)	Must be equal to the SCAN SPEED setting of the Quad Control Unit and must be greater than 10.
/SP:	The sampling speed	Allowed values are 0 to 15. This controls the number of data point per second (see Table 9).
/RS:	The reschedule time (sec)	Must be greater than or equal to 2 times the /TM: value
/SZ:	Sample size	In milligrams
/RE:	Resolution setting of Quad-1110	870 is currently used
/SE:	S.E.M. voltage setting	M (Maximum)
/EC:	Emission Current	720 (=0.720)
/RA:	Range setting of ESA-75 electrometer	B (A, B, C or D)
/FI:	Filter setting	4 (1, 2, 3, 4 or 5 counting from MIN)

Table 9. CAMAC Module Period Clocking

(Crystal Frequency = 6.5802 MHz)

Speed (sp:)	Divisor (Program)	Divisor (fixed)	Period (sec)	Data Rate (1/sec)
0	6336	1024	0.98600	1.014
1	4224	1024	0.65725	1.532
2	2880	1024	0.44825	2.231
3	2355	1024	0.36650	2.729
4	2112	1024	0.32875	3.042
5	1056	1024	0.164225	6.089
6	528	1024	0.082175	12.2
7	264	1024	0.041075	23.3
8	176	1024	0.027400	36.5
9	158	1024	0.024588	40.7
10	132	1024	0.020543	48.7
11	88	1024	0.013695	73.0
12	64	1024	0.010270	97.4
13	44	1024	0.006848	146.0
14	33	1024	0.005135	194.7
15	16	1024	0.002500	400.0

Note: QUS will ring the bell on the terminal at the end of each sample (scan) period.

3. To stop QUS:

```
MCR>HEL [1,1]cr
MCR>CAN ···QUScr
```

(Turn the heater off after QUS finishes sampling the last scan)

f. Running the QRDMAS Program:

```
MCR>HEL [201,7]cr              (cr = carriage return key)
MCR>RUN QRDMAS/TIME:4H$        ($ = ALTHODE or ESC key)
QUS>WANT TO INVOKE OPTIONS?-no
DAT>FILENAME=filename·qus
DAT>OUTPUT FILENAME=filename·qms
```

Note: The small lettered words and a carriage return are typed by the user. QRDMAS will process data until finished. Error messages will be printed on the terminal.

g. Running the QMS Program:

```
MCR>HEL [201,7]cr
MCR>RUN QMS$
```

Note: QMS is a computer terminal interactive program which allows the user to select analytical functions to be performed on the "filename·qms" data file created by QRDMAS. QMS will ask simple questions (mostly yes or no questions) and will repeat the questions until the proper answers are given by the user. Detailed instructions for running QMS written for non-computer oriented user were written by Graham (Ph.D. thesis, 1978,

Appendix A). The best way to understand QMS is to run it and try various options. Nothing can be destroyed by running QMS.

h. Planning for Future Experiments

The instructions given in parts (c) and (d) of this Appendix are designed for vaporization studies presented in this thesis (or other similar experiments). When planning for new experiments which require modification of the QUS control parameters, the following should be considered in addition to the system limitations given in Section III-D-3 of this thesis.

1. M/e = 16, 17, 18, 28, and 44 must appear in the mass spectrum. They are required by ARDMAS for the assignment of m/e values to all mass peaks in the mass spectrum.
2. For a mass scan of a specific mass range and the number of data points per scan to be sampled by QUS there must be at least 7 data points per mass peak-envelope to define the peak. For example, a mass scan covering a range of 100 amu and with sp:=9 (40.7 points/sec, see Table 9) and TM: 30, there will be approximately 1221 data points in this scan (i.e. 12 data points per mass peak).

APPENDIX D

Quadrupole Mass Spectrometer Data Acquisition System Software Documentation

1. QUS -- Real-time Data Acquisition Program

a. General Information

QUS is a pseudo-handler, written in assembly code, used to control a CAMAC module for acquiring data from the quadrupole mass spectrometer system. The electronic circuit for the CAMAC module is kept in the chemistry department computer room and a blueprint is kept in the mass spectrometry lab(HIG-414). The QUS program is stored in UIC=[201,100] on the disk and is backed-up on two magnetic tapes labelled 'QUS'. One of the tapes is kept in the computer room (BA-209) and the other is kept in the mass spectrometry lab. A complete documentation of QUS had been written by G. Gulden and is stored in a file called QS-RNO in UIC=[201,100]. The QUS program is called QUS·MAC; its associated command files are given below.

b. Assembly command file (QUSMAC·CMD)

```
QUS,QUS/-SP=[1,1]BIOMAC/ML.[201,100]QUS
```

c. QUS task command file (QUS·CMD)

```
QUS/-FP/TA-CP/-AB/-DS/-FX/PR,QUS/-SP=QUS,[1,1]EXEC.
STB.BIOMACIO
LIBR=SYSRES:RO
PRI-150
TASK=...QUS
STACK=80
ASG=SY:1
ASG=SY:2
ASG=TI:3
//
```

2. QRDMAS -- Data Analysis Program

a. General Information

QRDMAS is a FORTRAN program consisting of a main program and a set of subroutines. The QRDMAS programs are documented in the FORTRAN source codes and the flow charts of some of these programs are given in this appendix for convenient reference. The QRDMAS programs are stored in UIC=[201,6] on the disk and are backed-up on two magnetic tapes labelled 'QRDMAS'. One of the tapes is kept in the computer room (BA-209) and the other is kept in the mass spectrometry lab (HIG-414). A copy of the QRDMAS task file (QRDMAS·TSK) is ketp in UIC=[201,7] on the disk.

All the QRDMAS programs are listed in a FORTRAN command file. The QRDMAS FORTRAN command file, task command file and task overlay file are given in this appendix.

b. QRDMAS FORTRAN command file (QRDMAS·CMP)

```
QRDMAS,QRDMAS/-SP=QRDMAS
DATQUS,DATQUS/-SP=DATQUS
NORQUS,NORQUS/-SP=NORQUS
PLTQUS,PLTQUS/-SP=PLTQUS
PEKQUS,PEKQUS/-SP=PEKQUS
LBRSUB,LBRSUB/-SP=LBRSUB
PRTDAT,PRTDAT/-SP=PRTDAT
MASSID,MASSID/-SP=MASSID
SEARCH,SEARCH/-SP=SEARCH
MASSUB,MASSUB/-SP=MASSUB
ASGMAS,ASGMAS/-SP=ASGMAS
QRDOUT,QRDOUT/-SP=QRDOUT
SKIP,SKIP/-SP-SKIP
LSQ,LQS/-SP=LSG
```

c. QRDMAS task command file (QRDMAS·CMD)

```
QRDMAS,QRDMAS/SH/-SP=QRDMAS/MP
LIBR=FORBES:RO
PRI=65
ASG=SY:1
```

```
ASG=TI:5
ASG=TI:6
ASG=LP:4
//
```

d. QRDMAS task overlay file (QRDMAS·ODL)

```
          .ROOT    ROOT=*(A1,A4,A4,A5,A6)
ROOT:     .FCTR    QRDMAS-LBRSUB-PRTDAT-NORQUS-SKIP
A1:       .FCTR    DATQUS
A3:       .FCTR    PLTQUS-[1,1]TEKNEW.OLB/LB
A4:       .FCTR    PEKGUS
A5:       .FCTR    MASSID-SEARCH-MASSUR-ASGMAS-LSQ
A6:       .FCTR    QRDOUT
          .END
```

e. Flow charts of ARDMAS programs

Figure 46. Flow Chart Diagram of QRDMAS

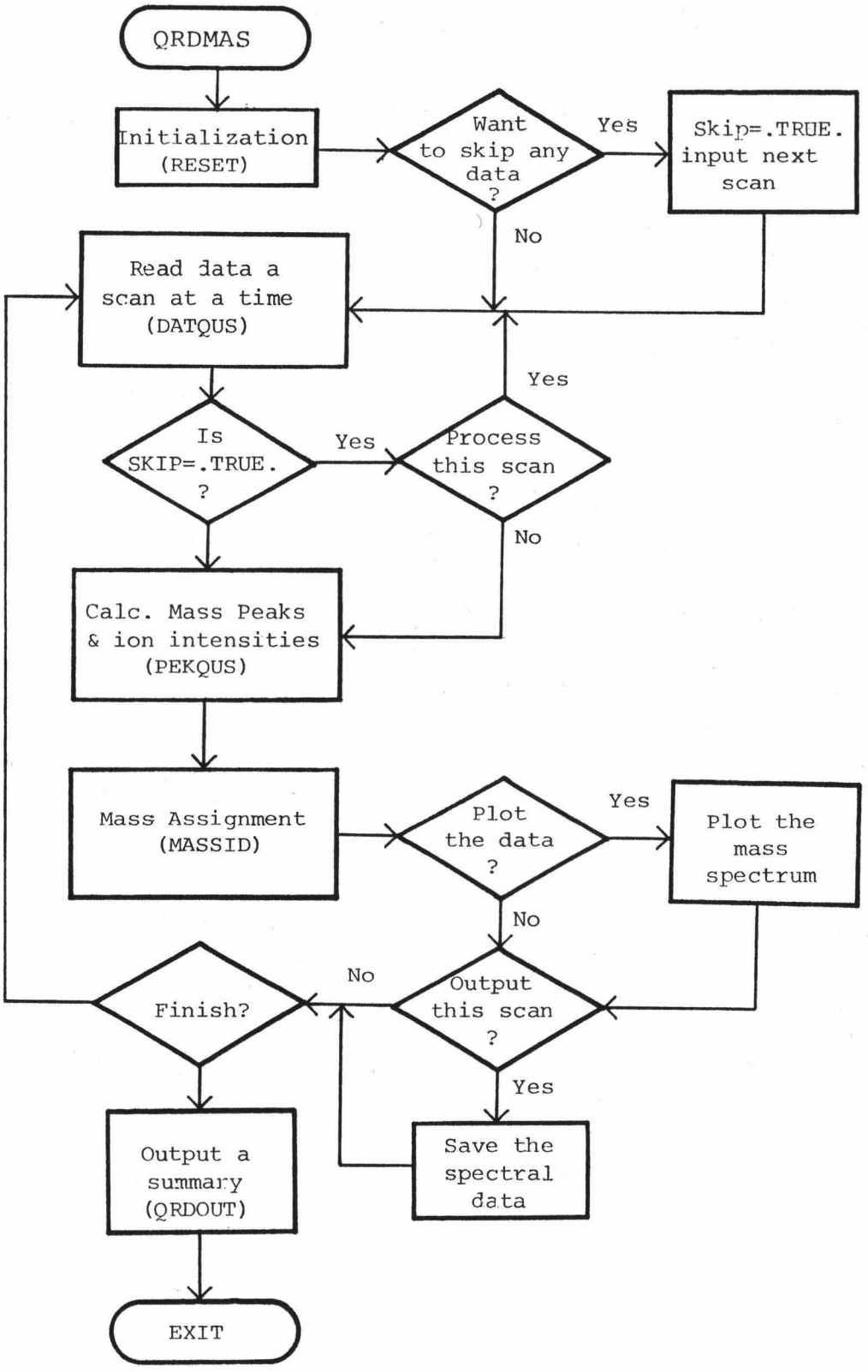

Figure 47. Flow Chart of Subroutine DATQUS

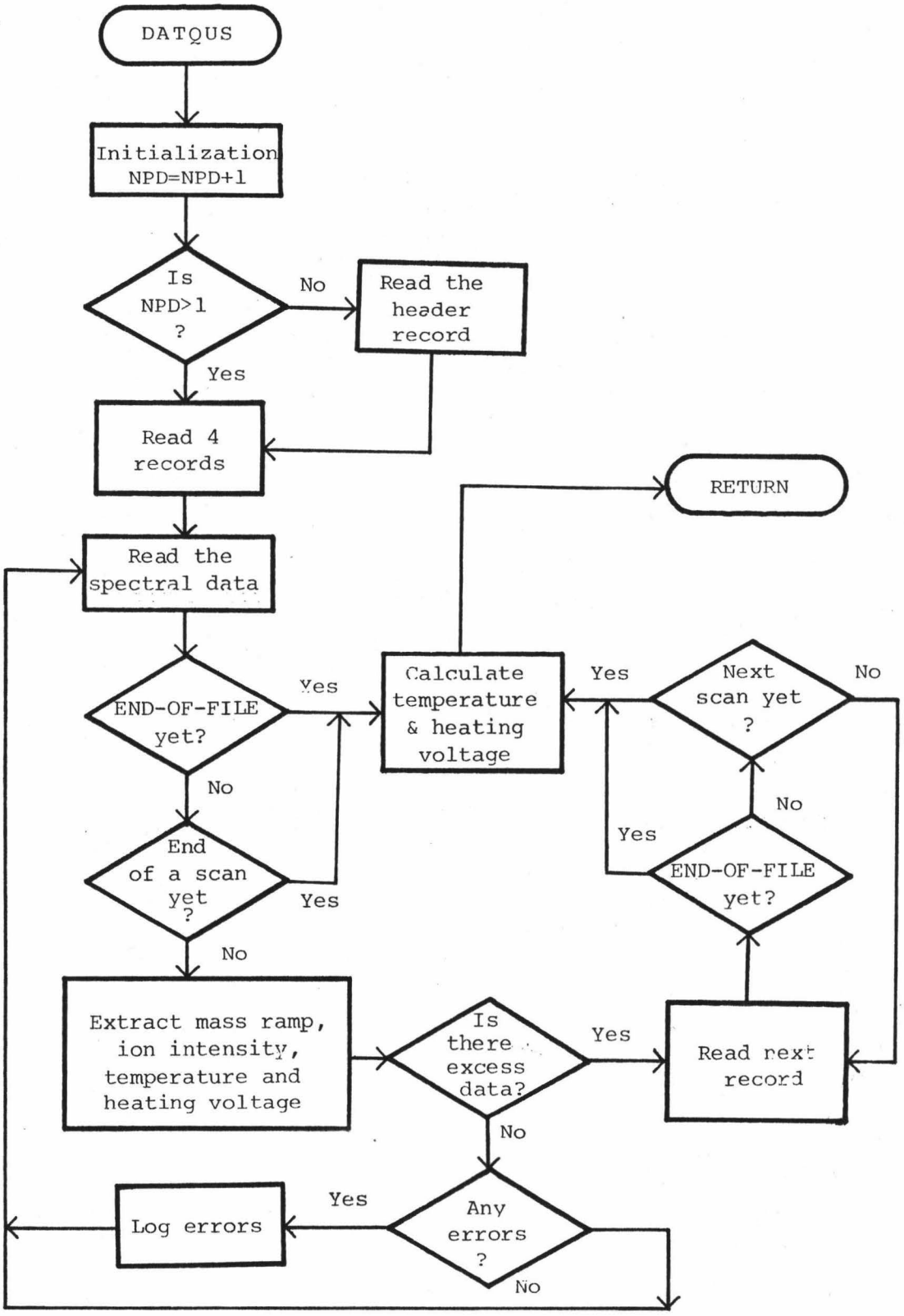

Figure 48. Flow Chart of Subroutine PEKQUS

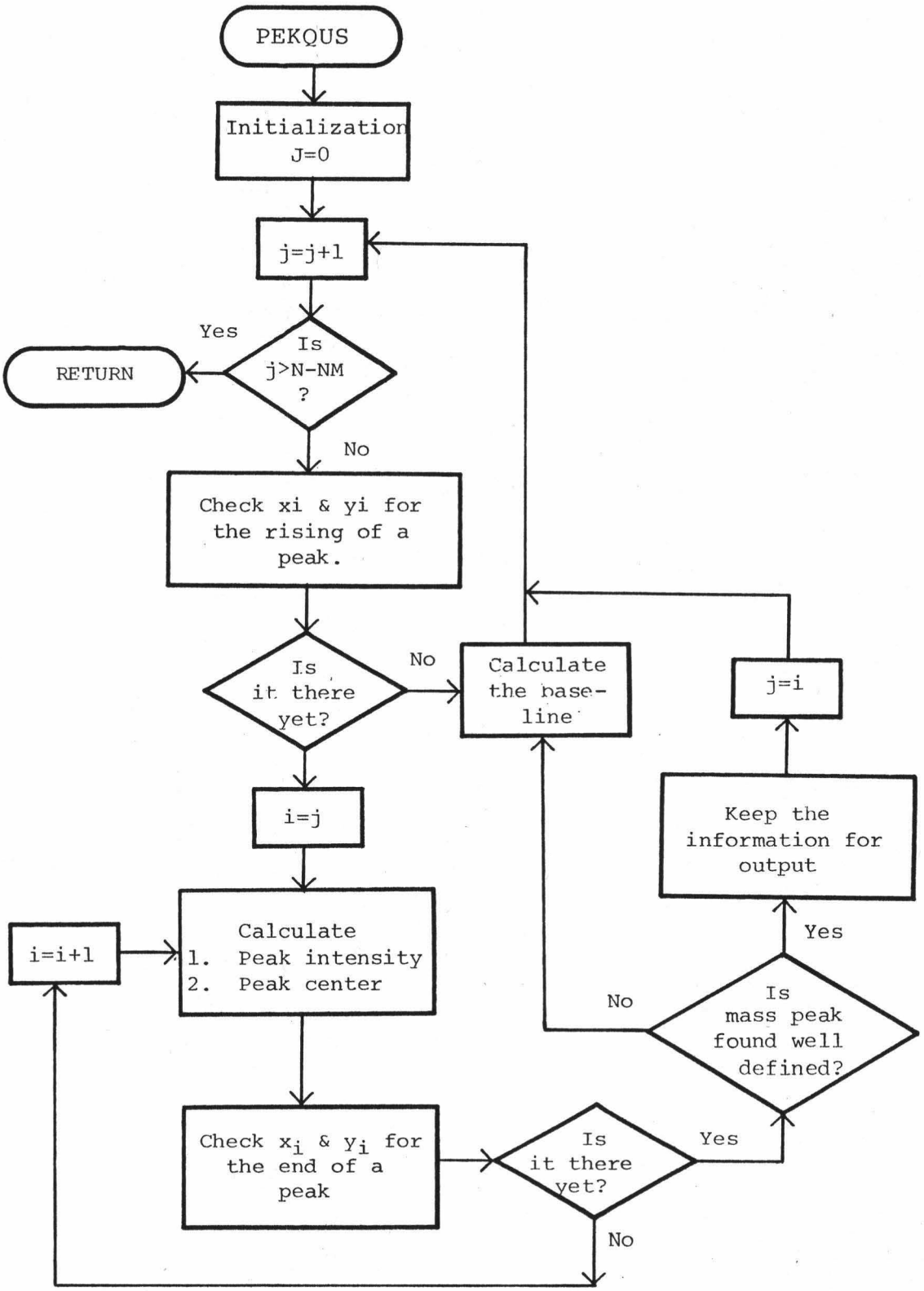

Figure 49. Flow Chart of Subroutine MASSID

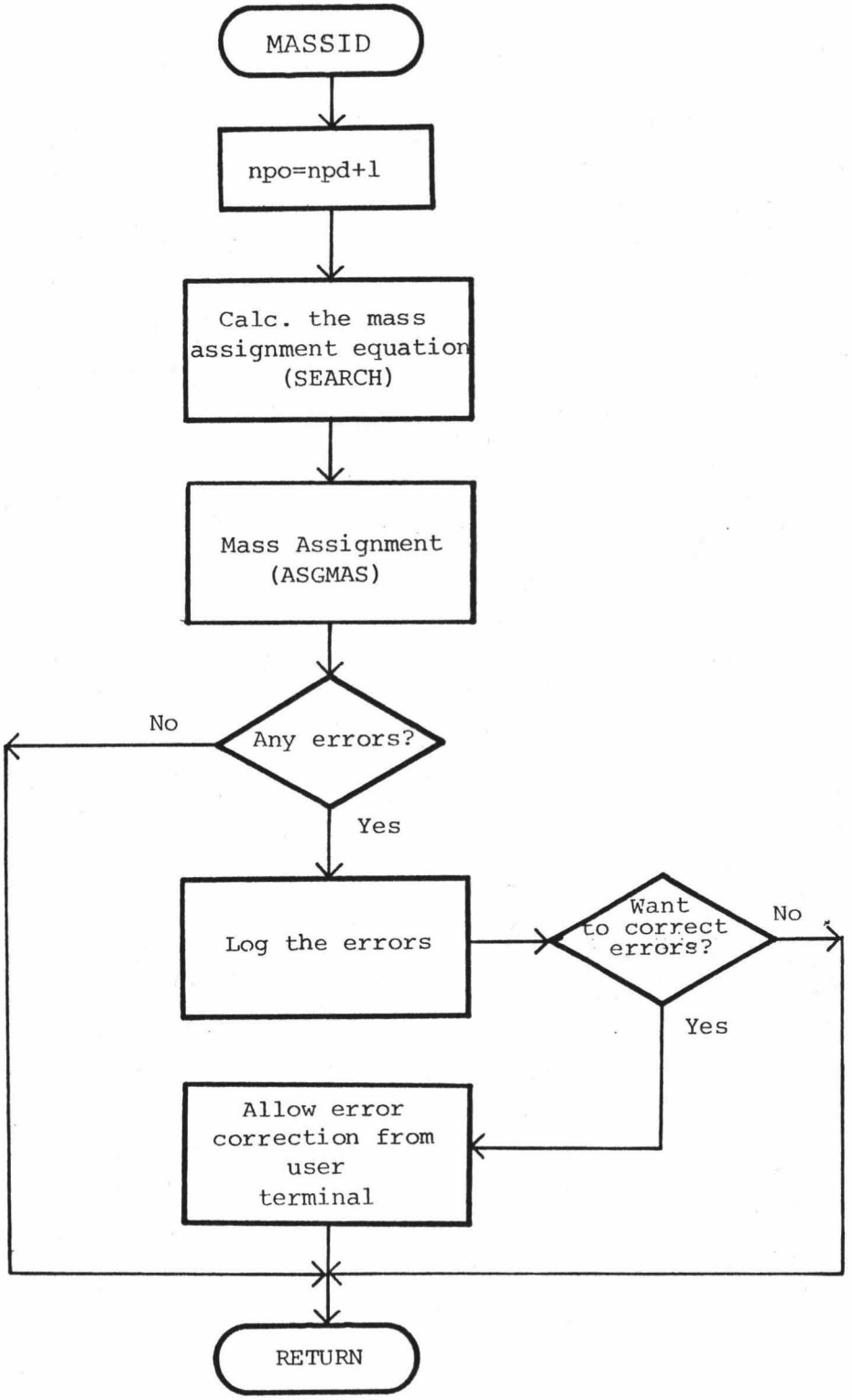

Figure 50. Flow Chart of Subroutine SEARCH

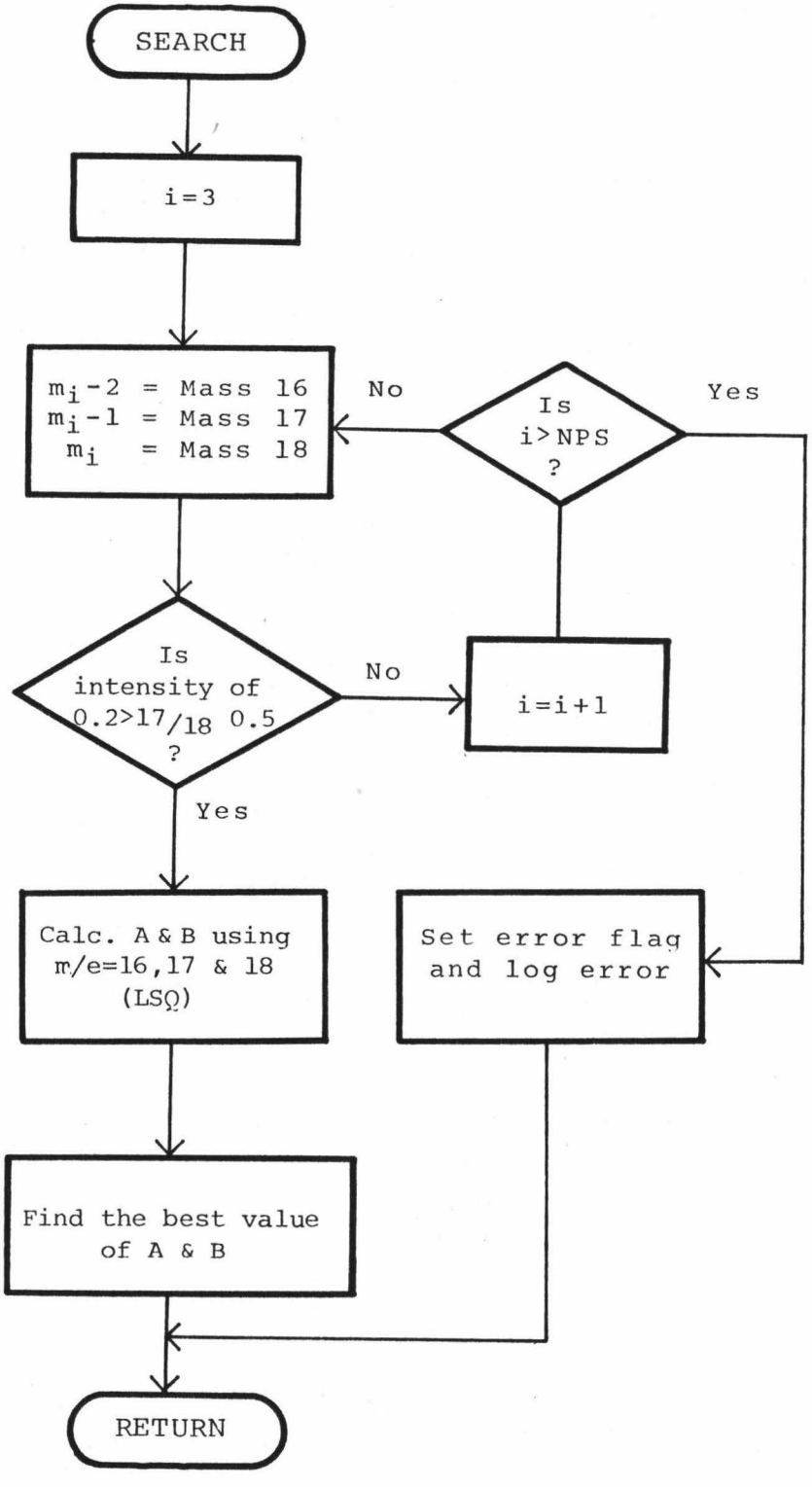

Figure 51. The Flow Chart Diagram of Subroutine BEST

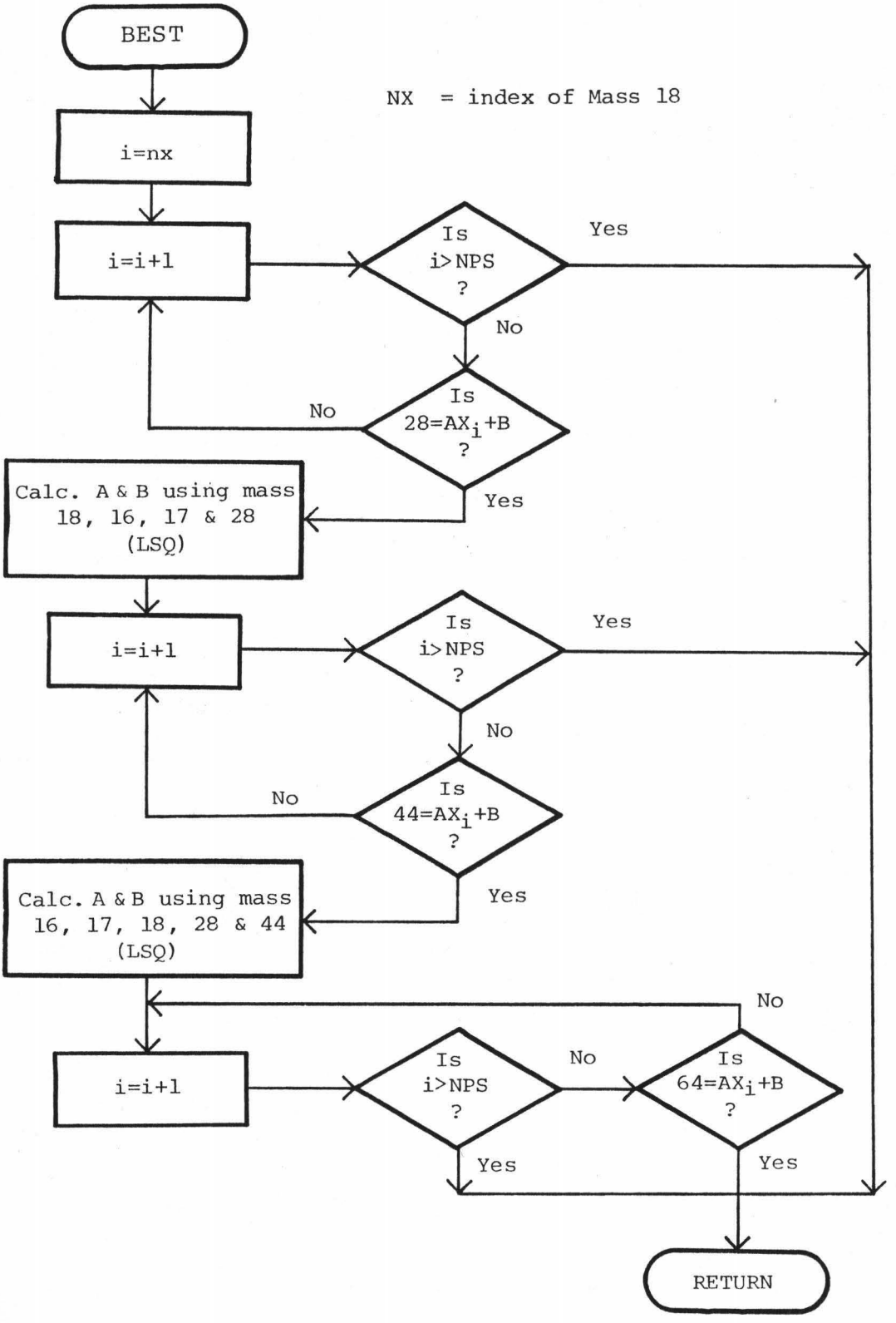

Figure 52. Flow Chart of Subroutine ASGMAS

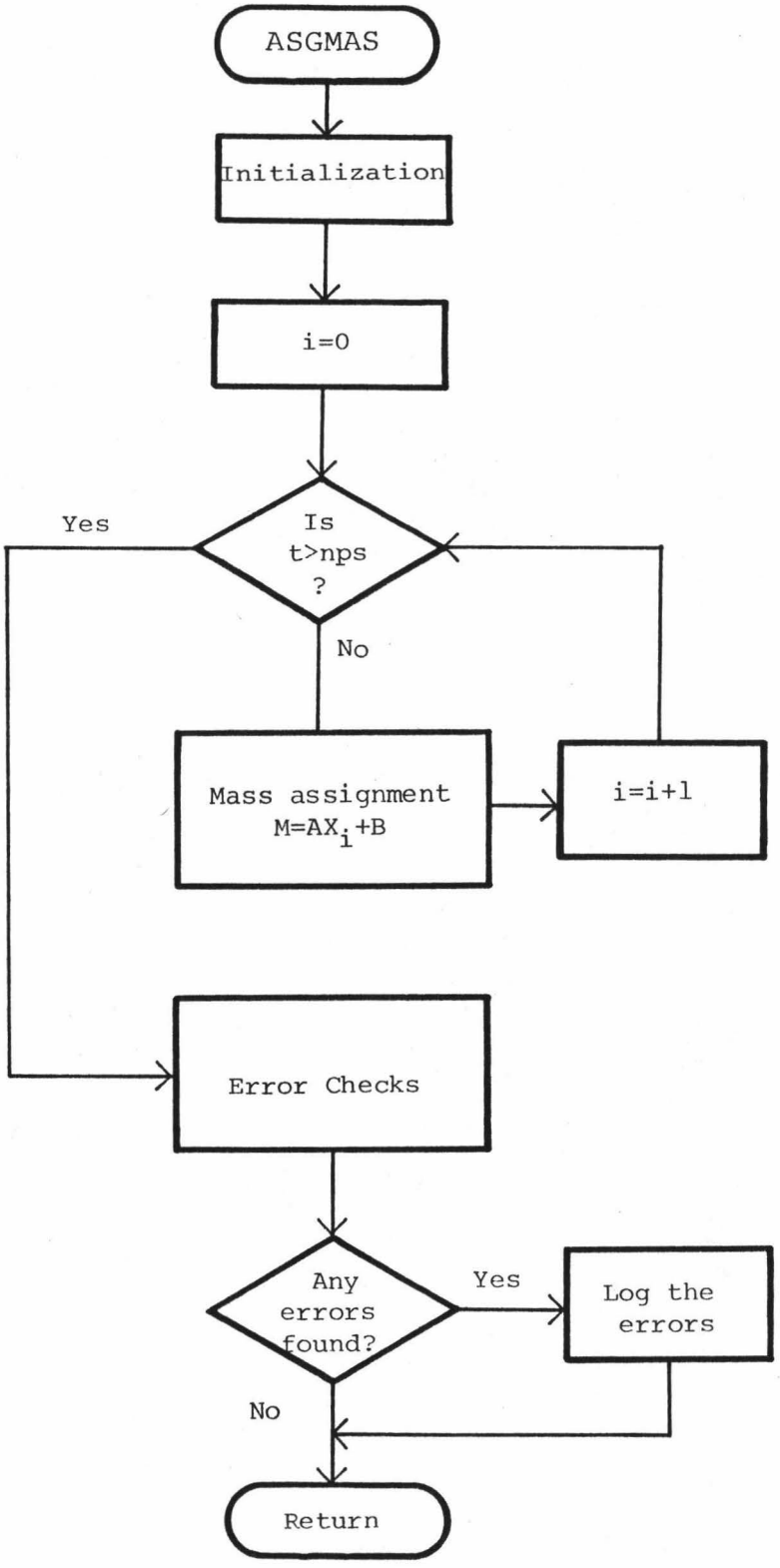

3. QMS -- Data Analysis Program

a. General Information

QMS is a FORTRAN program consisting of a main program and a set of subroutines. The QMS programs are documented in the FORTRAN source codes and the flow charts of some of these programs are given in this appendix for convenience reference. The QMS programs are stored in UIC=[201,1] on the disk and are also backed-up on two magnetic tapes labeled 'WMS'. One of the tapes is kept in the computer room (BA-209) and the other is kept in the mass spectrometry lab (HIG-414). A copy of the QMS task file (QMS-Tsk) is kept in UIC=[201.1] on the disk.

All the QMS programs are listed in a FORTRAN command file. The QMS FORTRAN command file, task command file and the task overlay file are given in this appendix.

b. QMS FORTRAN command file (QMS·CMP).

```
QMS,QMS/-SP=QMS
LSQ,LSQ/-SP=LSQ
AREA,AREA/-SP=AREA
DELH,DELH/-SP=DELH
MERG,MERG/-SP=MERG
PEAK,PEAK/-SP=PEAK
PYRO,PYRO/-SP=PYRO
START,START/-SP=START
BGDCOR,BGDCOR/-SP=BGDCOR
LBRSUB,LBRSUB/-SP=LBRSUB
PLTDEL,PLTDEL/-SP=PLTDEL
QMSBGD,QMSBGD/-SP=QMSBGD
QMSDAT,QMSDAT/-SP=QMSDAT
QMSERR,QMSERR/-SP=QMSERR
RATIOS,RATIOS/-SP=RATIOS
SMOOTH,SMOOTH/-SP=SMOOTH
TNTPLT,TNTPLT/-SP=TNTPLT
HELP,HELP/-SP=HELP
```

c. QMS task command file (QMS·CMD).

```
WMS/MU/WMS/SH/-SP=QMS/MP
LIBR=FORBES:RO
ASG=TI:6
ASG=SY:1
ASG=SY:4
//
```

d. QMS task overlay file (QMS·ODL)

```
            .ROOT    ROOT-*(A1,A2,A3,A4,A5,A6)
ROOT:       .FCTR    QMS-LBRSUB
A1:         .FCTR    QMSDAT-QMSBGD-START-BGDCOR-
                     QMSERR-LSG
A2:         .FCTR    RATIOS-LSQ-PEAK-AREA
A3:         .FCTR    PYRO-TNTPLT-[1,1]TEKNEW.OLB/LB
A4:         .FCTR    DELH-PLTDEL-LSQ-[1,1]TEKNEW.OLB/LB
A5:         .FCTR    MERG-SMOOTH
A6:         .FCTR    HELP
            .END
```

e. Flow charts of QMS programs

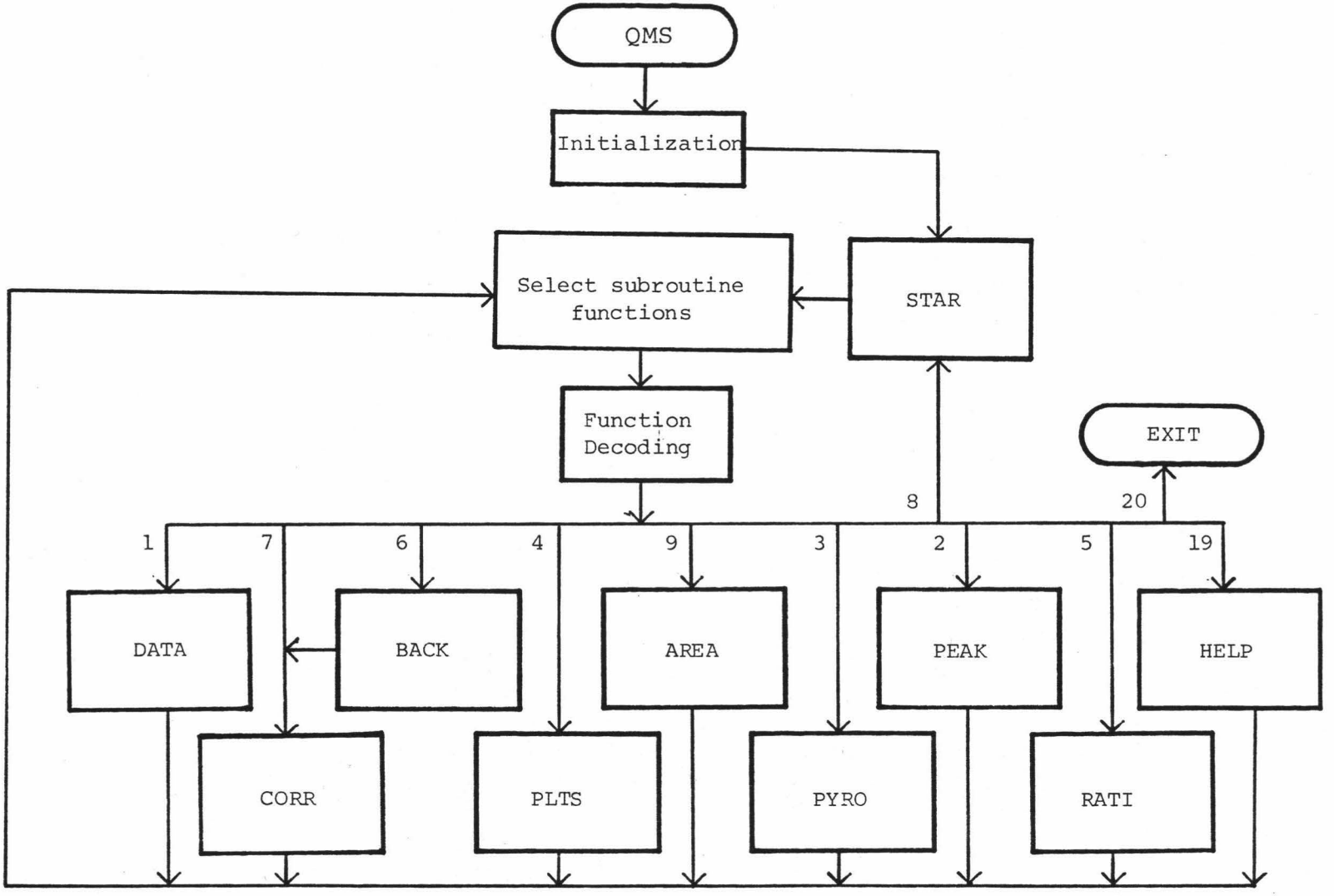

Figure 53. Flow Chart of QMS Main Program

Figure 54. Flow Chart of Subroutine AREA

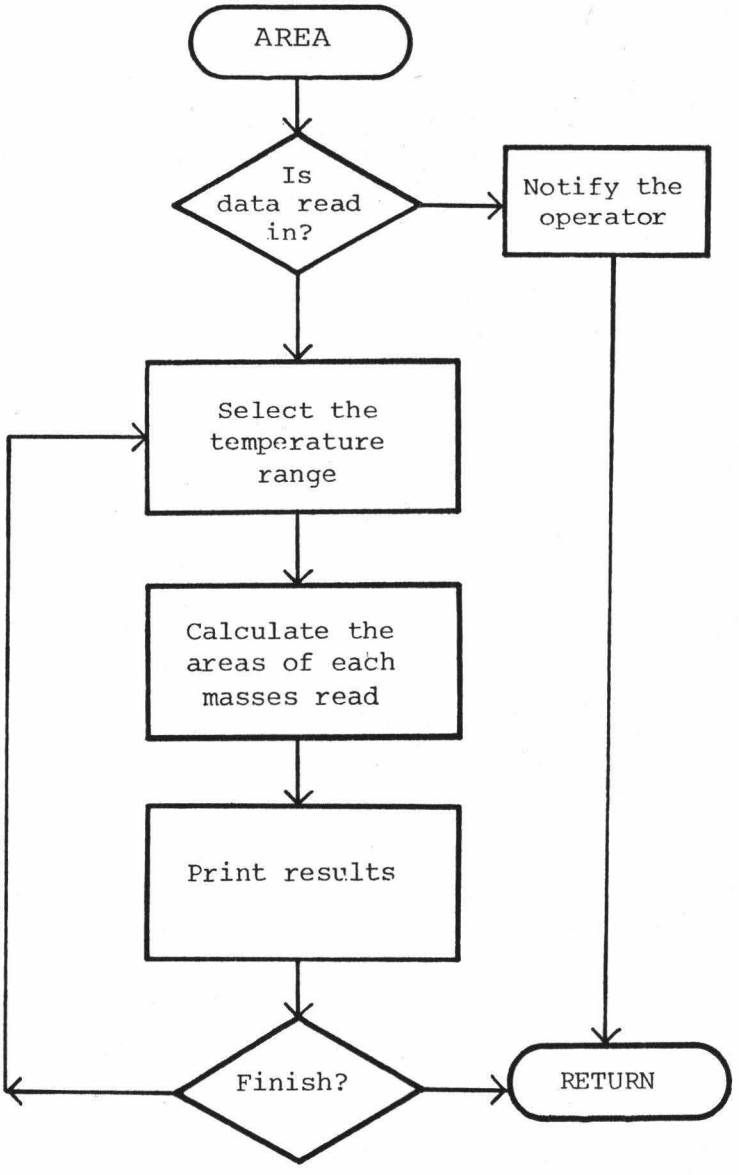

Figure 55. Flow Chart of Subroutine BACK

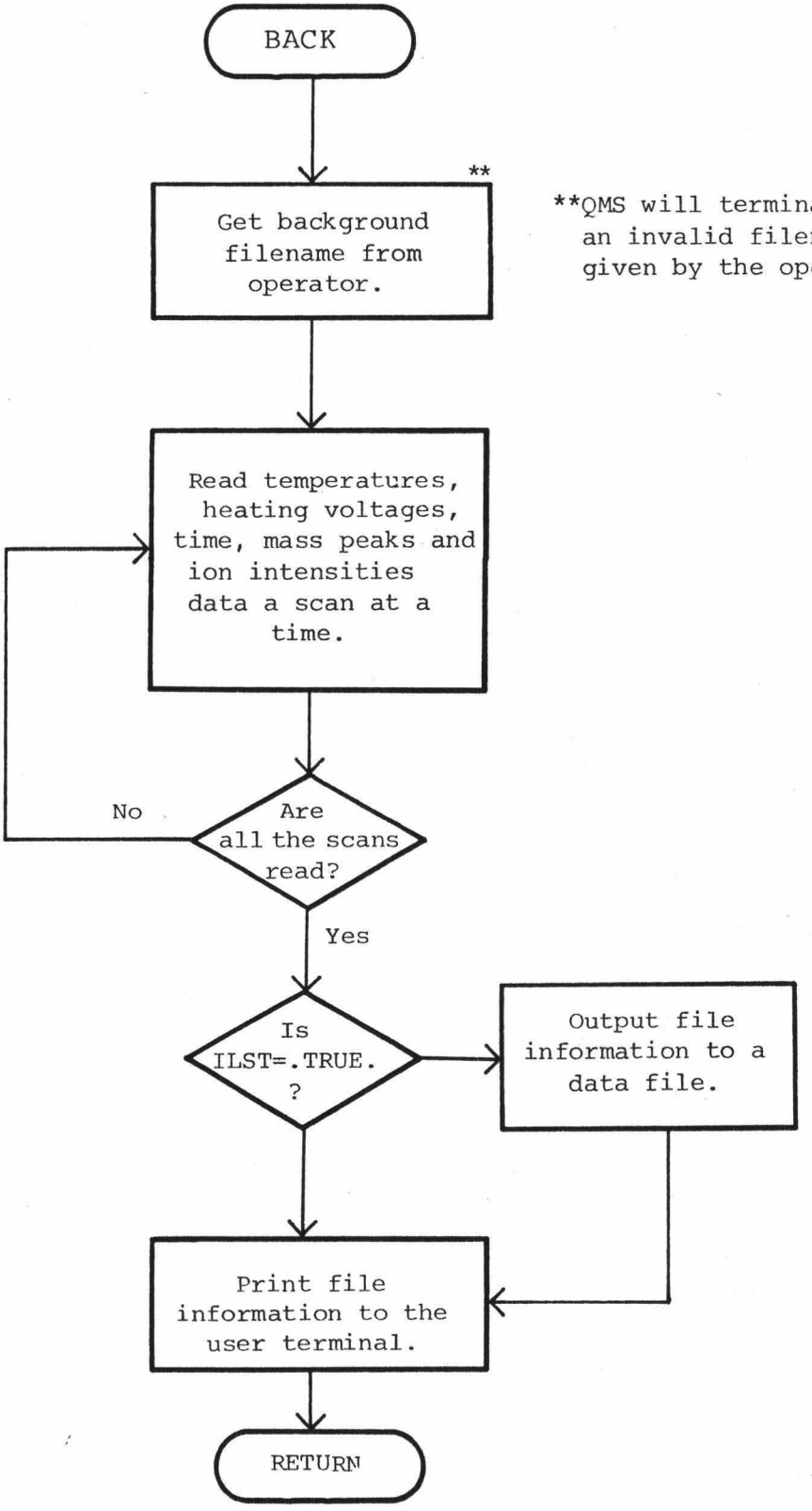

Figure 56. Flow Chart of Subroutine DATA.

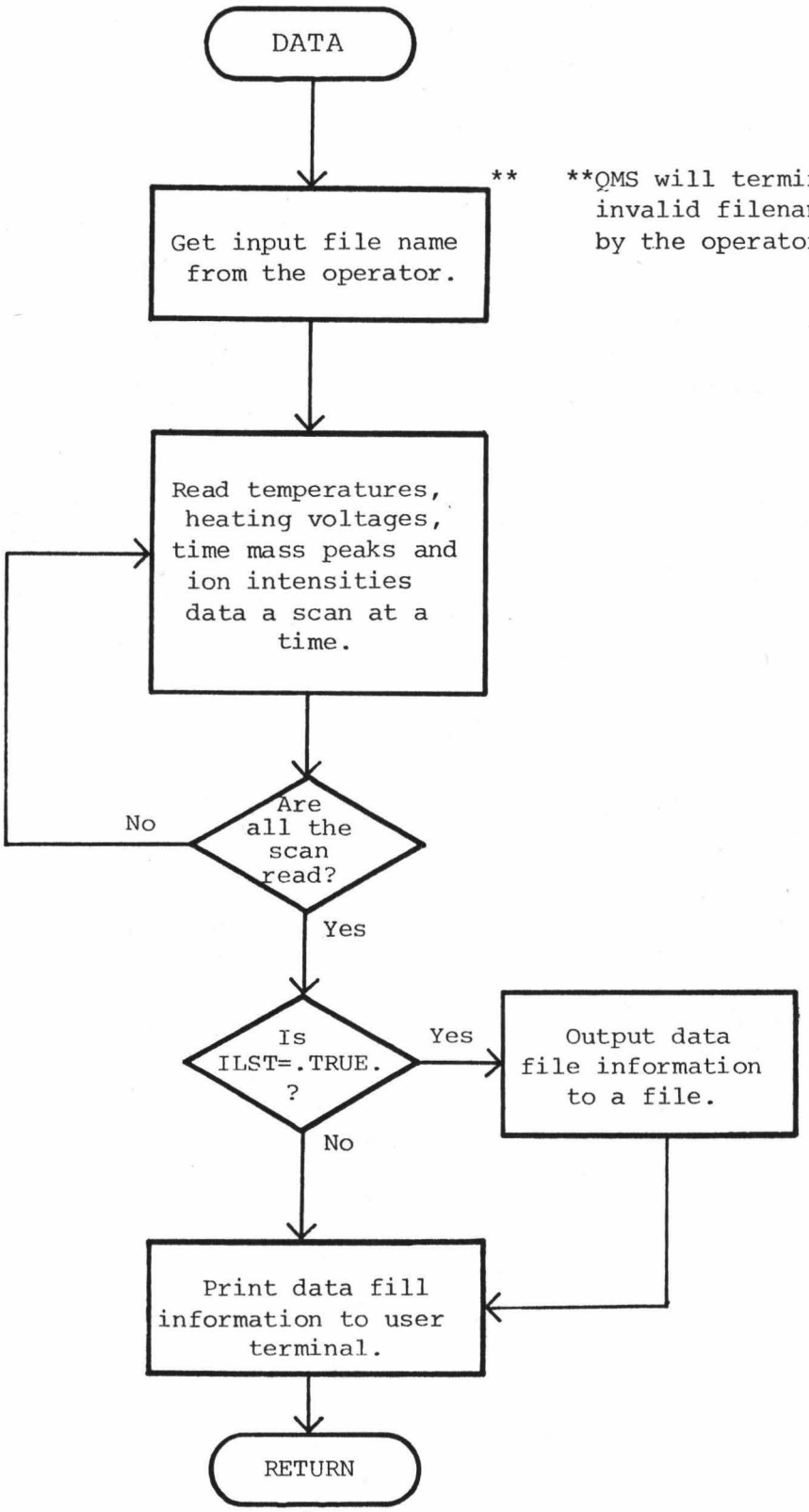

Figure 57. Flow Chart of Subroutine PEAK

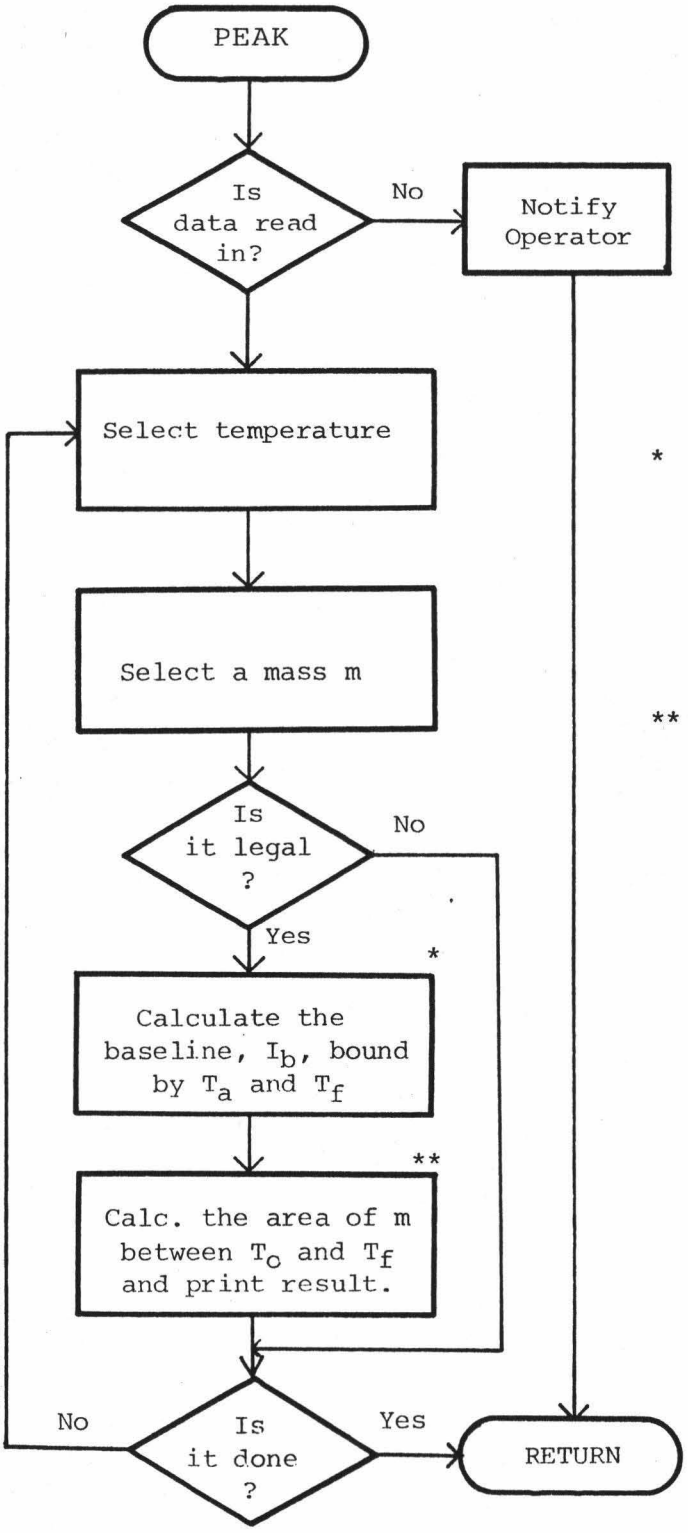

* The base line, Z_b, is calc. from the ion intensity of m at T_o and T_f using a least square method.

$$I_b = m T_i + B$$

** $$\text{Area} = \sum_{i=j}^{k} (I_i - I_b) T_i^{1/2}$$

j,k = index of the ion intensity of m by T_i and T_f

Figure 58. Flow Chart of Subroutine PLTS

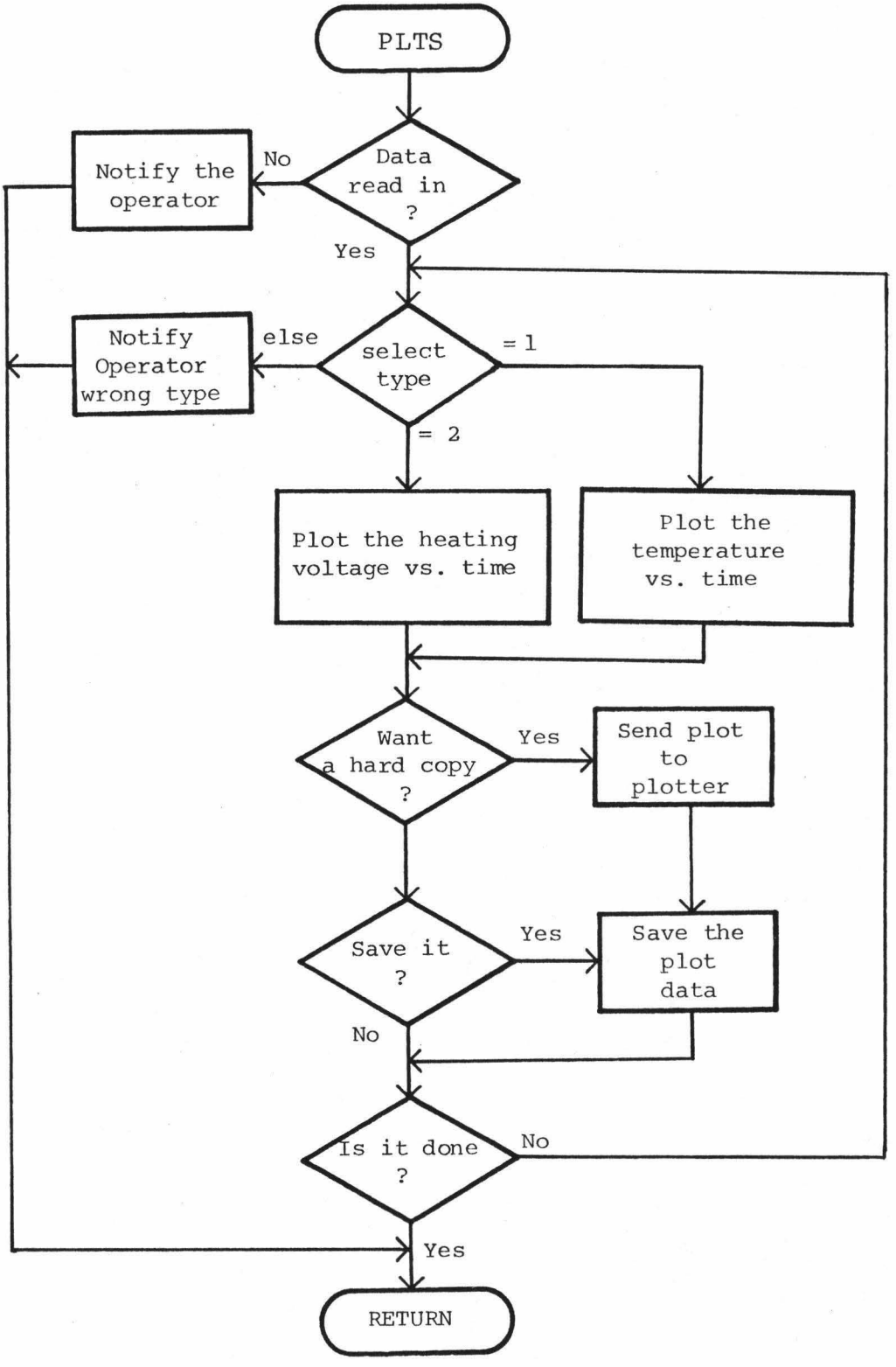

Figure 59. Flow Chart of Subroutine PYRO

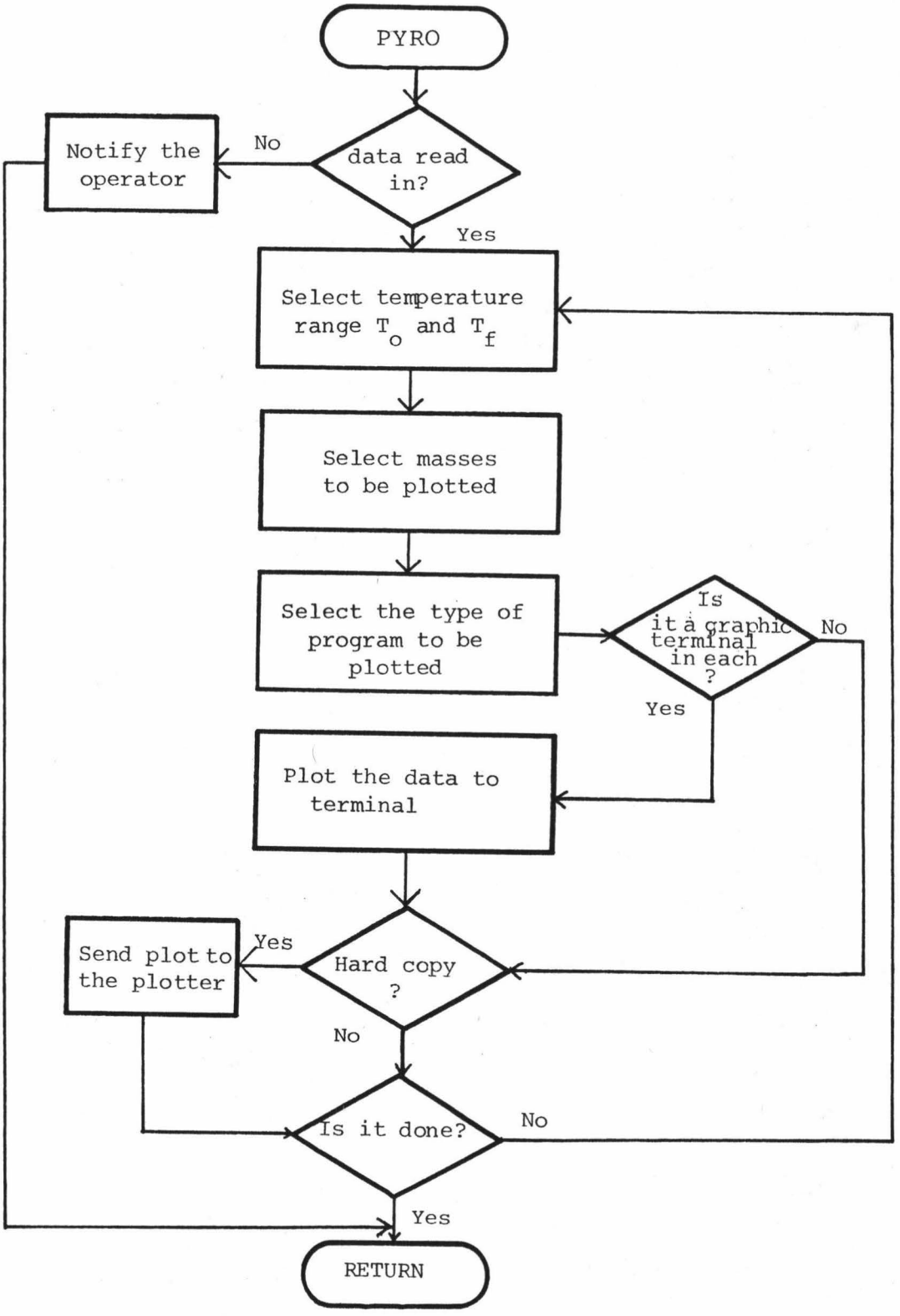

Figure 60. Flow Chart of Subroutine RATIO

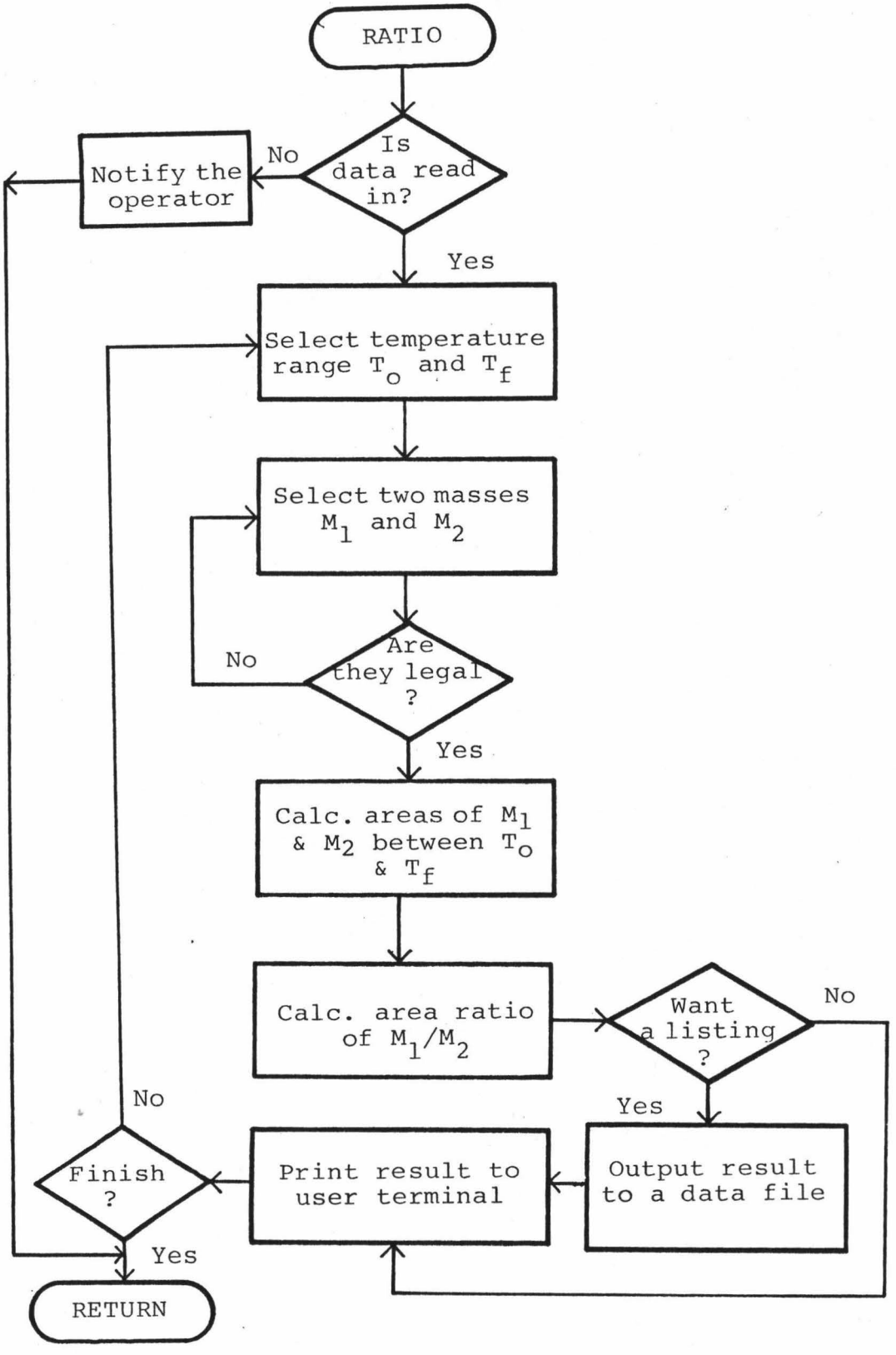

Figure 61. Flow Chart of Subroutine START

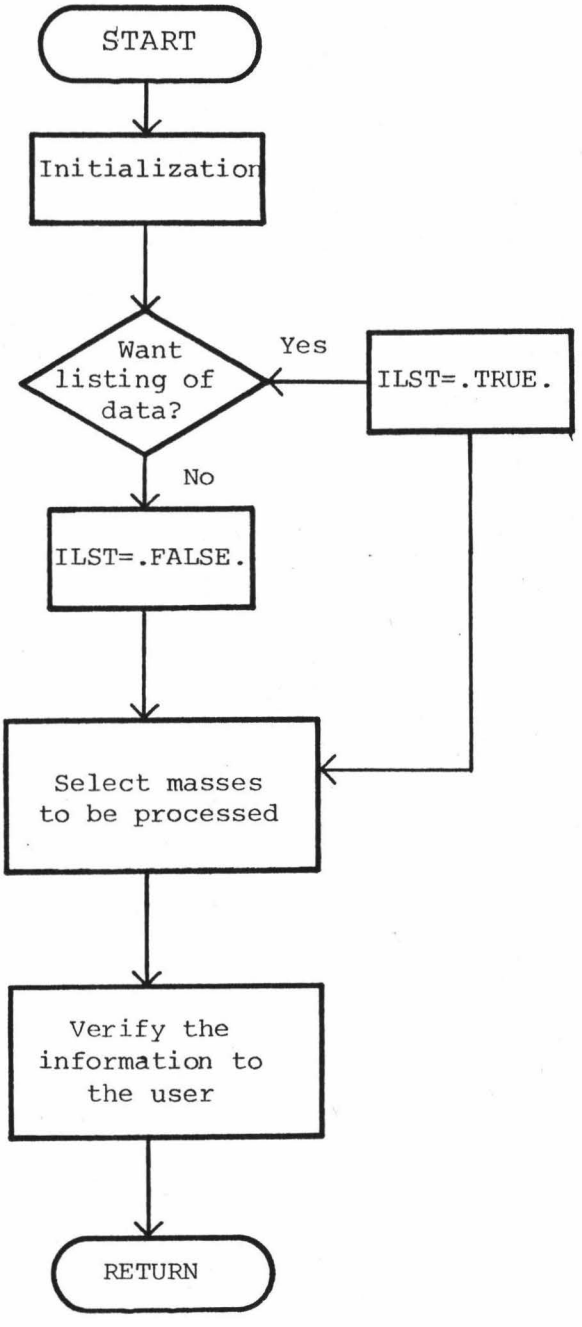

APPENDIX E

Quadrupole Mass Spectrometer Interface Electronic Circuits

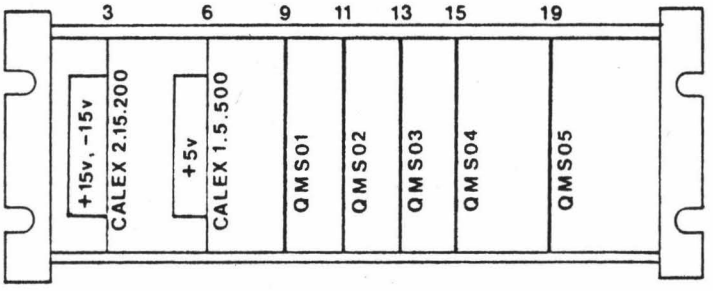

Circuit Card Used:

DOUGLAS ELECTRONICS INC.

24-DE-3 (QMS01, QMS02)
12-DE-3 (QMS03, EMS04, QMS05)
18-DE-3 (Power supplies)

Connector; 44C

Figure 62. QMS Circuit Configuration and Connector Diagrams.

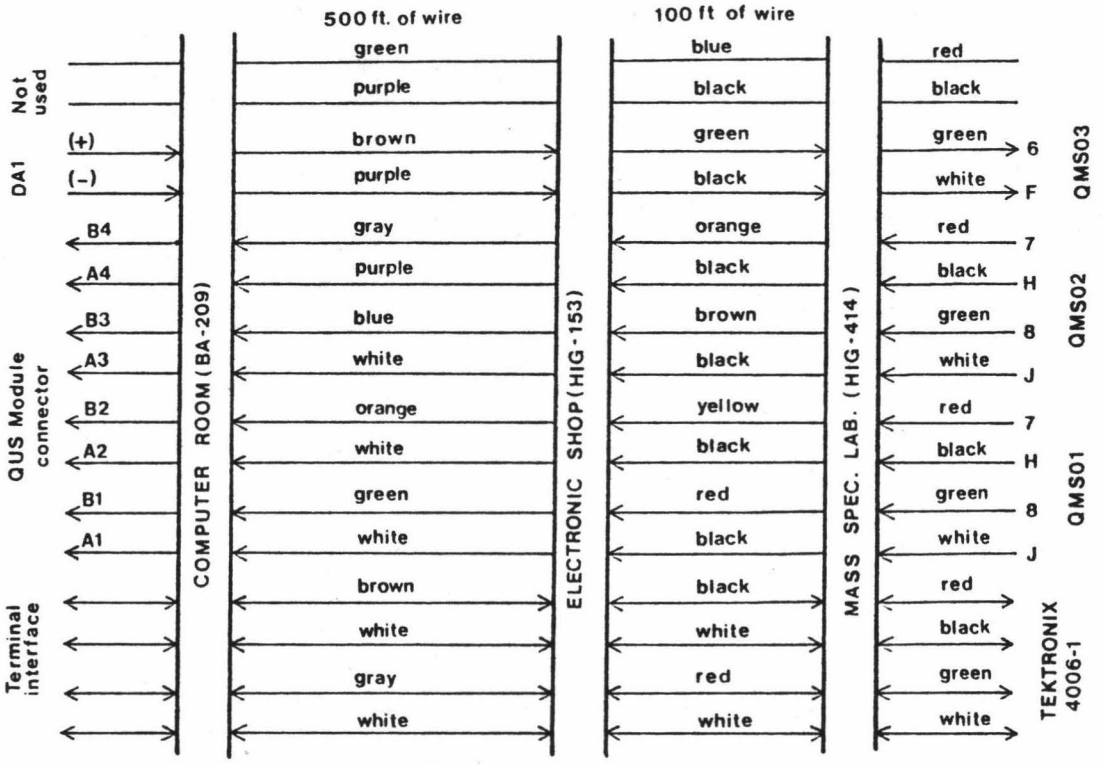

Figure 63. QMS Interface Cabling Diagram

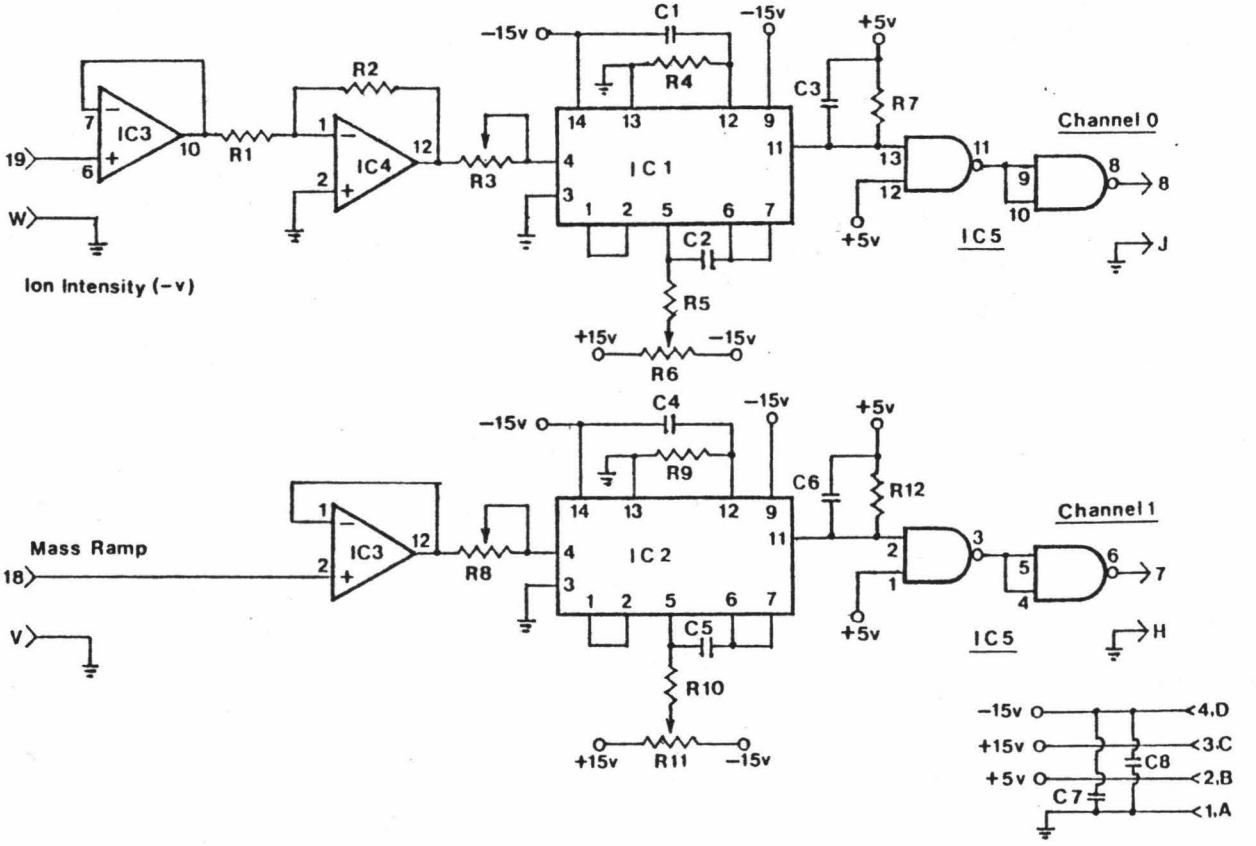

Figure 64. QMS01 -- V/F Circuits for Ion Intensity and Mass Ramp.

Figure 65. QMS01 Circuit Card Layout

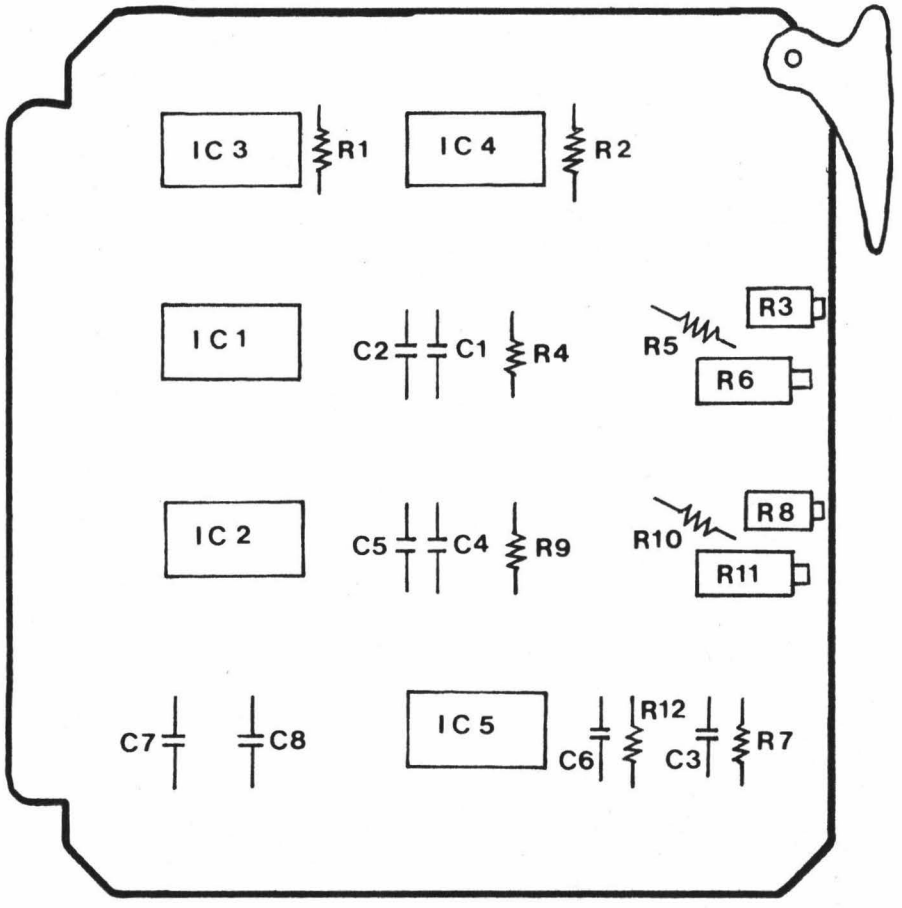

ICS

IC1 - INTECH A-8400
IC2 - INTECH A-8400
IC3 - SN72747
IC4 - SN72747
IC5 - SN7400N

Capacitors

C1 - 100 pf
C2 - 2200 pf
C3 - 100 pf
C4 - 100 pf
C5 - 2200 pf
C6 - 100 pf
C7 - 15µf, 20v
C8 - 15µf, 20v

Resistors (ohm)

R1 - 3.3K
R2 - 3.3K
R3 - 2K
R4 - 4.7K
R5 - 10M
R6 - 10K
R7 - 3.9K
R8 - 2K
R9 - 4.7K
R10 - 10M
R11 - 10K
R12 - 3.9K

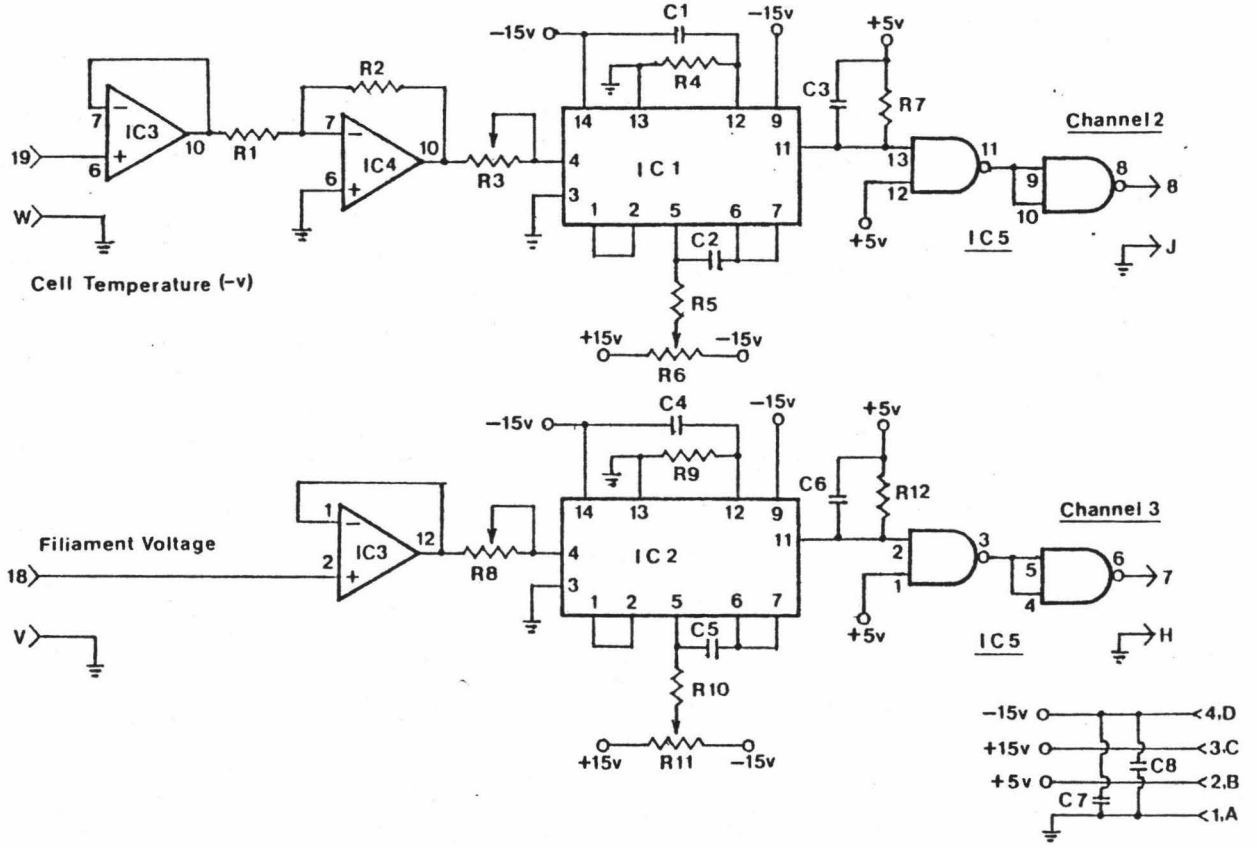

Figure 65. QMS02 -- V/F Circuits for Cell Temperature and Resistance Element Voltage.

Figure 67. QMS02 Circuit Card Layout.

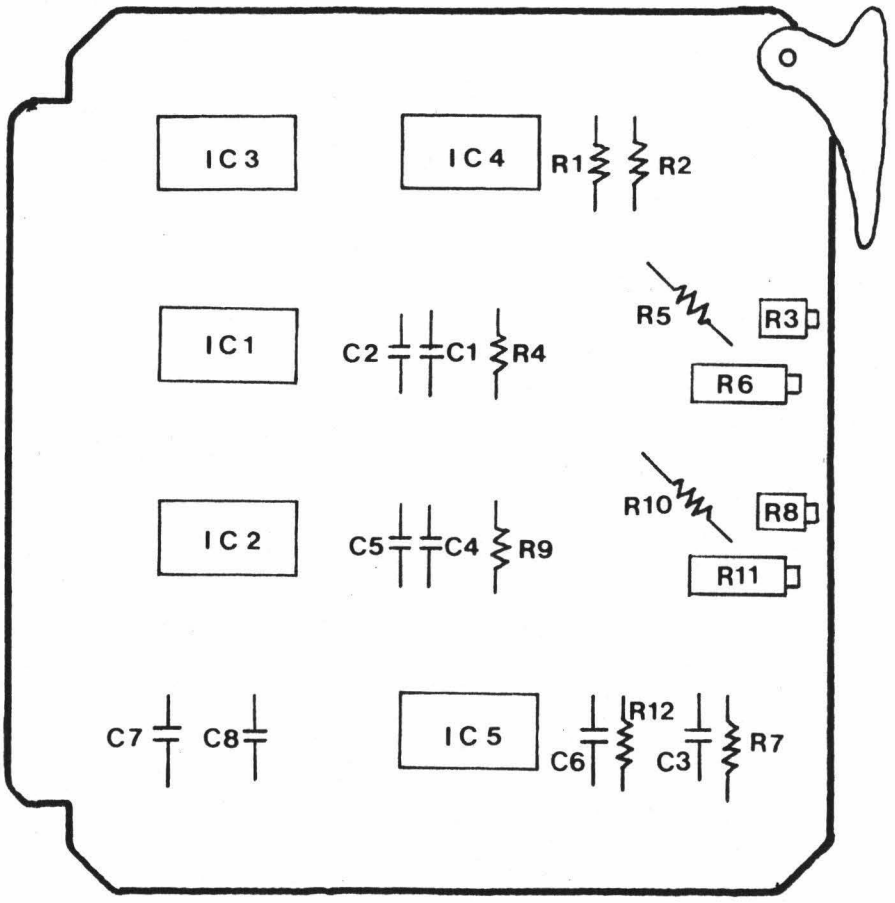

ICS	Capacitors	Resistors (ohm)
IC1 - INTECH A-8400	C1 - 100 pf	R1 - 1K
IC2 - INTECH A-8400	C2 - 2200 pf	R2 - 4.7K
IC3 - SN72747	C3 - 100 pf	R3 - 2K
IC4 - SN72747	C4 - 100 pf	R4 - 56K
IC5 - SN74132N	C5 - 2200 pf	R5 - 10M
	C6 - 100 pf	R6 - 10K
	C7 - 15µf, 20v	R7 - 4.7K
	C8 - 15µf, 20v	R8 - 2K
		R9 - 56K
		R10 - 10M
		R11 - 10K
		R12 - 4.7K

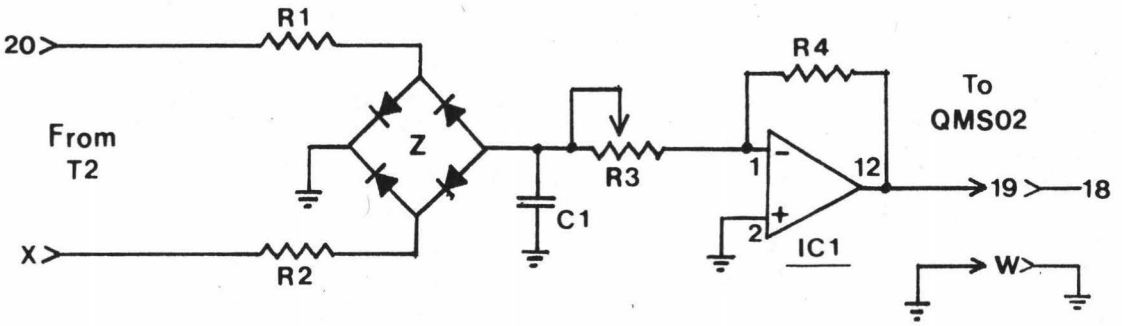

a. Resistance Element Voltage Monitoring Circuit.

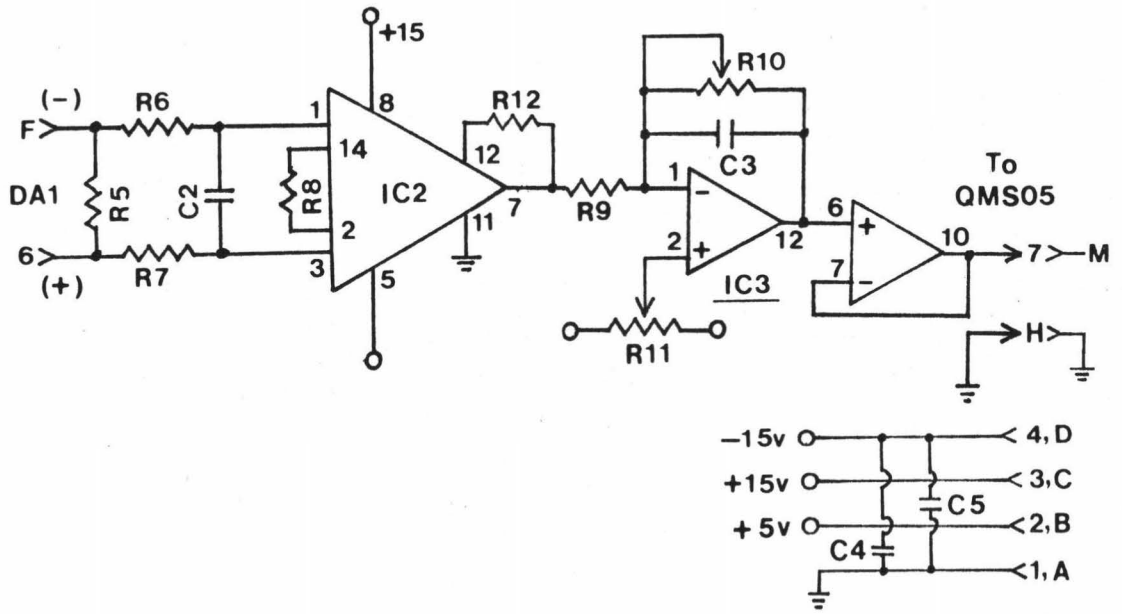

b. Computer Controlled Cell-Temperature Ramp Buffer Circuit

Figure 68. QMS03 Circuits

Figure 69. QMS03 Circuit Card Layout.

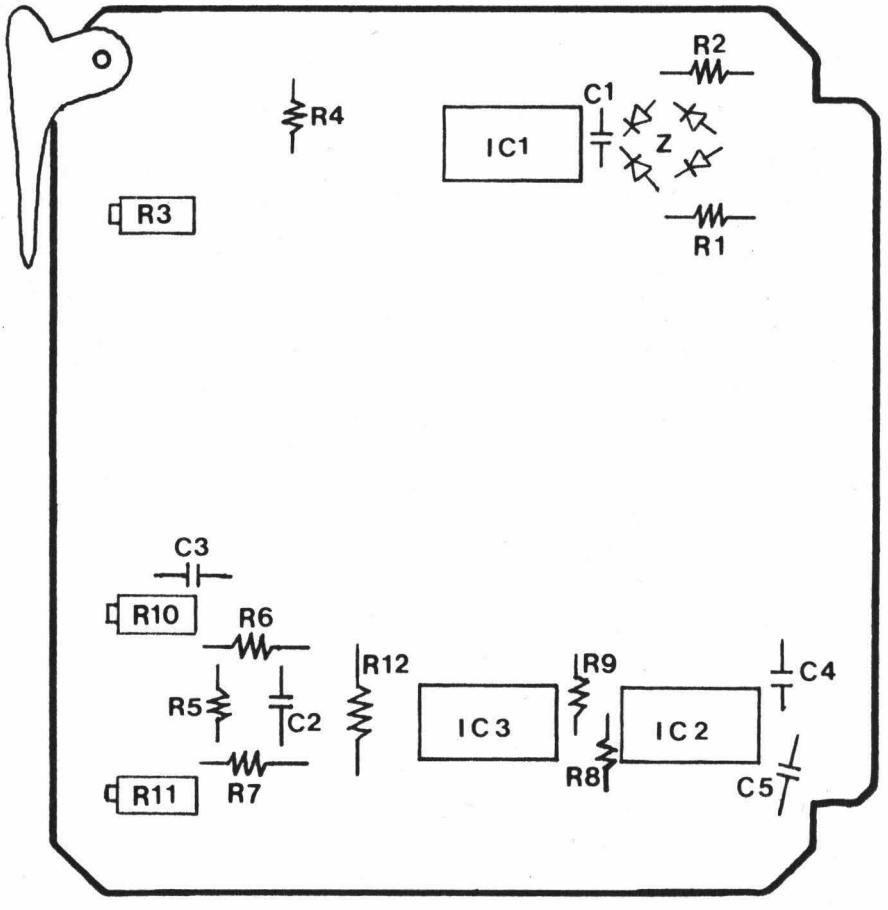

ICS	Resistors (ohm)	Capacitors (µf)
IC1 -- SN74747N	R1 - 100K	C1 -- 20, 15v
IC2 -- AD521JD	R2 - 100K	C2 -- 1
IC3 -- SN74747N	R3 - 100K	C3 -- 1
	R4 - 100K	C4 -- 6.8, 20v
	R5 - 1K	C5 -- 6.8, 20v
	R6 - 10K	
	R7 - 10K	
	R8 - 100K	
	R9 - 10K	
	R10 - 10K	
	R11 - 10K	
	R12 - 10K	

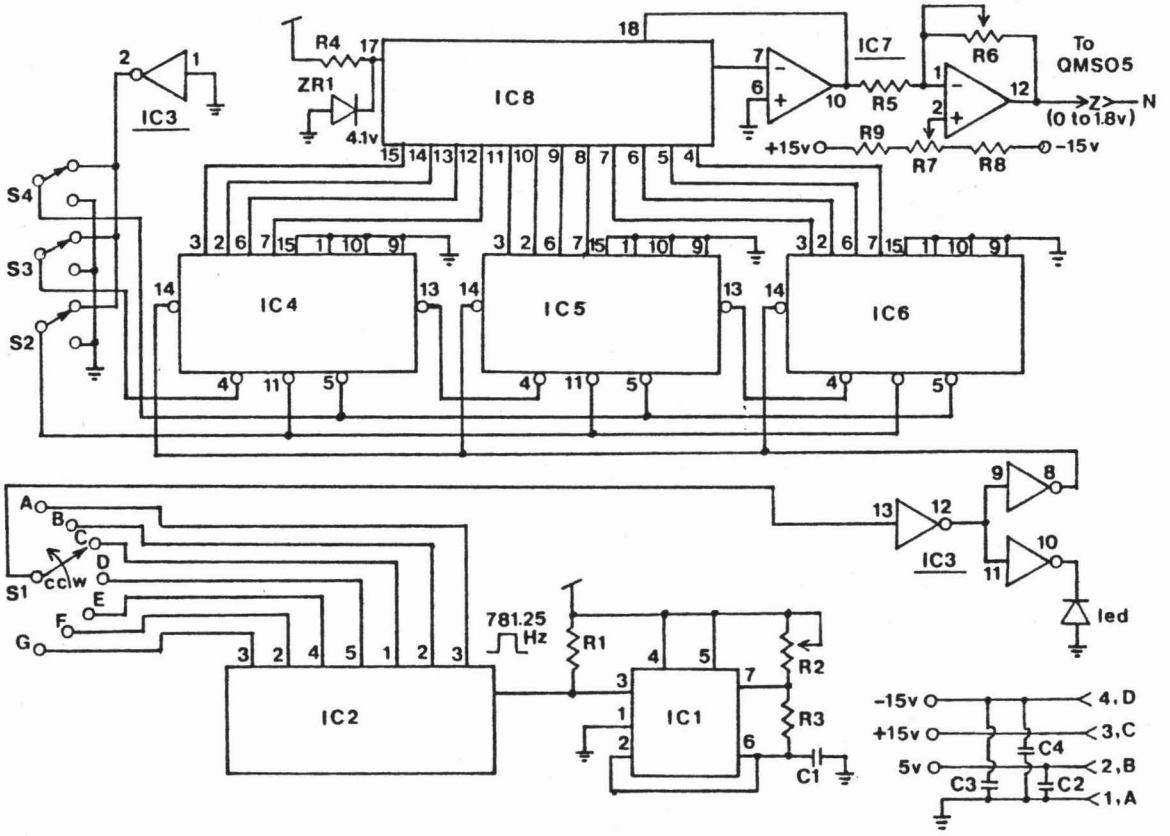

Figure 70. QMS04 Cell Temperature Control Ramp Circuit.

Figure 71. QMS04 Circuit Card Layout

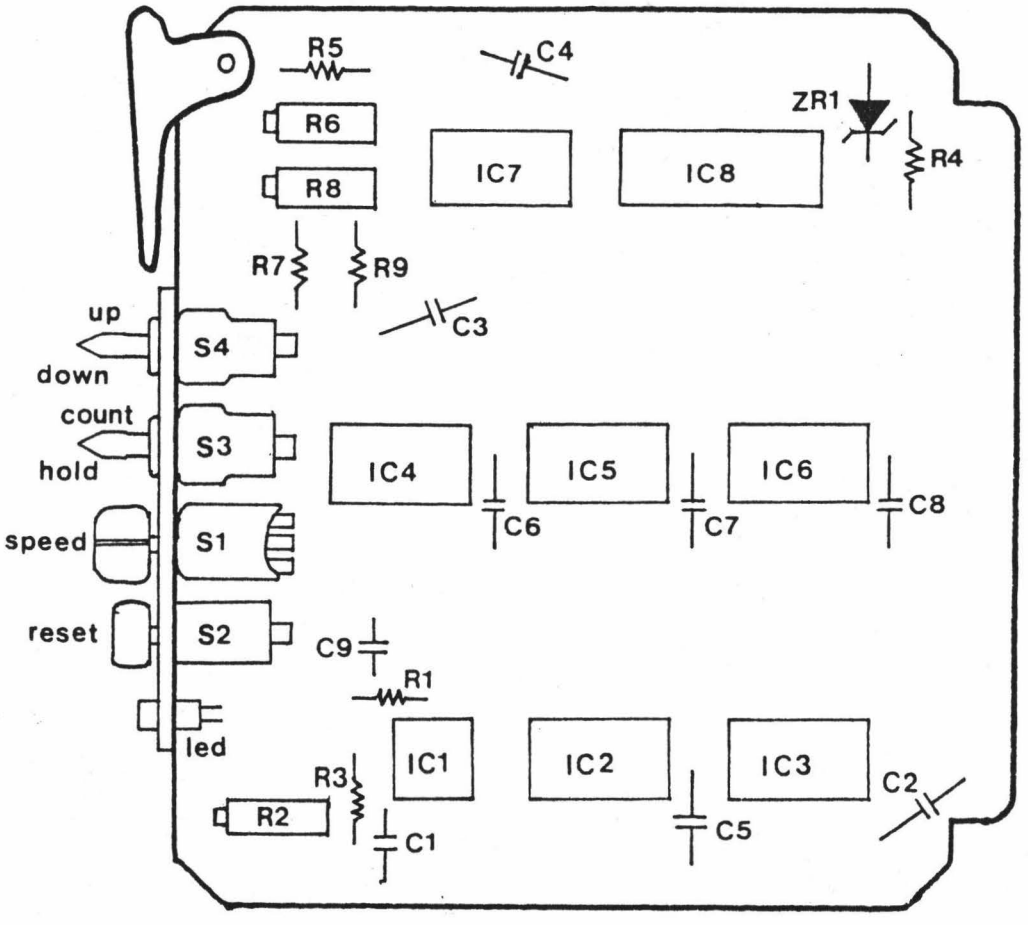

ICS	Capacitors (µf)	Resistors (ohm)
IC1 - NE555V	C1 - 0.01	R1 - 1.5K
IC2 - TP40204N	C2 - 15, 20v	R2 - 100K
IC3 - SN74LS04N	C3 - 15, 20v	R3 - 2.2K
IC4 - SN74LS191N	C4 - 15, 20v	R4 - 2.2K
IC5 - SN74LS191N	C5 - 0.01	R5 - 49.9K
IC6 - SN74LS191N	C6 - 0.01	R6 - 100K
IC7 - SN72747	C7 - 0.01	R7 - 100K
IC8 - AD7521LD	C8 - 0.01	R8 - 10K
	C9 - 0.01	R9 - 100K
		ZR1 - Zener Diode 4.1 v

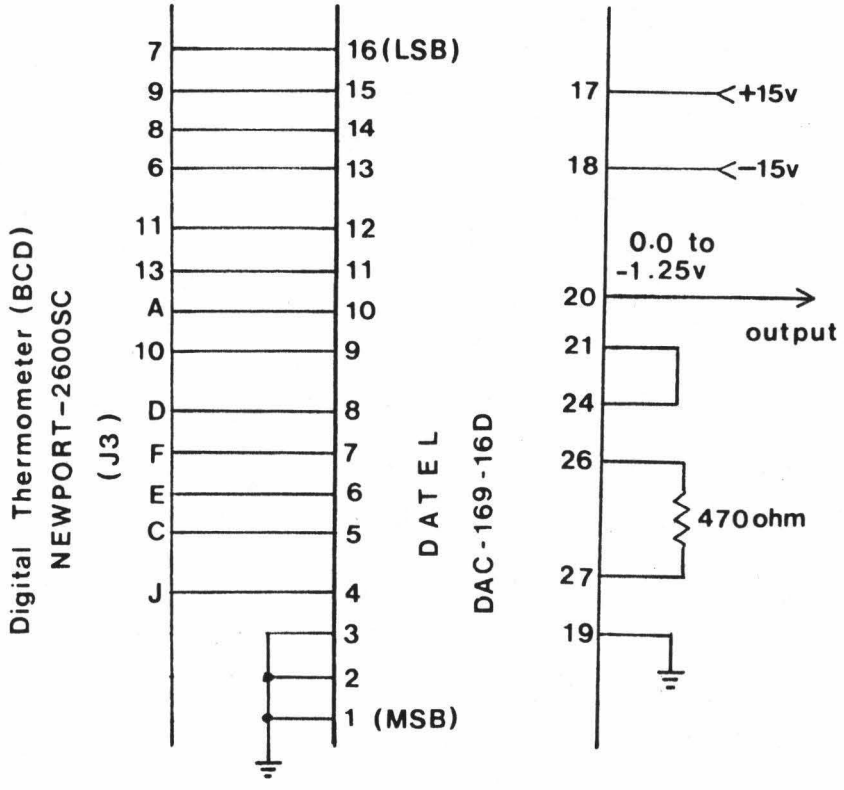

Figure 72. Cell Temperature Feed-Back Circuit. This circuit is located within the Knudsen cell heating voltage control box next to the digital thermometer. The output goes to 5.1 (summing resistor of the voltage circuit) and Pin 2 of QMS02.

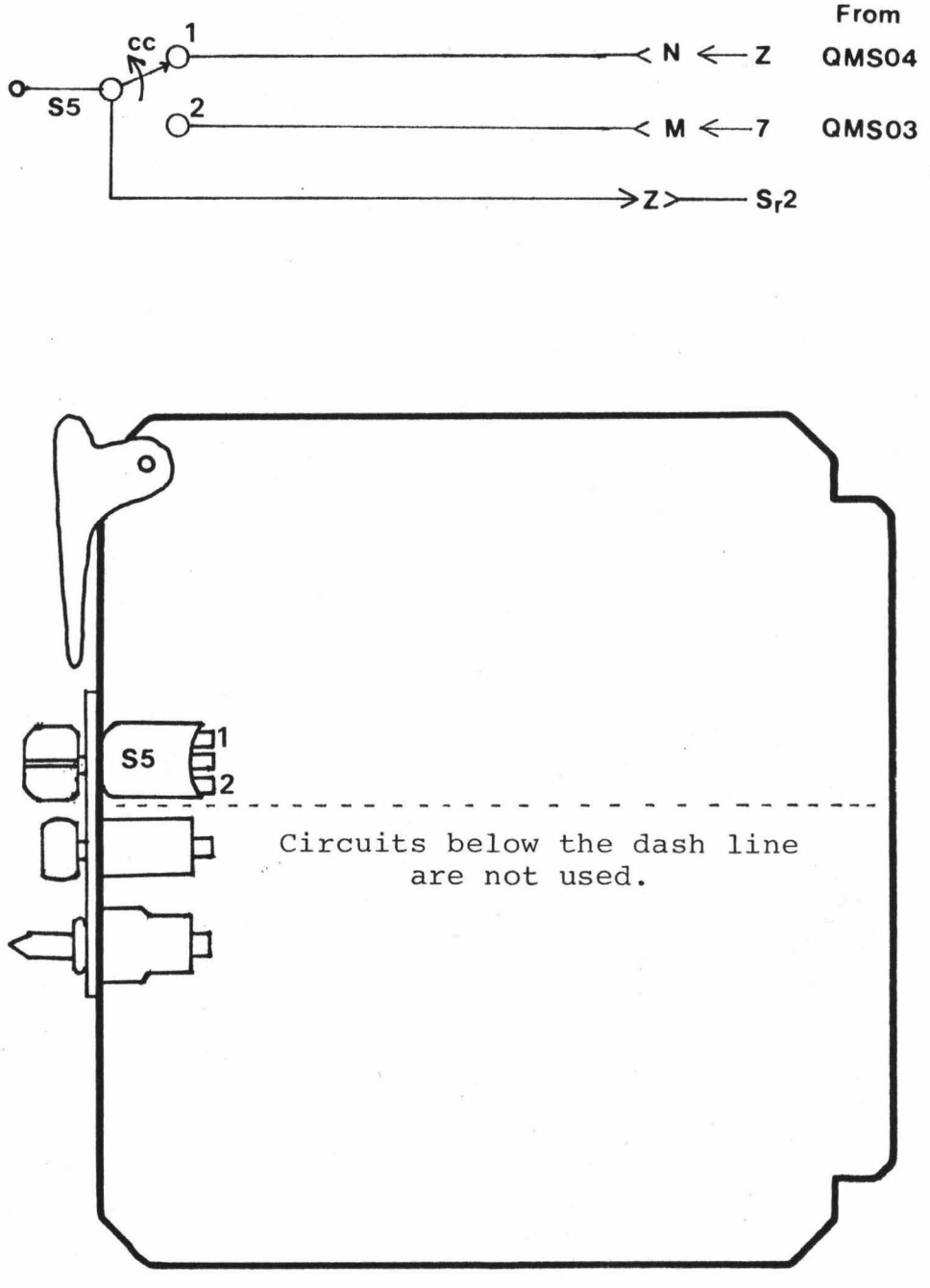

Figure 73. Cell Temperature Control Ramp Selection Switch Circuit and Circuit Card Layout.

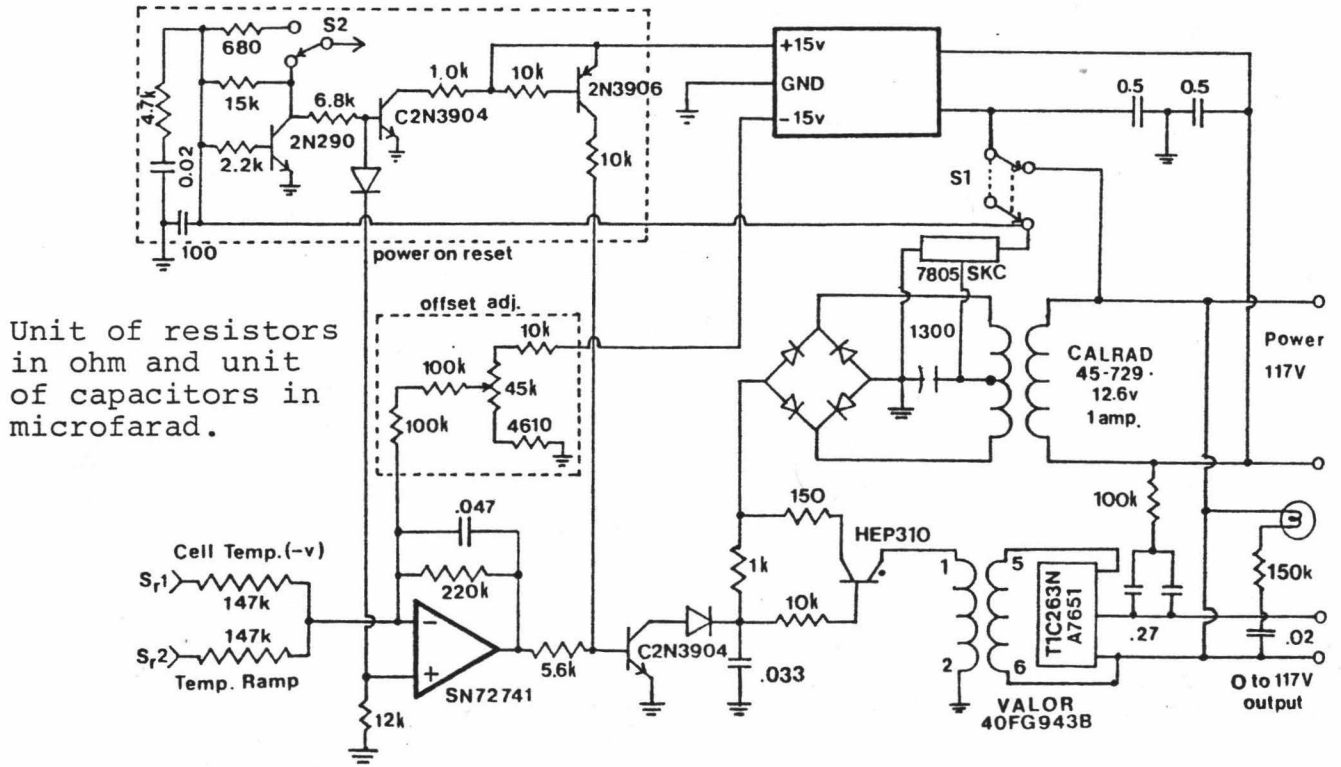

Figure 74. Knudsen-Cell Heating Voltage Control Circuit. This circuit is located within a metal box next to the NEWPORT-2600SC digital thermometer.

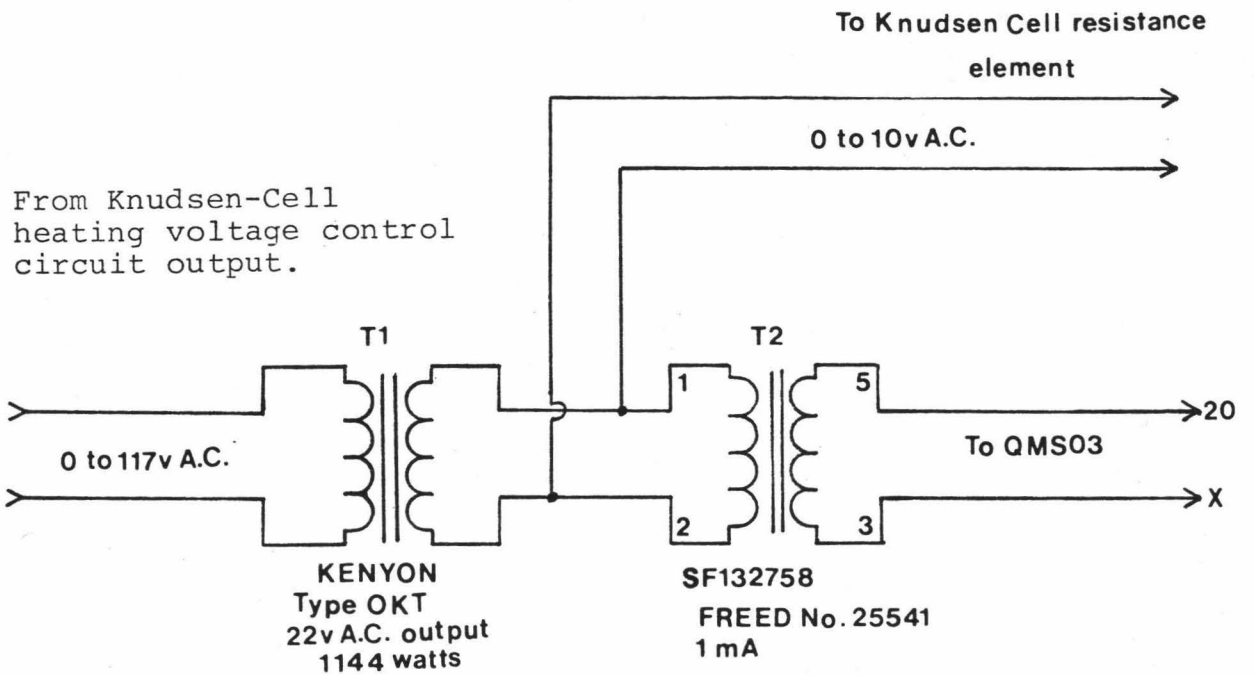

Figure 75. Resistance Element Current Supply Circuit.

REFERENCES

Anderson, A.T. (1975) Some basaltic and andesitic gases: Rev. Geophys. Space Phys., vol. 13, 37-56.

Armstrong, R.L. (1968) A model for the evolution of the strontium and lead isotopes in a dynamic earth: Rev. Geophysics, vol. 6, 175-199.

_____ (1971) Isotopic and chemical constraint on models of magma genesis in volcanic arcs: Earth Planet. Sci. Lett., vol. 12, 137-142.

Boetteher, A.L. (1977) The role of amphiboles and water in circum-Pacific volcanism; in High Pressure Research: Applications in Geophysics; M. H. Manghani and S.-I. Aimoko, eds.: Academic Press, New York, 107-125.

Brubaker, W.M. (1960) Proceedings of the Fith International Instruments and Measurements Conference, Stockholm, 1960, (Acad. Press Inc., N.Y. 1961), p. 305.

Burlingame, A.L., Hauser, J.S., Simoneit, B.R., Smith, D.H., Biemann, K., Mancuso, N., Murphy, R., Flory, D.A. and Reynolds, M.A. (1971) Preliminary organic analysis of the Apollo 12 cores: Proc. Second Lunar Sci. Conf., Geochim. Cosmechim. Acta. Suppl. 2. M.I.T. Press, 1891-1899.

Craig, H. and Lupton, J.E. (1976) Rare gases and volatiles in oceanic basalt, (Abst): E.O.S., Trans. Am. Geophys. Union, Vol. 57, p. 408.

Dawson, P.H. and Whetten, N.R. (1969) Mass Spectroscopy using RF quadrupole fields; Advan. Electron. Electron Phys., 27, 59-185.

Delaney, J.R. (1977) Ph.D. dissertation, The University of Arizona.

Delaney, J.R., Muenow, D.W., and Graham, D. G. (1978) Abundance and distribution of water, carbon and sulfur in the glassy rims of submarine pillow basalts: Geochim. Cosmochim. Acta, in press.

Dietrich, V., Emmermann, R., Oberhansli, R. and Puchelt, H. (1978) Geochemistry of basaltic and gabbroic rocks from the west Mariana basin and the Mariana Trench: Earth Planet, Sci. Lett., Vol. 39, 127-144.

Eggler, D. H. (1976) Does CO_2 cause partial melting in the low-velocity layer of the mantle?: Geology, Vol. 4, 69-72.

Eggler, D.H. and Rosenhauer, M. (1968) Carbon dioxide in silicate melts: II. Solubilities of CO_2 and H_2O in $CaMgSi_2O_6$ (diopside) liquids and vapors at pressure to 40 kb: Am. Jour. Sci., Vol. 278, 64-94.

Garcia, M.O. (1978a) Volatiles in submarine volcanic rocks from the Marianas Island Arc and Trough: Abstract Geol. Soc. Am.

Garcia, M.O. (1968b) Personal communication.

Garcia, M.O., Muenow, D.W. and Liu, N.W.K. (1978) Volatiles in submarine volcanic rocks from the Mariana Island-Arc and Trough: Submitted to Geochim. Cosmochim. Acta.

Gibson, E.K., Jr. (1973) Thermal analysis - mass spectrometer computer system and its application to the evolved gas analysis of green river shale and lunar soil samples: Thermochimica Acta, 5, 243-255.

Gibson, E.K., Jr. and Moore, G.W. (1973) Volatile-rich lunar soil: evidence of possible cometary impact: Science. 179, 69-71.

Gibson, E.K., Jr., Moore, G.W. and Johnson, S.M., (1974) Summary of analytical data from gas release investigations, volatization experiments, elemental abundance measurements on lunar samples, meteorites, minerals, volcanic ashes and basalts: NASA Report, Houston.

Gooding, J.L. (1975) M.S. thesis, University of Hawaii.

Gooding, J.L. and Muenow, D.W. (1977) Experimental vaporization of the Holbrook Chondrite; Meteoritics, Vol. 12, No. 4, 401-408.

Graham, D.G. (1978) Ph.D. dissertation, University of Hawaii.

Grimley, R.T. (1967) Mass Spectrometry. In The Characterization of High Temperature Vapors (editor J.L. Margrave), Wiley. 195-243.

Hawkins, J.W. (1976) Petrology and geochemistry of basaltic rocks of the Lau Basin: Earth Planet. Sci. Lett., Vol. 28, 283-297.

Hawkins, J.W. (1977) Petrologic and geochemical characteristic of marginal basins basalts: in Island Arcs, Deep Sea Trenches and Back-Arc Basins, M. Talwani and W. C. Pitman, eds., AGU Maurice Ewing Series, Vol. 1, 355-365.

Holland, P.T., Simoneit, B. R., Wsolek, P.C., McFadden, W.H. and Burlingame, A.L. (1972) Carbon chemistry of Apollo 14 size-fractionated fines: Nature (Phys. Sci.) 235, 106-108.

Holloway, J.R. and Burnham, C.W. (1972) Melting relations of basalt with equilibrium water pressure less than total pressure: J. Petrol., Vol. 13, 1-29.

Howkesworth, C.J., O'nions, R.K., Pankhurt, R.J., Hamilton, P.J. and Evansen, N.M. (1977) A geochemical study of island-arc and back-arc tholeiites from Scotia Sea: Earth Planet. Sci. Lett. Vol. 36, 253-262.

Killingley, J.S. and Muenow, D.W. (1974) A mass spectrometric method for the determination of the size distribution of CO_2 inclusions in olivines: Am. Mineralogist, Vol. 59, 863-967.

Killingley, J.S. (1975) Ph.D. dissertation, University of Hawaii.

Killingley, J.S., and Muenow, D.W. (1975) Volatiles from Hawaiian submarine basalts determined by dynamic high temperature mass spectrometry: Geochim. Coscochem. Acta. 39, 1467-1473.

_____ (1975b) Thermal stress-induced release of CO_2 inclusions in olivine on cooling from high temperatures: Am. Mineralogist, vol. 60, 148-151.

Klimowski, R.J., Venkataraghavan, R. and McLafferty (1970) A small on-line computer system for high-resoolution mass spectrometers: Organic Mass Spectrometry, Vol. 4, 17-39.

Kushiro, I. (1973) Origin of some magmas in oceanic and circumoceanic regions: Tectonophysics, Vol. 17, 211-222.

Meijer, A. (1974) Ph.D. dissertation, UCSB.

Meijer, A. (1976) Pb and Sr isotopic data bearing the origin of volcanic rock from the Mariana island-arc system: Geol. Soc. Am. Bull., Vol. 87, 1358-1369.

Moore, J.G. and Fabbi, B.P. (1971) An estimate of the juvenile sulfur content of basalts: Contrib. Mineral. Petrol., Vol. 33, 118-127.

Muenow, D.W., Graham, D.G., Liu, N.W.K. and Delaney, J.R. (1978) Water-poor glass-vapor inclusions in phenocrysts from Hawaiian tholeiitic pillow basalts. In prep.

Muenow, D.W. (1973) Occurrence of volatile nitrides from silicates in low pressure, high temperature, reducing environments: Geochim. Cosmochim. Acts, 37, 2523-2528.

Naughton, J.J., Derby, J.V. and Glover, R.B. (1969) Infrared measurements on volcanic gas and fume: Kilauea Eruptions, 1968: Jour. Geophys. Res., Vol. 74, 3273-3277.

Paul, W., Reinhard, H.P. and von Zahn, U. (1958) Das elektrische massenfilter als massenspektrometer und isotopentrenner; Z. Phys. 152, 143-182.

Ringwood, A.E. (1974) The petrological evolution of island arc systems: Geol. Soc. Lond. J., Vol. 130, 183-204.

Ringwood, A.E. (1975) Composition and Petrology of the earth's mantle, McGraw-Hill, p. 156.

Roedder, E. (1965) Liquid CO_2 inclusions in olivine-bearing nodules and phenocrysts from basalts: Amer. Mineral, Vol. 50, 1746-1782.

Roedder, E. and Weibler, P.W. (1972) Petrographic features and petrologic significance of melt inclusions in Apollo 14 and 15 rocks: Proc. Third Lunar Sci. Conf., Geochim. Cosmochim. Acta Suppl, Vol. 4, 251-279.

_____ (1973a) Petrology of melt inclusions in Apollo samples 15598 and 62295, and of clasts in 67915 and several lunar soils: Proc. Fourth Lunar Sci. Conf. Geochim. Cosmochim Acta Suppl, Vol. 4, 681-703.

_____ (1973b) Petrology of some lithic fragments from Luna 20: Geochim. Cosmochim. Acta, Vol. 37, 1031-1052.

Roboz, J. (1968) Introduction to Mass Spectrometry, Interscience Publishers, p. 107.

Sigvaldason, G.E. and Oskarsen, N. (1976) Chlorine in basalts from Iceland: Geochim. Cosmochin. Acta, Vol. 40, 777-789.

Simoneit, B.R. and Burlingame, A.L. (1972) Organic contamination analysis. High resolution mass spectrometric analysis of surface organics on selected areas of Surveyor 3. In Analysis of Surveyor 3 Material and Photographs Returned by Apollo 12: NASA SP-284. U.S. Gov. Printing Office, 127-142.

Simoneit, B.R., Wszolek, P.C., Christiansen, P., Jackson, R.F. and Burlingame, A.L. (1973) Carbon chemistry of luna 16 and Luna 20 samples: Geochim. Cosmochim. Acta. 37, 1063-1974.

Toksoz, N.M. (1975) The subduction of the lithosphere: Readings from Scientific American, Continents Adrift and Continents Aground, p. 116.

Unni, C.K. and Schilling, J.G. (1978) Cl and Br degassing by volcanism along the Reykjanes Ridge and Iceland: Nature, Vol. 272, 19-23.

Watson, E.B. (1976) Glass inclusions as samples of early magmatic liquid: Determinative method and application to a south Atlantic basalt: Jour. Volcanol. Geotherm. Res., 1, 73-84.

Wyatt, J.R., Pressley, G.A., Jr., and Stafford, E.A. (1971) On-line computer control and data acquisition for a high temperature/molecular beam mass spectrometer: High Temperature Science 3, 130-137.

Wyllie, P.J. (1973) Experimental petrology and global tectonics -- a review: Tectonophysics, Vol. 17, 189-209.